Molecular Geometry and the Mulliken–Walsh Molecular Orbital Model. An *Ab Initio* Study

ROBERT J. BUENKER* and SIGRID D. PEYERIMHOFF

Department of Chemistry, University of Nebraska, Lincoln, Nebraska 68508, and Lehrstuhl für Theoretische Chemie, Universität Bonn, 53 Bonn, West Germany

Received January 15, 1973 (Revised Manuscript Received April 30, 1973)

Contents

I. Introduction

The geometrical arrangements of molecules in their ground and excited states has been a subject of long-standing interest in virtually every major field of chemistry. Of the rather large number of theoretical models thus far developed to deal with this question, that given by Mulliken[1] and Walsh[2] in terms of generalized orbital binding energy correlation diagrams has certainly proved itself to be one of the most useful. Furthermore because of its clear association with the more general molecular orbital (MO) theory, this particular geometrical model has been viewed by many authors as being particularly susceptible to straightforward mathematical analysis with reference to the basic concepts of quantum mechanics itself. Unquestionably the most salient feature of this stereochemical model, which has come to be known in its simplest form as Walsh's rules, is its conclusion that molecular geometry is determined to a very great extent simply by the *number of valence electrons* in a given system. The latter observation is especially poignant in view of the fact that essentially the same conclusion has been reached by various other authors[3-6] approaching the subject from apparently quite different directions, in particular *via* the VB theory of Pauling.[7]

In its original form[1,2] the Mulliken–Walsh model (hereafter referred to simply as the MW model) has been used to rationalize certain empirically determined geometrical trends on a qualitative, or at most a semiquantitative, basis, but its clear success in this endeavor has prompted more detailed investigations into this general question in an attempt to obtain quantitative justification for the methodology of this simple theory. One of the most exhaustive of such studies has been made by means of *ab initio* SCF calculations with an eye toward drawing a close connection between the canonical orbital energies resulting therefrom and the *empirical* quantities plotted in the aforementioned MW correlation diagrams. Because calculations of this type involve fairly extensive computations, publication of these results has occurred over a period of at least 5 years,[8-10] and it is thus the objective of the present paper to summarize the findings of these investigations and to evaluate their contribution to the goal of not only establishing the methodology of the MW model on firmer theoretical grounds but also of attaining a more generally applicable theory of molecular geometry which encompasses at least a significant portion of certain well-defined exceptions not covered in the original empirical scheme.

To these ends problems of relating the results of quantum mechanical calculations to the various aspects of the empirical theory of Mulliken and Walsh are considered in section II. In section II.A, a number of quantities used previously for the construction of MW correlation diagrams are discussed in light of certain objective criteria. The use of canonical SCF orbital energies and particularly the importance of Koopmans' theorem for understanding the operations of the MW model are investigated

*Author to whom inquiries should be addressed at Lehrstuhl für Theoretische Chemie.

in section II.B; in particular, certain corrections are determined which must be applied to the original theory when comparing systems of differing covalency. In section II.C, extensions in the scope of the MW model are discussed, particularly as they relate to the possibility of using the same correlation diagram for more than one class of molecular systems. The third section of the paper deals with specific applications of the resultant modified theory of molecular geometry, with special emphasis on results obtained from *ab initio* SCF treatments of molecules containing from one to four heavy (nonhydrogenic) atoms. Finally the last section briefly summarizes what has been learned and comments upon the probable directions of future investigations on the general subject of molecular geometry in ground and excited states. Alternative geometrical models based on valence bond theory, atomic radii, electronegativity differences, Jahn-Teller distortions, and various other concepts are given only brief consideration in this review, primarily because the calculations under discussion are not at all so easily related to the latter approaches to the study of molecular structure as they are to that proposed by Mulliken and Walsh.

II. Theoretical Aspects

A. What Is Plotted in Walsh's Diagrams?

The central theoretical tool employed in the structural theory of Mulliken and Walsh is the correlation diagram, essentially a plot of a series of rather loosely defined quantities (generally referred to as orbital energies) as a function of some internuclear coordinate (usually an angular variable); a typical example of such a correlation diagram is given in Figure 1a, in this case for the AH_2 series of molecules, as originally discussed by Walsh in 1953. Each of the curves in this diagram corresponds to a particular molecular orbital of a general AH_2 system such as water, H_2O; in each case the key point of interest in whether the orbital energy decreases with angular deformation of the molecule (as for the $3a_1$ species in Figure 1a), remains essentially constant (as for the $1b_1$ MO), or increases with such geometrical changes (as for the $1b_2$).

Arguments for the behavior of the various orbital energy curves with molecular bending are based on a series of simple theoretical concepts pertaining to the effects of AO mixing on the stability of the MO's in question. For example, the $1b_1$ orbital energy is assumed to remain constant with $\angle$HAH changes because the constitution of this MO remains pure $p\pi$ at all stages of the bending process. That of the $1b_2$ is said to increase with molecular bending because the possibilities for constructive overlap between the $p\sigma$ orbital of the central A atom and the 1s AO's of the two hydrogenic species are clearly diminished as the system deviates from the linear arrangement of nuclei. The opposite trend is assumed for the $3a_1$ species since in this case bending out of the linear geometry causes the MO in question to be transformed from a pure $p\pi$ species (degenerate with the $1b_1$) to a hybrid orbital of both s and p character. To a certain extent, of course, it must be acknowledged that the primary motivation in these interpretations for the shapes of the various orbital energy curves is largely empirical, but the fact remains that for the most part such trends can be anticipated quite effectively on the basis of the stability arguments introduced by Mulliken and Walsh in their original work.

Conclusions relative to the geometry of molecules in a given family are then made quite easily on the basis of which of the MO's are occupied in a particular electronic

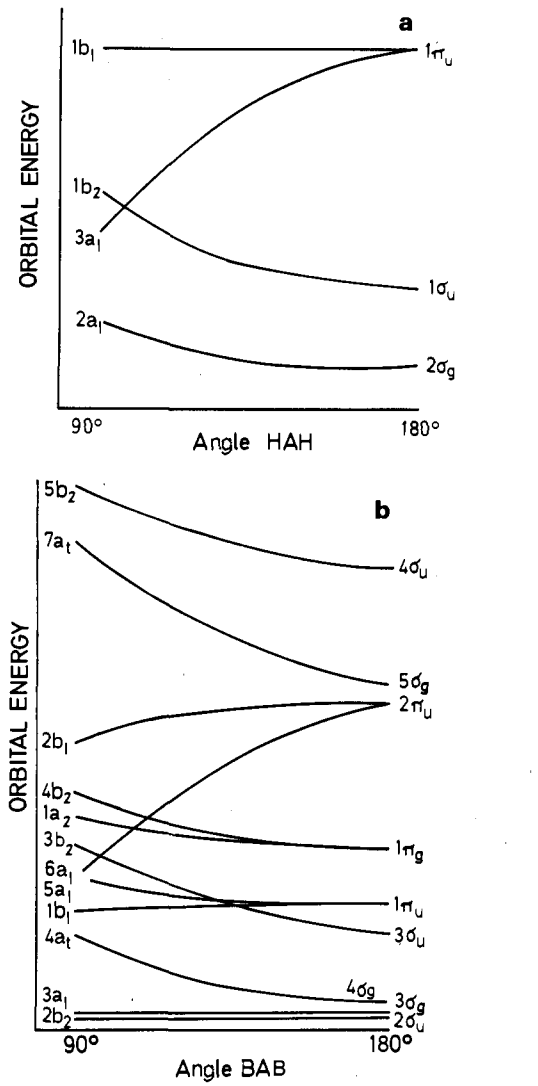

Figure 1. Empirical angular correlation diagrams for general AH_2 (a) and AB_2 (b) systems, after the work of Mulliken and Walsh.[1,2]

state of interest. Basically, occupation of a level whose orbital energy curve is decreasing with diminishing internuclear angle is said to produce a trend toward bent geometry while the opposite effect is, of course, expected for population of an MO whose energy increases for such deformations out of the linear nuclear arrangement. Thus while AH_2 systems with four valence electrons are predicted to be linear in their ground states (with double occupation of all levels up to and including the $1b_2$ species), those with five and six (such as BH_2 and BH_2^-, respectively) are expected to prefer increasingly smaller HAH angles, as the direct result of occupation of the $3a_1$ MO, with its aforementioned preference toward bent geometries. On the other hand, the MW model predicts no change in geometry to occur in going from the BH_2^+ ground state to the $^2B_1$ excited state of BH_2, since in this case the differentiating orbital ($1b_1$) possesses an energy curve which does not vary with changes in internuclear angle. Clearly the key point in this model is that the geometry of a molecule in a given state is very much dependent on its characteristic electronic configuration.

For other classes of molecular systems it is merely necessary to introduce different correlation diagrams, the behavior of whose constituent orbital energy curves can be explained in essentially the same manner as has been described above for the AH_2 family. The corresponding diagram for molecules of AB_2 type is shown in Figure 1b,

again patterned after that given by Walsh[2] in 1953 and, to a lesser extent, after that introduced by Mulliken[1] in 1942. In this case it is possible, for example, to understand why systems of this type possess progressively more strongly linear ground-state structures as the number of valence electrons increases from 12 to 16, respectively, as a result of successive population of the $1\pi_g$–($4b_2$, $1a_2$) pair of MO's, with their marked aversion to bent nuclear geometries. Similarly it is clear from such a diagram that occupation of the next most stable species, the $6a_1$ MO, reverses this trend quite dramatically by virtue of the strongly bent tendency exhibited by its orbital energy curve (Figure 1b). Again it can scarcely be overemphasized that such argumentation appears to be equally valid for both ground and excited states, thereby underscoring the fact that the MW model is easily applicable to the understanding of the stereochemical changes which occur in electronic transitions.

Despite the very definite relationship between the MW model, on the one hand, and MO theory, on the other, there is still considerable question as to just how this empirical structural model can be justified on the basis of a *priori* quantum mechanical theory. In attempting to formulate a quantitative realization of the MW model of molecular geometry, the single most critical question which needs to be answered is that of the identity of the ordinate in the Walsh (correlation) diagrams. In introducing the concept in 1942 Mulliken invariably referred to the ordinate in such diagrams as "ionization energies," whereas Walsh apparently preferred the physically less precise term "orbital binding energies." To a certain extent it must be said that the identity of the aforementioned quantities cannot be determined with mathematical certainty since their behavior as a function of some geometrical distortion has been derived from largely *empirical* considerations. Despite this fundamental difficulty, however, there is considerable merit in establishing certain objective criteria for judging the degree to which a given mathematical construct is able to realize the essential features of such an empirical quantity.

1. Criteria

In all the writings which have followed upon the introduction of the MW model, the characteristic most generally believed to be essential for a given mathematical quantity to be employed as a valid realization of the "orbital binding energy" is its proper behavior with changes in molecular geometry; *i.e.*, the correlation diagram constructed with such quantities should *basically* reproduce the gross features of the original Walsh diagram. Occasional disagreements between the shapes of corresponding curves in calculated and empirical diagrams can be ignored, of course, if they do not lead to a conflict with experimental data. The second and third criteria generally considered are closely connected to the first, requiring merely that the quantities plotted in the diagrams be clearly related to *orbitals* which have definite symmetry characteristics and that as a result of this fact the shapes of the various curves be interpretable (predictable) on the basis of elementary considerations of the bonding and antibonding character of the orbitals themselves.

The fourth and fifth criteria are generally considered less critical, requiring identification of the plotted quantities with the negative of the ionization potentials of the corresponding orbitals, and also clear association between *differences* in such orbital energies and the transition energies between various electronic states of the system. The last and by far the most controversial standard by which types of orbital energies have been judged involves the question of how such quantities are used to obtain the geometrical predictions ultimately forthcoming from the MW model. To many authors the most straightforward method of obtaining such information has simply been to use the *sum of orbital energies* as the potential term for motion along a given geometrical coordinate, but there is considerable evidence that such an identification represents an overly restrictive view of how the MW model arrives at its predictions.

2. Suggested Quantities

One of the first attempts to achieve a quantitative realization of the Mulliken–Walsh model was made in terms of united atom (UA) calculations by Wulfman[11,12] and Bingel[13] and later by Saturno.[14] The correlation diagrams constructed by these authors for AH_2, AH_3, and AH_4 systems using the eigenvalues of a UA Hamiltonian closely resembled those given empirically by Walsh,[2] but nevertheless the same treatment was found to be much less successful when applied to systems with more than one heavy atom[11,12] (notably AB_2 molecules), a result which was not altogether unexpected in view of the nature of the UA method itself. Perhaps more fundamentally these calculations raised the question[13] of just how the repulsion between the nuclei in such molecular systems should be taken into account in the framework of the MW model.

At about the same time Schmidtke and Preuss[15] and Schmidtke[16,17] carried out some LCAO–MO calculations with a simplified Hamiltonian in order to study the same problem. Again these authors were quite successful in reproducing Walsh's AH_2 and AH_3 diagrams in their calculations, but they too reported some difficulties in the case of the AB_2 systems. The question of how to include the nuclear repulsion in such calculations was also a source of some concern to these authors since the definition of their orbital energies does not include explicit contributions from this seemingly essential potential term.

The question of the missing nuclear repulsion term was also given serious consideration by Coulson and Neilson,[18,19] but discussion of their proposed solution to the problem is best deferred until the following subsection in which the more general question of how to relate the results of *ab initio* SCF or Hartree–Fock calculations to the methodology of the MW model is investigated. Chronologically the next suggestion as to what to use for the orbital binding energies was given by Peters[20] in the form of a quantity described as the increase in ionization energy of a given MO upon molecule formation. Even though such a definition leads to a correlation diagram in which the orbital energy curve for the 1s orbital lies *between* and not below the corresponding curves for the valence species, Peters contended that these changes in binding energy are still easily identifiable with Walsh's orbital binding energies. Nevertheless, applications were only reported for AH_2 systems, and, in light of the experience of Schmidtke,[17] Wulfman,[11,12] and Bingel[13] with AB_2 systems, there is good reason to withhold judgment on the utility of this particular quantity until it is used to construct correlation diagrams for more general systems.

Shortly after the work of Peters, the first series of papers[21-24] was published in which it was suggested that the *canonical orbital energies* of nonempirical (*ab initio*) LCAO–MO–SCF calculations be used for the construction of the correlation diagrams of the MW model. At about the same time, Leclerc and Lorquet[25] reported the first Hückel-type (semiempirical) calculations on the general subject of Walsh's rules. These authors suggested the

use of the Hückel eigenvalues as the ordinate in the Walsh diagrams; shortly thereafter Allen and Russell[26] considered the same possibility. In both cases a great similarity was noted between such semiempirical calculations and those of *ab initio* SCF type, and thus further discussion of this work is deferred until after the following subsection dealing specifically with treatments of the latter type.

Two other attempts to obtain a quantitative realization of the Mulliken–Walsh model have been reported which make use of the virial and Hellmann–Feynman theorems, respectively. Following the work of Nelander[27] on the virial theorem for triatomic molecules (which showed that at any given internuclear angle the total energy is equal to the negative of the kinetic as long as the bond distances are optimal for that angle), Takahata and Parr[28] suggested the use of the negative of the *orbital* kinetic energy as the quantity to be plotted in the Walsh diagrams. The result for H_2O is a correlation diagram quite unlike that given by Walsh for general AH_2 systems, but interestingly enough the authors were able to draw a close connection between this work and a different geometrical model given by Gillespie,[29] which in turn stems from the valence bond theory.[7]

The Hellmann-Feynman theorem has recently been used with some success by Coulson and Deb[30] in reproducing the important features of the Walsh diagrams of AH_2, AH_3, and A_2H_2 systems, but this treatment abandons any attempt to relate the quantities plotted in the Walsh diagrams to ionization potentials and/or electronic transition energies. Furthermore, the shapes of the curves in these Walsh–Coulson diagrams are found to be very dependent on the nature of the force field assumed in such calculations, unlike the case in many other investigations reported to this point, notably those using the canonical SCF orbital energies[21-24] in the diagrams. The basic problem with the use of the Hellmann–Feynman theorem for this purpose is (not at all surprisingly) seen to be the need for wave functions of very high accuracy in order to obtain reliable results. In any event this approach offers an interesting answer to the question of what is really plotted in the Walsh diagrams, but the practical significance of this observation cannot really be satisfactorily assessed until a broader range of applications is reported.[31]

3. *Self-Consistent Field Eigenvalues and Related Quantities*

As indicated in the previous subsection, a great number of the various attempts to obtain a quantitative realization of the MW geometrical model have centered upon the quantitative LCAO–MO-SCF method, which in turn is an outgrowth of Hartree–Fock theory.[32] Such emphasis is hardly surprising in view of the close connection between the aforementioned geometrical model and the original MO theory of Mulliken[33] and Hund,[34] yet there has been considerable question as to how best to relate the results of such quantitative treatments to the study of the MW model. This uncertainty is caused in large part by the existence of at least three types of SCF quantities which might in principle be associated with the ordinate in the original Walsh diagrams.

The first of these theoretical quantities to be discussed is the canonical orbital energy, which is the eigenvalue of the Fock matrix (as originally defined[32]) for a given eigenvector (MO). The main advantage of this quantity in the present context is its near equality with the negative of the ionization potential; in fact, it has been shown by Koopmans[35,36] that the ionization energy calculated by employing only the SCF MO's of the un-ionized system is *exactly* equal to the negative of the orbital energy of the MO from which ionization is taking place. Thus the canonical orbital energy can be regarded as an accurate measure of the relative stabilities of the constituent MO's of a given system and therefore would appear to satisfy the fourth and fifth criteria listed in section II.A.1 to a sufficiently good approximation.[37] In addition the first of these criteria, namely the requirement that correlation diagrams constructed from such quantities basically reproduce those given empirically by Walsh,[2] is also satisfied quite well by canonical orbital energies, as has been demonstrated in case after case (see Figure 2a for an example) for a quite large range of molecular systems. In addition the shapes of these orbital energy curves are found to be susceptible to the same types of interpretation as are their empirical counterparts, and the MO's to which they correspond are found to exhibit nearly the same constitution and symmetry properties as those discussed in the original MW model.

On the other hand, it is well known that the sum of the canonical orbital energies $\Sigma\epsilon_i$ is *not* equal to the true total energy of SCF (or Hartree–Fock) theory, and thus it is not at all obvious how the use of these quantities *by themselves* could lead to reliable geometrical predictions, since ultimately only the total molecular energy determines the molecular structure. The quantity ϵ_i itself can be expressed as (closed-shell case)

$$\epsilon_i = \langle i| -\tfrac{1}{2}\nabla^2 - \sum_a \frac{Z_a}{r_a} |i\rangle + \sum_j^{occ} \{2[ii|jj] - [ij|ji]\} \quad (1)$$

and thus represents the mean value of the kinetic and nuclear attraction energies (one-electron quantities) of an electron in orbital i as well as the repulsive energy of this electron in the averaged field of all the other electrons in the molecule (two-electron quantity). Summing the canonical orbital energies consequently leads to the correct total kinetic and nuclear attraction energies but takes account of each electron repulsion term twice; the correct total molecular energy E_T is thus obtained by subtracting the (total) electronic repulsion energy V_{ee} once and at the same time by adding the missing (total) nuclear repulsion V_{nn}, namely as

$$E_T = \Sigma\epsilon_i + V_{nn} - V_{ee} \quad (2)$$

In order to take account of this discrepancy between E_T and $\Sigma\epsilon_i$, Coulson and Neilson[18,19] suggested another set of quantities e_i defined as

$$e_i = (\epsilon_i + E_i)/2 \quad (3)$$

with

$$E_i = \langle i| -\tfrac{1}{2}\nabla^2 - \sum_a \frac{Z_a}{r_a} |i\rangle$$

which do sum to the total energy *less the nuclear repulsion term* V_{nn} (see also Parr[38]). Using the nonempirical SCF results of Ellison and Shull[39] for H_2O, these authors found that the correlation diagram constructed from the calculated e_i values closely resembles the empirical counterpart for a general AH_2 system, but, of course, they were forced to explicitly add the V_{nn} term to their orbital energy sum in their rationalization, a feature which is completely absent in the original model. Peyerimhoff and Buenker[23] subsequently constructed a correlation diagram from the e_i quantities calculated for F_2O, and from these results (Figure 2b) it is quite clear that the early success obtained for this type of orbital energy was based almost exclusively on the fact that V_{nn} for the approach of two hydrogen atoms in H_2O is a relatively insignificant term in the total energy *variation* of this system with *bending*. Addition of the E_i terms (see eq 3) to

the canonical orbital energies in an AB_2 system produces quantities which all uniformly *decrease* toward smaller internuclear angles (and increased nuclear attraction); as a result there can be no question that the e_i values of eq 3 are definitely *not* what are plotted in Walsh's diagrams, since they do not generally satisfy the first of the objective criteria cited above.

Still another set of SCF quantities of interest in this connection results from the use of a Fock operator different from that given in the original formulation of Hartree–Fock theory.[32] Davidson[40] has shown that the choice of operators used in obtaining the SCF solutions is, in fact, somewhat arbitrary and that, in particular, a whole class of modified Fock operators can be defined which lead to sets of canonical orbitals that differ by only a unitary transformation from the conventionally defined set[36] and hence result in *identical total energy* values. Advantage can be taken of this certain arbitrariness in the SCF formalism to construct a set of canonical orbitals whose associated eigenvalues do, in fact, sum to the true total energy E_T of a given system (these quantities will hereafter be referred to as the internally consistent SCF energies ϵ_i^{ICSCF}). They are defined in such a way that a specific portion of the $(V_{nn} - V_{ee})$ term of eq 2 is included in each of the conventional canonical orbital energies, so that in fact

$$E_T = \Sigma\epsilon_i^{ICSCF} \qquad (4)$$

At present little is known about the actual behavior of these quantities, although it is clear that *the advantage of summability to the total energy is obtained at the expense of identification with ionization potentials via* Koopmans' theorem. Nevertheless, if correlation diagrams constructed from these ϵ_i^{ICSCF} values do turn out to resemble quite closely those of the MW model, there would be good reason to assert that these quantities represent a quite satisfactory quantitative realization of the ordinates in the Walsh diagrams.

In lieu of such developments, however, there is still good reason to take a closer look at the conventional canonical orbital energies, especially in light of the fact that their failure to sum to the total energy does not in itself *preclude their use in making geometrical predictions.* The missing term $(V_{nn} - V_{ee})$ might, for example, be quite generally unaffected by structural changes, in which case it would be of no greater significance for obtaining geometrical predictions than is the choice of a zero of energy for the potential curves. Or perhaps the entire question of using the sum of the orbital energies as a substitute for the total molecular energy might represent an unnecessary restriction placed upon the behavior of the ordinate in such diagrams in the first place, introduced merely because of an improperly rigid view of how to translate the methodology for the MW model into purely mathematical terms.

B. How to Use the Canonical Orbital Energies in the Mulliken–Walsh Model

1. *Molecular Geometry and* $\Sigma\epsilon_i$

The fact that the canonical orbital energy sum $\Sigma\epsilon_i$ cannot be equated with the total molecular energy E_T does not in itself preclude the possibility that these two quantities may *vary* in a *parallel* fashion with various structural changes and hence lead to identical predictions of the equilibrium geometries for whole classes of molecular systems. Clearly the key relationship to be considered for this purpose is not that of eq 2 but rather some differential form thereof

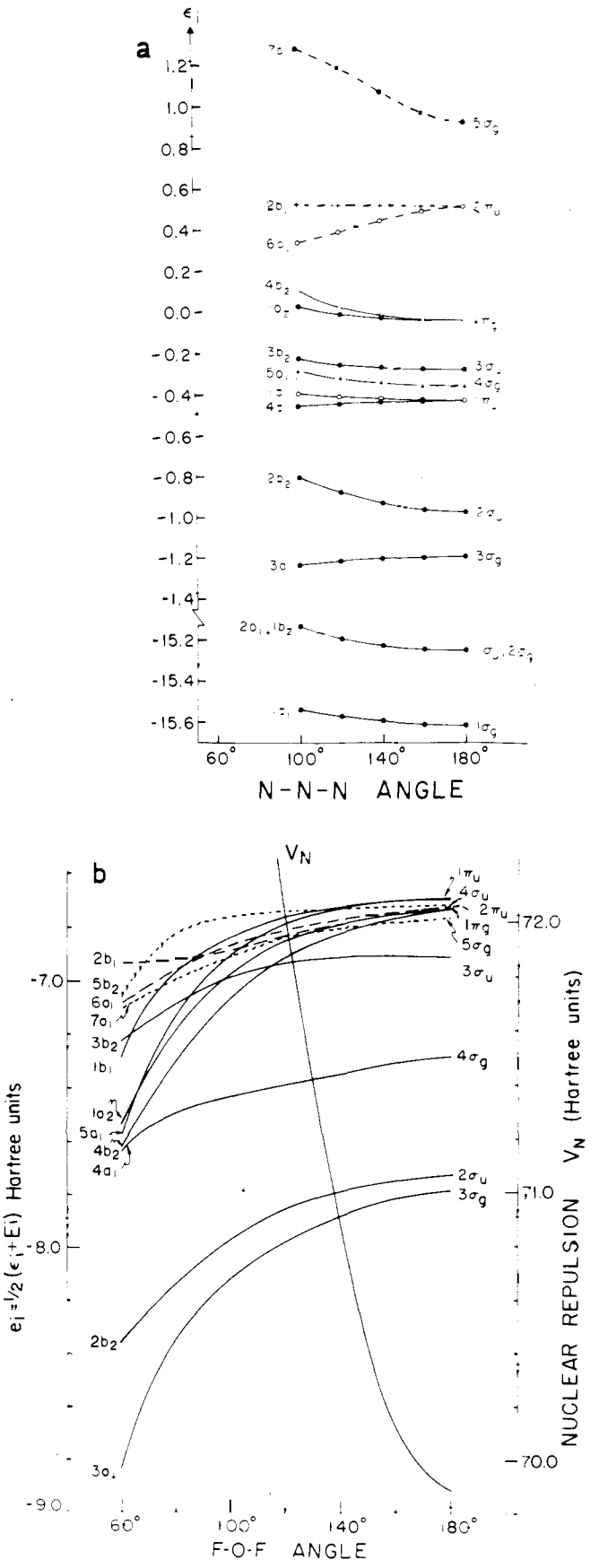

Figure 2. Angular correlation diagram (a) for an AB_2 molecule (plotted are the canonical orbital energies of the N_3^- ground state as a function of the internuclear NNN angle[24]), and related diagram (b) for F_2O constructed from the one-electron quantities e_i as suggested by Coulson and Neilson.[18,19] Throughout this paper all energy values are given in hartrees, unless stated otherwise.

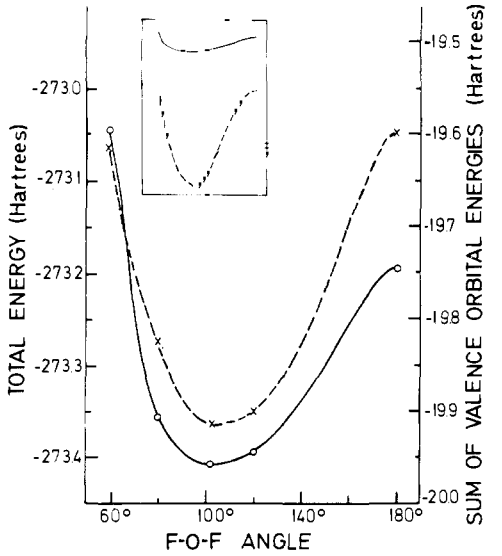

Figure 3. Total SCF energy (solid line) and sum over canonical valence orbital energies $\Sigma\epsilon_i$ (dashed line) for F_2O as a function of internuclear angle.[23] The insert shows in a schematic way a comparison between the calculated canonical $\Sigma\epsilon_i$ (again dashed line)[23] and corresponding Hückel $\Sigma\epsilon_i^H$ (solid line).[26]

$$\partial E_T/\partial R = \partial\Sigma\epsilon_i/\partial R + \partial(V_{nn} - V_{ee})/\partial R \qquad (5)$$

where R is some generalized geometrical variable. If the derivative of the term $(V_{nn} - V_{ee})$ were of negligible magnitude for a sufficiently large range of R values in the neighborhood of equilibrium, the shape of the $\Sigma\epsilon_i$ curve would parallel very closely that of the total (SCF) energy in that region and therefore would be for all practical purposes of *equal* value in obtaining the desired geometrical predictions.

A cancellation of errors in neglecting *both* the derivatives of nuclear (V_{nn}) and electronic (V_{ee}) repulsion in eq 5 would clearly justify the use of $\Sigma\epsilon_i$ as the quantity upon which the predictions of the MW model are ultimately based, provided, of course, that it occurred under quite general circumstances. Leclerc and Lorquet[25] spoke of just such a cancellation in their early work, pointing to the success of Boer, Newton, and Lipscomb[41] in approximating atomization energies with the quantity $\Sigma\epsilon_i^a - \Sigma\epsilon_i^m$ (difference of the canonical orbital energy sum in the molecule m and in the separated atoms a). At about the same time, the present authors in collaboration with Allen[21] attempted to clarify this possibility further by introducing several rather obvious inequalities as conditions for the sufficiency of the canonical orbital energy sum in predicting equilibrium geometries, which may be summarized as

$$\left|\frac{\partial}{\partial R}(V_{nn} - V_{ee})\right| \leq \left|\frac{\partial}{\partial R}(\Sigma\epsilon_i)\right| \qquad (6)$$

If this inequality is satisfied everywhere within a sufficiently large interval containing the equilibrium position[42] of R, then it follows that the *slopes* of corresponding E_T and $\Sigma\epsilon_i$ curves have the same sign at every point within this interval (see eq 5) and hence *vanish for identical R values*, as is, of course, required if $\Sigma\epsilon_i$ is to lead to the same geometrical predictions as E_T. Satisfaction of this inequality clearly does not mean, however, that the $\Sigma\epsilon_i$ and E_T curves are parallel, as is necessary if other potential quantities such as force and anharmonicity constants are also to be accurately predicted strictly on the basis of $\Sigma\epsilon_i$. In order to be even more consistent with the MW model, eq 6 can be modified so that only the valence orbital energy sum $\Sigma^{val}\epsilon_i$ is used

$$\left|\frac{\partial}{\partial R}(V_{nn} - V_{ee} + \sum^{core}\epsilon_i\right| \leq \left|\frac{\partial}{\partial R}(\sum^{val}\epsilon_i)\right| \qquad (7)$$

where $\Sigma^{core}\epsilon_i$ is merely the difference between the sum of all canonical orbital energies and that of the valence orbital energies only.

While it is obvious that the inequalities of eq 6 and 7 cannot be expected to hold in the region in which the orbital energy sum derivative vanishes (unless, of course, the repulsion derivative vanishes at exactly the same value of R, *i.e.*, perfect agreement with $\partial E_T/\partial R$ at R_0 is obtained), this fact in itself cannot be construed as *proof* that these inequalities are not obeyed to a *sufficiently good approximation* so as to effectively explain the basis for the general success of the MW model in such geometrical studies. To delve into this matter more carefully, it is necessary to test the foregoing inequalities numerically, and this has been done by means of a fairly large series of *ab initio* SCF calculations.[21-24] The results were encouraging for AH_2 and AH_3 molecules,[21] for which the $\Sigma\epsilon_i$ and E_T curves not only show *minima* at very nearly the *same internuclear angle* θ_0 but also exhibit very nearly parallel behavior in very wide regions in the neighborhood of θ_0; on the other hand, the results of earlier investigations[11-13,15-17] cautioned against optimism on this point until similar results could be obtained for larger systems. Yet analogous calculations by the present authors[23] for the nonhydrogenic system F_2O again found quite satisfactory agreement between the shapes of angular $\Sigma^{val}\epsilon_i$ and E_T curves, as can be seen from Figure 3. At the same time it was noted that the *calculated correlation diagrams* for both the aforementioned hydrogenic systems and the various AB_2 systems considered (obtained using the canonical orbital energies as ordinates in the theoretical plots) bear strong resemblance to the corresponding Walsh diagrams (see Figure 2a, for example).

Nevertheless, faith in the cancellation-of-errors axiom began to dwindle quickly when still more numerical data became available. Analogous calculations for ground and certain closed-shell (SCF) excited states of ozone[24] do not lead to uniformly parallel relationships between corresponding $\Sigma^{val}\epsilon_i$ and E_T angular potential curves (Figure 4a,b). Although a clear resemblance can be seen between corresponding curves for some of the states, the potential surface for the interesting cyclic state of ozone (curves labeled 3 in Figure 4a,b) is reproduced very badly by $\Sigma^{val}\epsilon_i$. A similar result has been obtained[24] for certain states of the azide ion N_3^-. Yet, even in the cases where large discrepancies in the two types of potential curves are found to occur for O_3 and N_3^-, it must be pointed out that the $\Sigma^{val}\epsilon_i$ data clearly distinguish bent from linear structures (curve 3 in Figure 4b merely fails to show a minimum at small angles, for example, and thus, in fact, only overestimates the tendency toward bent geometry in this electronic state), and it could, of course, be argued that the MW model itself is not capable of providing more accurate *quantitative* information. Nevertheless, it is clear that the inequalities of eq 7 (and also of eq 6) are violated in such exceptional cases, and this fact by itself raises serious questions about the wisdom of employing $\Sigma\epsilon_i$ or $\Sigma^{val}\epsilon_i$ as a substitute for the total energy in trying to explain the validity of the empirical model under consideration.

Further numerical applications did not result in any lessening of concern in this regard as violation of the inequalities of eq 6 and eq 7 began to occur with greater and greater frequency. In studying the potential surface of diborane[22] B_2H_6 in going from an umbrella ethane-like geometry to its preferred bridged structure, for example, it is found that the $\Sigma^{val}\epsilon_i$ curve is initially arched upward

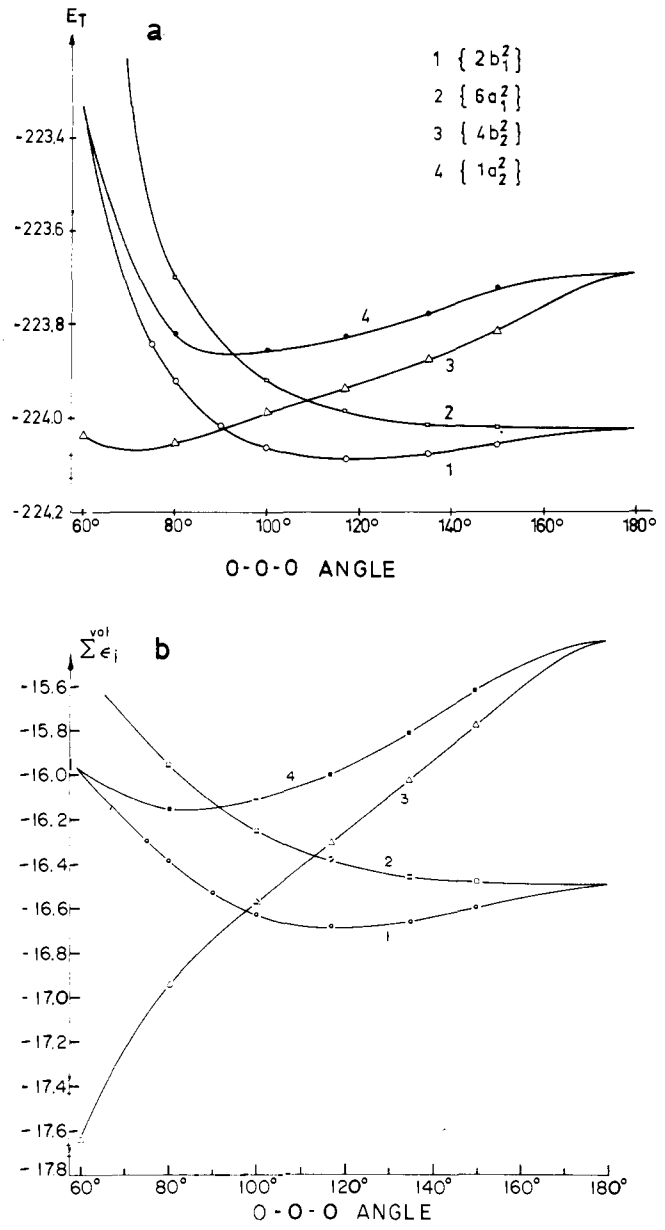

Figure 4. Total SCF energy E_T (a) and corresponding sum over canonical valence orbital energies $\Sigma\epsilon_i$ (b) for various $^1A_1$ states of ozone as a function of the internuclear OOO angle. (The notation $\{2b_1^2\}$, for example, indicates that of the four MO's $2b_1$, $1a_2$, $6a_1$, $4b_2$, only the $2b_1$ is *not* doubly occupied.)

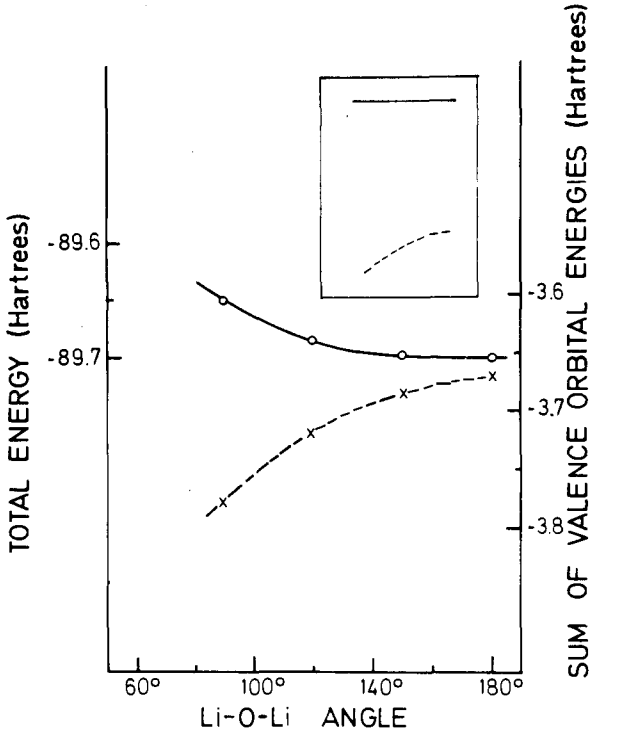

Figure 5. Total SCF energy (solid line) and sum over canonical valence orbital energies $\Sigma\epsilon_i$ (dashed line) for Li_2O as a function of the internuclear angle.[23] The insert shows in a schematic way a comparison between the calculated canonical $\Sigma\epsilon_i$ (again dashed line) and corresponding Hückel $\Sigma\epsilon_i^H$ (solid line).[26]

(see Figure 12 of ref 22) before dropping quite sharply toward the equilibrium geometry, whereas the corresponding SCF total energy curve shows a monotonic (and much more gradual) decrease throughout the entire geometrical deformation, in obviously better agreement with the actual experimental situation. In this case the discrepancy occurs for geometrical changes in a molecular ground state and thus would seem to rule out the possibility that such disagreement between $\Sigma\epsilon_i$ and E_T variations occurs only for excited SCF states.

Even more critical is the finding that in a few cases $\Sigma^{val}\epsilon_i$ angular potential curves cannot even correctly predict whether the preferred molecular geometry is *linear* or *bent*. Calculations[23] on Li_2O find that while the SCF total energy curve correctly predicts a linear equilibrium structure, the corresponding $\Sigma^{val}\epsilon_i$ species shows a maximum for this nuclear arrangement (Figure 5). This result is not so surprising in light of the fact that the conventional application of the MW model itself *incorrectly* predicts the equilibrium geometry of this system, since it obviously has the same number of valence electrons as water H_2O and hence should be thought to possess a bent structure similar to that of the dihydride.

Another example was soon found, however, which shows that $\Sigma^{val}\epsilon_i$ can make an incorrect prediction of equilibrium angle even where the MW model is apparently in complete agreement with experiment. The first hint that such a situation actually exists came from the study of hypofluorous acid[23] FOH whose E_T and $\Sigma^{val}\epsilon_i$ curves are compared in Figure 6. The fact that the valence orbital energy sum greatly overestimates the tendency toward bent geometry for this system raised considerable doubts as to whether this trend could be reversed for HAB systems with four less electrons such as hydrogen cyanide HCN, which is well known to be linear. Speculation that the $\Sigma^{val}\epsilon_i$ curve for HCN might still lead to the correct prediction of a linear geometry for this system was certainly *not* supported by the fact that the sum of FOH valence orbital energies *weighted according to the orbital population in HCN* (that is, for isoelectronic FOH^{4+}) is also found to decrease from the linear geometry, although the resulting curve is decidedly *less steeped* in this direction than that of the full FOH valence orbital energy sum shown in Figure 6. Subsequently Pan and Allen[43] showed that even if the HCN $\Sigma^{val}\epsilon_i$ curve is calculated on the basis of SCF results obtained explicitly for this system, the curve still fails to show a minimum for the linear geometry actually preferred experimentally, even though, just as in the case of our results[23] for Li_2O, the SCF total energy itself does show the correct behavior.

To this point it should be quite clear that one cannot rely with certainty on the satisfaction of the inequalities of eq 6 and 7 in the general case, although it must be said that on the whole there are many more cases in which $\Sigma^{val}\epsilon_i$ and E_T *angular* potential curves show roughly parallel behavior than in which they do not. Rath-

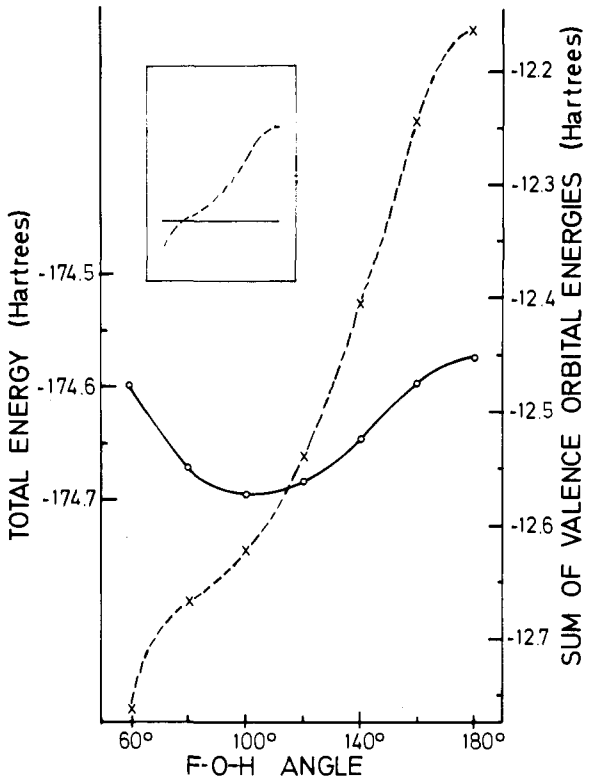

Figure 6. Total SCF energy (solid line) and sum over canonical valence orbital energies $\Sigma\epsilon_i$ (dashed line) for FOH as a function of the internuclear angle.[23] The insert shows in a schematic way a comparison between the calculated canonical $\Sigma\epsilon_i$ (again dashed line) and corresponding Hückel $\Sigma\epsilon_i^H$ (solid line).[26]

er than to present evidence for the latter qualification, however, it seems much more pertinent to move away from the subject of internuclear angle predictions to discuss the equally important topic of bond distance determinations, especially since there is good reason to believe that the cancellation-of-error inequalities of eq 6 and 7 are, in fact, *never* satisfied for potential curves of this type.

A series of calculations carried out by the present authors and Whitten[44] for the purpose of studying this latter point shows that in each of the cases of CO_2, BeF_2, NH_2^+, BH_2^-, BH_2^+, BH_3, and CH_3^+ the sum of valence orbital energies decreases with bond contractions long after the corresponding total energy has reached its minimum at the position of equilibrium (see Figure 7 for the CO_2 results). In fact, none of the calculated $\Sigma^{val}\epsilon_i$ curves shows a minimum anywhere in the bond distance regions considered, and in most cases their downward slopes are observed to become even greater as the nuclei come still closer together.

The underlying cause for this behavior is not at all difficult to understand once the relationship between derivatives of the total energy E_T and the sum of canonical orbital energies $\Sigma\epsilon_i$ is considered (eq 5). The magnitude of the $(V_{nn} - V_{ee})$ derivative is not at all negligible in the case of bond stretching, far outweighing that of $\Sigma\epsilon_i$, in fact, and as a result the inequalities of eq 6 and 7 are clearly not satisfied. The physical meaning behind this statement is merely that the repulsion of the nuclei, which are fixed in the calculations at each internuclear distance because of the Born–Oppenheimer approximation, increases much faster with decreasing R than does the total repulsion between the electrons, whose distribution is continually adjusted as the nuclei approach each other.

In summary then, it is quite clear from the foregoing discussion that the question of whether the total SCF energy E_T and the sum of the (conventional) canonical orbital energies $\Sigma\epsilon_i$ (or $\Sigma^{val}\epsilon_i$) vary *in general* with some geometrical distortion in a nearly parallel manner *cannot be answered in the affirmative.* And yet it has always been possible to use the canonical orbital energies to draw the same types of *qualitative* conclusions about variations in geometry with the number of electrons that have clearly been the most attractive feature of the MW model, simply because *correlation diagrams constructed from these quantities invariably resemble quite closely those given empirically.* The question is thus whether the utility of the canonical orbital energies in discussing various aspects of molecular geometry has simply been obscured by a decided overemphasis upon the prospect of establishing a close relationship between the *sum of the ordinates* in the Walsh diagrams, on one hand, and the truly legitimate potential quantity in the SCF method, on the other, namely the total molecular energy E_T. To answer this question, it is necessary to reexamine the physical significance of the canonical orbital energy itself as suggested by the consequences of Koopmans' theorem.

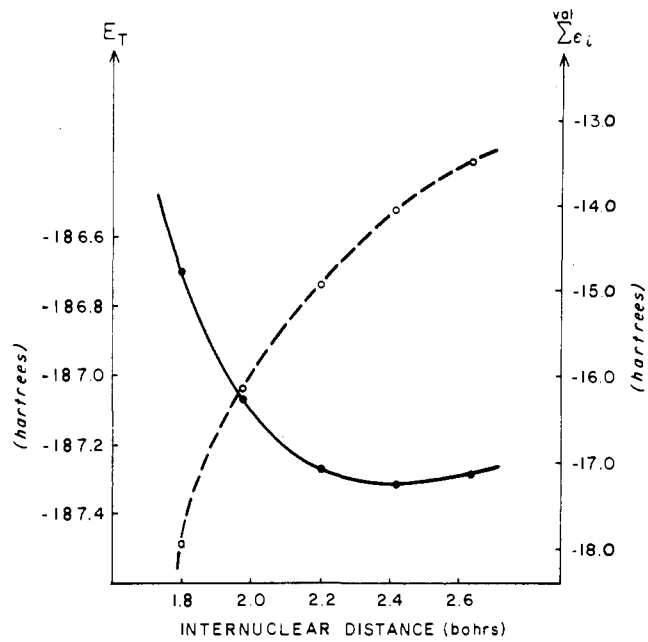

Figure 7. Total SCF energy E_T (solid line) and sum over canonical valence orbital energies $\Sigma\epsilon_i$ (dashed line) for CO_2 as a function of the internuclear CO distance.[44]

2. *Molecular Geometry and Koopmans' Theorem*

The aforementioned calculations of bond-stretching potential curves for various polyatomic molecules[44] illustrate most emphatically that the quantity $\Sigma\epsilon_i$ is by itself a hopelessly poor indicator of equilibrium bond distances. Yet even though neither Mulliken[1] nor Walsh[2] included stretching correlation diagrams *explicitly* in their original papers, some very definite information for understanding trends in the bond distances of various classes of systems is unquestionably available from their general model; indeed, the whole idea of relating geometrical trends to electron orbital populations had its origin in the study of bond distances, notably those of diatomic molecules.[33] Some of the very first applications of the molecular orbital theory of Mulliken and Hund made use of the fact that σ_g and π_u MO's in homonuclear diatomics are bonding (and hence have orbital energies which decrease with approach of the nuclei) while those of σ_u and π_g type are antibonding. Successive occupation of *bonding* MO's, as occurs in going from Be_2 to N_2, is directly responsible for the observed regular *decrease in*

equilibrium bond length (and also increase in binding energy) through this series while the opposite trend in going from N_2 to the mythical Ne_2 system can be attributed similarly to the successive occupation of *antibonding* MO's. Perhaps more interesting in the present context is the corollary observation that the bond lengths of ions relative to those of the corresponding neutral systems can be predicted by the same type of analysis; this fact can easily be proven in a straightforward manner[44] on the basis of Koopmans' theorem and hence by means of *canonical orbital energies*.

According to Koopmans' theorem the (SCF) total energy E_T of the various positive ions of a given system A is directly related to the total energy of A itself and the canonical orbital energy ϵ_D of the MO ψ_D from which ionization takes place.

$$E_T(A) = E_T(A^+) + \epsilon_D \tag{8}$$

In this relationship the same set of MO's is used in the wave functions of both A and A^+; the quantity ϵ_D is calculated in the field of A. Experience has generally shown that such relationships hold to a rather good approximation in comparison to experimental measurements of ionization potentials, but since the main interest in the present discussion is geometry, this result in itself is not *directly* relevant. But it certainly becomes relevant upon differentiation of the previous equation with respect to some geometrical variable R, namely

$$\partial E_T(A)/\partial R = \partial E_T(A^+)/\partial R + \partial \epsilon_D/\partial R \tag{9}$$

From this equation it is clear that the term $\partial \epsilon_D/\partial R$ represents, at least *within the approximation of Koopmans' theorem*, the difference in the respective slopes of the total energy curves of A and A^+ *at any value of the geometrical variable* R; consequently, knowledge of the *variation* of the canonical orbital energy ϵ_D with R can be combined with analogous information for the total energy of A to give an estimate *for the potential energy curve of the corresponding positive ion.*

The quantitative relationship of eq 9 is totally consistent with the aforementioned qualitative interpretations by Mulliken and Hund with respect to bond length magnitudes based on the bonding or antibonding characteristics of differentiating orbitals. If ψ_D is a bonding orbital, its canonical orbital energy ϵ_D decreases with diminishing R, and hence $\partial \epsilon_D/\partial R > 0$. Ionization from such an orbital requires according to eq 9 that $\partial E_T(A)/\partial R$ also be positive when evaluated at the equilibrium position $R_0(A^+)$ of the ion, at which point, of course, $\partial E_T(A^+)/\partial R$ vanishes; in other words

$$\partial E_T(A)/\partial R|_{R_0(A^+)} > 0 \text{ if } \psi_D \text{ is bonding} \tag{10}$$

If the curvature of $E_T(A)$ is greater than zero at $R_0(A^+)$ [as it invariably is since such a region is also in the neighborhood of a *minimum*[42] of $E_T(A)$], eq 10 implies in turn that $\partial E_T(A)/\partial R$ vanishes at a smaller value of R than $R_0(A^+)$; thus

$$R_0(A) < R_0(A^+) \text{ if } \psi_D \text{ is bonding} \tag{11a}$$

The reverse order is obtained if ionization occurs from an antibonding orbital defined by $\partial \epsilon_D/\partial R < 0$; *i.e.*

$$R_0(A) > R_0(A^+) \text{ if } \psi_D \text{ is antibonding} \tag{11b}$$

Similarly it can be concluded that the greater the bonding or antibonding character of the differentiating orbital (as measured by $\partial \epsilon_D/\partial R$) the greater the expected difference between equilibrium bond distance values of the original and the ionized systems, respectively.

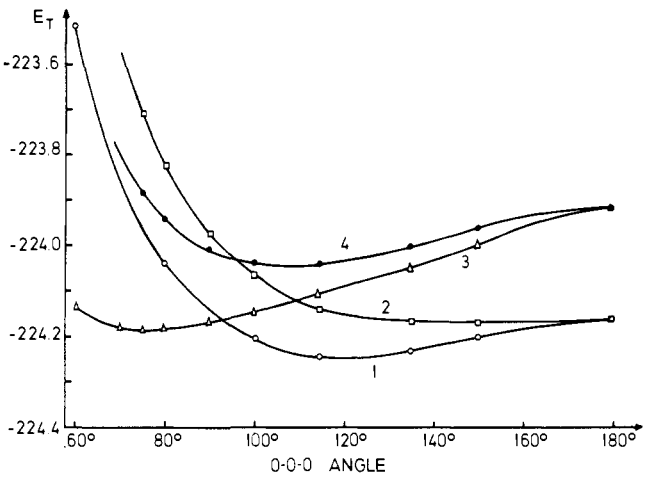

Figure 8. Angular potential curves for the four $^1A_1$ states of ozone considered in Figure 4a constructed *via* Koopmans' theorem. (The states 2, 3, 4 are constructed from the 1-state of O_3, the 1-state itself from the original 3-state in Figure 4a; the absolute values are adjusted.)

To this point the discussion has been restricted to relationships between singly positive ions and the corresponding un-ionized species, but if one continues to assume that the *same set of MO's* can be used to calculate the potential curves of both A and A^+ and also *makes the additional assumption* that the shapes of corresponding canonical orbital energy curves are the same for both these entities, it is clear that eq 9 can be generalized to account for geometrical changes in *multiple ionizations* as well. To accomplish this goal it is only necessary to substitute A^{2+} for A^+ and A^+ for A in eq 9 for the next stage of ionization and then proceed in a completely analogous manner for still greater reductions in the number of electrons in this system. Furthermore, the same pair of assumptions enables one to draw relationships between potential curves of the various *negative ions* of A, in which case it is only necessary in the first stage to substitute A^- for A and A for A^+ in eq 9. Finally, since literally *any electronic configuration* in *any stage of ionization* can be obtained by successive addition and/or deletion of electrons from an appropriate series of molecular orbitals, one easily concludes that *as long as both of the aforementioned assumptions are valid* that the geometry of any excited state of the original system can be deduced by means of *successive application of eq 9.* If, on the other hand, the MO's of the two states being compared are greatly different or if their corresponding orbital energy curves have significantly different shapes, then it must be expected that such a straightforward use of eq 9 will not be adequate for the prediction of the desired relationships; nevertheless, the very success of Mulliken and others in applying these concepts of molecular orbital theory *on a qualitative basis* suggests that such situations fortunately occur only rather infrequently.

Thus far the mathematical treatment has been confined to deductions relative to the structure of the positive (and negative) ions of the *same* molecule, but it is clear that the relationships derived are of much more general significance because of the basic precept of the MW model (and indeed MO theory in general) that *isoelectronic molecules belonging to the same family exhibit similar equilibrium structures.* If therefore one wishes to compare the geometry of system B with n−m electrons to that of system A containing n, it is only necessary (according to the model) to obtain an estimate of the pertinent potential curve of the m-th positive ion of A by *successive application* of the differential form of *Koopmans'*

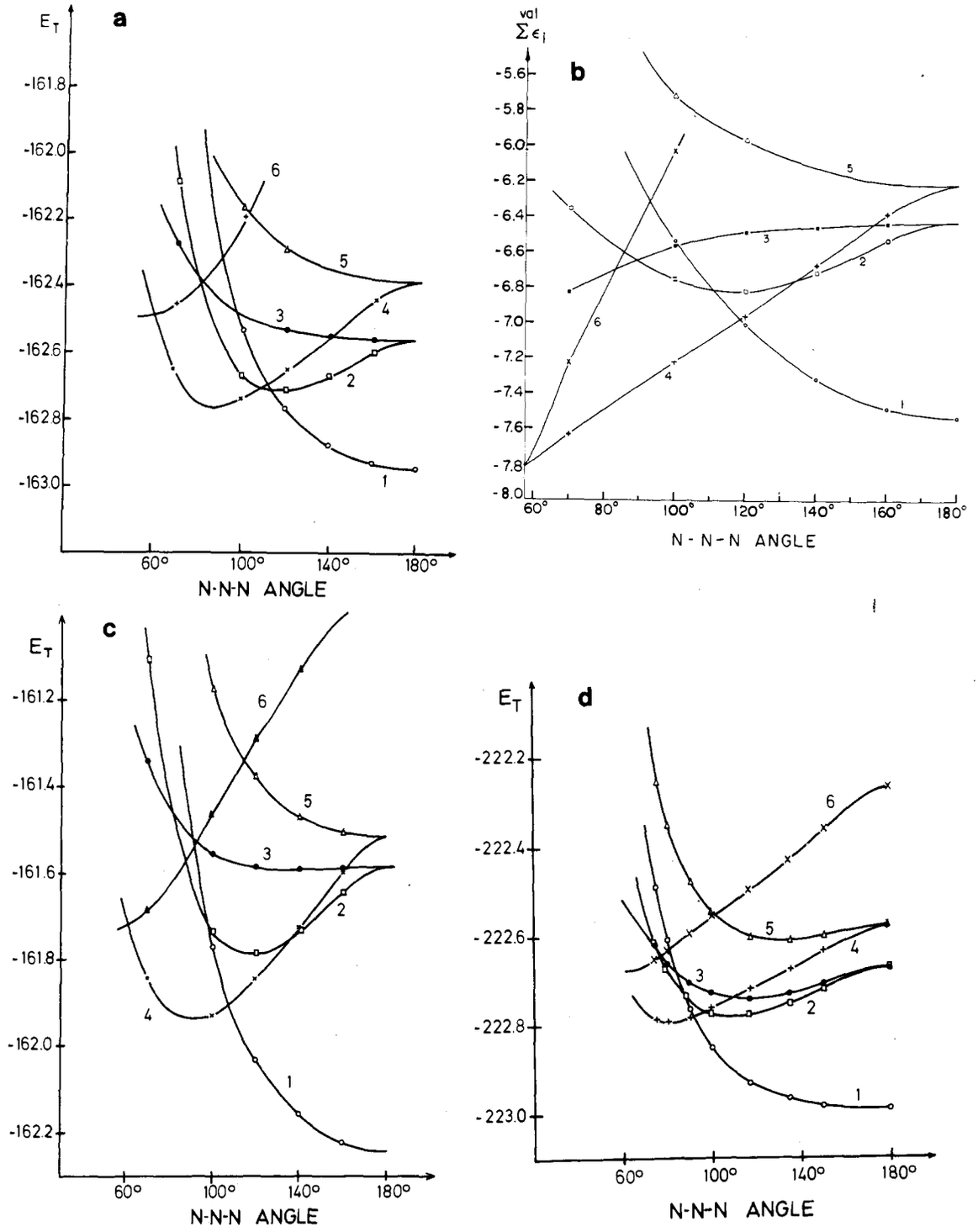

Figure 9. Angular potential curves for six different $^1A_1$ states of N_3^-: (a) calculated total SCF energy E_T; (b) calculated sum over canonical valence orbital energies $\Sigma\epsilon_i$; (c) calculated *via* Koopmans' theorem from N_3^- states; (d) calculated *via* Koopmans' theorem from an O_3 state.

theorem (eq.9). Such a procedure is *hopelessly inadequate* for predicting *the total energy* of B *on an absolute scale*, but in the great majority of cases it will be seen to lead to a *quite reasonable approximation* for the *variation* of E_T *with* a *given geometrical variable*, the only information required for determination of equilibrium geometry (and also associated spectroscopic constants). Furthermore, the same type of reasoning can be used to deduce potential curves for *molecular excited states* merely by adding or subtracting appropriate canonical orbital energies weighted according to their population in the electronic configurations being compared.

To illustrate how these ideas can be applied in practice, the various potential curves discussed in the previous subsection will be considered again, with particular emphasis on those cases for which corresponding E_T and $\Sigma^{val}\epsilon_i$ curves have quite different appearance. In the first example shown in Figure 8, the angular potential curves for various closed-shell states of ozone are constructed by successive application of Koopmans' theorem based on the SCF results of a single O_3 state, as discussed in the preceding paragraph; for easier comparison with the corresponding E_T and $\Sigma^{val}\epsilon_i$ curves their position on the energy scale has been adjusted. It is

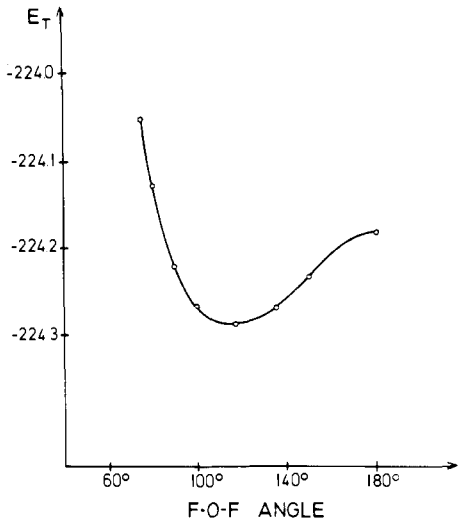

Figure 10. Angular potential curve for the ground state of F_2O calculated *via* Koopmans' theorem from an O_3 state. This potential curve should be compared with the actual SCF counterpart given earlier (Figure 3).

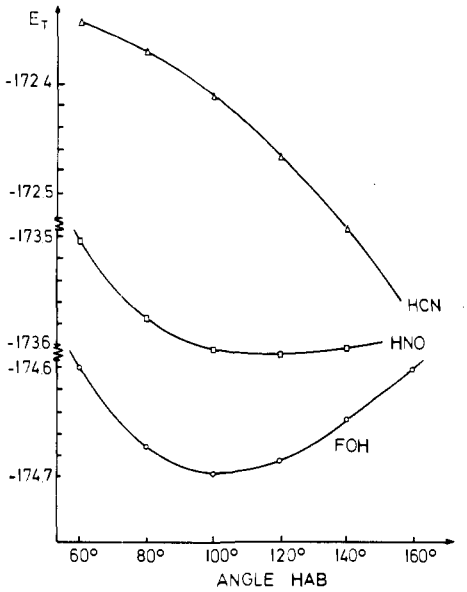

Figure 11. Angular potential curves for the ground states of HCN and HNO constructed *via* Koopmans' theorem from the calculated ground-state SCF curve of FOH also given.

seen that the shapes of these curves are in every case very similar to those of the corresponding total energy curves of Figure 4a; in particular, contrary to the case of the $\Sigma^{val}\epsilon_i$ plot, the Koopmans' theorem curve for the cyclic state of ozone (labeled 3 in all pertinent figures) is seen to resemble quite closely its corresponding E_T species.

A similar comparison is made in Figures 9a–d for six states of N_3^-. In Figure 9c the various N_3^- states have been constructed *via* Koopmans' theorem from the total energy and the corresponding canonical orbital energies of an N_3^- state, while in Figure 9d the necessary E_T and ϵ_D data have been taken for the same purpose *from the calculation of the ozone ground state.* Both sets of Koopmans' theorem potential curves are clearly superior approximations to the corresponding E_T species (Figure 9a) than is that obtained using $\Sigma^{val}\epsilon_i$ (Figure 9b) for each N_3^- state. To be sure some small discrepancies between corresponding curves (particularly in no. 3 and 5) can be noted between Figures 9c–d and Figure 9a, but it will be shown subsequently that even these distinctions are not inconsistent with the predictions of the MW model. The ground-state E_T and ϵ_i curves of O_3 have also been used to obtain a potential curve for F_2O (or O_3^{2-}), which is shown in Figure 10 for comparison with corresponding E_T and $\Sigma^{val}\epsilon_i$ data given earlier in Figure 3. Again the agreement between *Koopmans' theorem* and *SCF total energy* angular potential curves is quite good, although in this case the corresponding $\Sigma^{val}\epsilon_i$ species also approximates the E_T curve very satisfactorily.

The HAB molecules FOH and HCN provided another interesting example for which the $\Sigma^{val}\epsilon_i$ quantity fails to even approximately reproduce the behavior of the corresponding SCF total energy curve, as has been discussed in section II.B.1. If one uses Koopmans' theorem (eq 9) in connection with the SCF E_T and ϵ_i results for FOH in order to construct an angular potential curve for HCN, the result is seen to be quite different (Figure 11), however; these calculations correctly predict both the *linear geometry of HCN and the nonlinear nuclear arrangement known for HNO.* The use of Koopmans' theorem also corrects the problem noted earlier in connection with the $\Sigma^{val}\epsilon_i$ potential curve for distortion of diborane from its equilibrium bridged structure to an ethane-like umbrella nuclear conformation. Furthermore, it is even successful in predicting trends in equilibrium *bond distances* in AB_2 systems on the basis of the aforementioned SCF results[44] for CO_2 symmetric stretch potential curves.

It does not, of course, add anything new to the question of why Li_2O is linear and water is bent because the *valence electron populations* in both of these systems (at least formally) are *identical.* It is also of no help in explaining the significant differences between the bond lengths in CO_2 and BeF_2 (R_{CO} = 1.162 Å, R_{BeF} = 142 Å), since both systems possess identical ground-state electronic configurations. The important point in this connection, however, is that the MW model itself, at least in its simplest form in which a single correlation diagram is used for *all* systems in a given family, is not able to explain these distinctions either, since it merely *assumes that systems in the same class of molecules possessing identical electronic configurations should exhibit approximately the same equilibrium nuclear geometries.* In fact, even in the cases of curves no. 3 and 5 in Figures 9a–d for N_3^-, in which corresponding total energy and Koopmans' theorem potential curves disagree as to the favored nuclear conformation in the associated excited states, a closer look at the predictions which must be made on the basis of the pertinent Walsh diagram shows that the empirical model either leads one to expect the same answer *given by the Koopmans' theorem* analysis or is *not able to make any clear judgement either way.*[45] Thus it is seen that *once the thesis of substituting* $\Sigma^{val}\epsilon_i$ *for the (SCF) total energy is abandoned and emphasis is placed instead on the role of Koopmans' theorem in deducing the desired geometrical relationships, use of SCF canonical orbital energies is able to produce a convincing quantitative realization of the original MW model,* succeeding in its predictions whenever its qualitative counterpart has been successful, failing when it has not.

The close connection found to exist between Koopmans' theorem and the MW model can be of considerable advantage in clarifying the logical framework underlying this empirical scheme. Its basic premise may be summarized in terms of a schematic diagram in which all the systems in a given molecular family (at least in their ground states) are classified according to the number of valence electrons they contain; each combination of nuclei is represented by a *vertical column* in such a table while *complete sets of isoelectronic systems* (of the same electronic configuration) with different nuclear

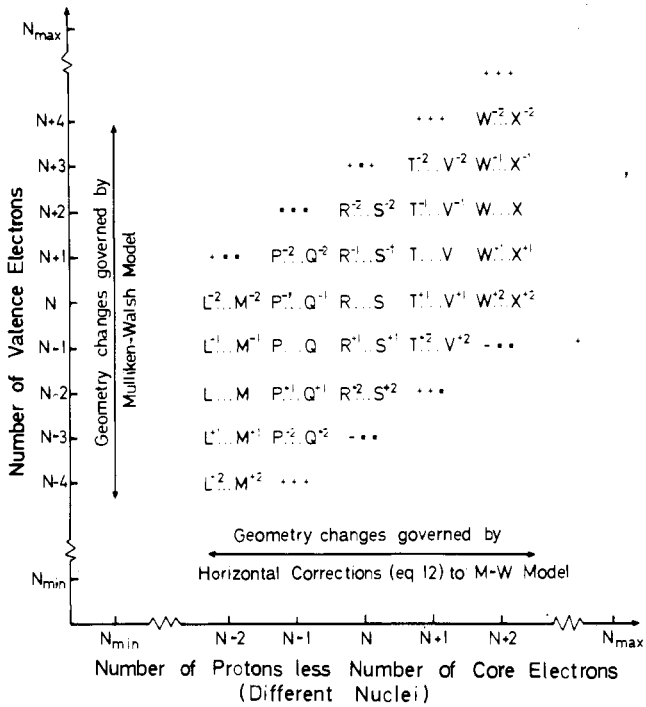

Figure 12. Schematic diagram arranging the various systems in a given molecular family according to the number of protons (less the number of core electrons) and the number of valence electrons each contains. Isovalent systems with the same formal charge (such as CO_2 and BaF_2) are grouped in the same column (and the same row). Ionic series such as N_3^+, N_3, N_3^-, etc., corresponding to vertical columns of the figure and structural differences between such systems are found to be governed quite well by the differential form of Koopmans' theorem (eq 9). Geometrical distinctions between isovalent systems (with identical electronic configurations) are governed by the secondary principle of eq 12, which takes account of differences in the AO composition of corresponding MO's in such species (hence referred to as a horizontal correction). In principle then, all differences in equilibrium geometry between any pair of systems in such a family can be ascertained by appropriate application of eq 9 and/or eq 12, as indicated by the respective location of each of these species in the diagram.

framework are located in the *same row* of this diagram (as, for example, in Figure 12). *Geometrical changes within a column* of the table (that is, among the ions of a given system) *are controlled almost exclusively by the operation of the appropriate differential form of Koopmans' theorem* (eq 9); horizontally *across a given row* it is merely assumed that *no significant changes are possible*. The latter assumption seems to hold to a very good degree if bonding in the systems being compared is of nearly equal covalency, but, on the other hand, it is apparently likely to fail if comparison is made between a largely ionic species and one possessing considerable covalent character (as, for example, in the case of Li_2O and water and also that of CO_2 and BeF_2). It was recognized by Mulliken and Walsh that such a simplified view of the trends which occur in molecular geometries cannot be expected to hold quantitatively, but it nevertheless represents an elementary principle which satisfactorily explains (albeit only qualitatively) a broad range of geometrical phenomena and at the same time provides a starting point from which more detailed theoretical investigations into this question may proceed.

3. *Toward a Horizontal Correction for the Mulliken–Walsh Model*

The geometrical trends predicted by the MW model are borne out to a very high degree by actual experimental observations, and this fact has provided the primary motivation in obtaining a quantitative realization for this simple theory. Nevertheless, it is clear that certain aspects of the model are oversimplified, particularly the principle that all members in a given class of molecules which possess *identical electronic configurations* should exhibit nearly equivalent equilibrium geometries. The available experimental evidence (see Table I) indicates on the contrary that isovalent systems with widely differing bonding characteristics such as Li_2O and water or CO_2 and BeF_2 do possess significantly different ground-state equilibrium geometries.

What is obviously needed then to improve the precision of the model is some supplementary principle which isolates the essential causes for differences in the geometries of such isovalent systems whenever they are found, and one which is also capable of predicting both the direction and the rough magnitude of such changes from one system to another; in terms of the diagram in Figure 12 we will speak of this desired principle as a *horizontal correction* to the MW model. Certainly one possible means of achieving this goal is to attempt to predict *differences in the correlation diagrams* of such isoelectronic systems, as Walsh, in fact, suggested in his original presentation,[2] but such a procedure obviously seems best suited for the use of orbital energy quantities whose sum varies in an exactly parallel manner as the corresponding (SCF) total energy; use of the conventional SCF canonical orbital energies, on the other hand, requires that the $(V_{nn} - V_{ee})$ term in the total energy expression of eq 2 be given simultaneous consideration.

It seems reasonable to assume that if a normally ionic system such as Li_2O were forced to maintain a charge distribution roughly equivalent[46] to that of some covalent species such as water, the differences in preferred geometries for the two systems would all but disappear. In such a constrained charge distribution (model distribution), the total energy E_T^0 could then be written as

$$E_T^0 = \Sigma\epsilon_i^0 + V_{nn} - V_{ee}^0 \qquad (2')$$

Clearly all terms in this expression for a given nuclear arrangement will in general possess different values from the corresponding quantities in eq 2 for the *optimal* (actual) charge distribution of this system in exactly the same geometry, with the obvious exception of the nuclear repulsion V_{nn} (hence no superscript for this quantity in eq 2'). Subtracting eq 2' from eq 2 therefore succeeds in eliminating the V_{nn} term entirely

$$E_T = E_T^0 + \Sigma\epsilon_i - \Sigma\epsilon_i^0 - V_{ee} + V_{ee}^0 = E_T^0 + \Delta\Sigma\epsilon_i + (-\Delta V_{ee}) \qquad (12)$$

where the definitions of $\Delta\Sigma\epsilon_i$ and $(-\Delta V_{ee})$ should be obvious.[47]

The quantity E_T^0 for the *model charge distribution* may then reasonably be assumed to vary in exactly the same manner with every possible geometrical change as the *actual calculated* (SCF) *total energy for the system being compared* (for example, E_T^0 for a suitably covalent Li_2O structure should lead to potential curves which are everywhere parallel to those actually observed for the water molecule); hence *structural differences between the two systems* must be attributed to the other two terms in eq 12. In general it does not always seem possible to predict which of the terms $\Delta\Sigma\epsilon_i$ or $(-\Delta V_{ee})$ is most sensitive to changes in a given geometrical variable R; in the case of the Li_2O–H_2O bending comparison, however, experience with actual SCF calculations[23,48] indicates that it is the orbital energy term which is of major importance, with $\Sigma\epsilon_i$ for Li_2O favoring a *bent* equilibrium geometry *less* than the water-like quantity $\Sigma\epsilon_i$ for the same sys-

TABLE I. Experimental Equilibrium Geometries of Various Triatomic Molecules in Their Ground States[a]

No.[b]	Molecule	Angle, deg	R_0	k_r	k_δ/R_0^2
12	C_3	180	1.277		0.0047[c]
13	CNC	180	1.245		
	CCN	180			0.15[c]
14	NCN	180	1.232		0.22[c]
	CCO	180[d]	1.160/1.279[d] (ass.)	7.97/14.06[d]	0.18[d]
15	CO_2^+	180	1.177		
	N_3	180	1.181		
	BO_2	180	1.265	11.73[i]	0.30,[i] 0.26[c]
	CS_2^+	180	1.564		
16	CO_2	180	1.162	16.02[i]	0.583[i]
	N_3^- (cryst)	180	1.12[e]		
	NO_2^+ (cryst)	180	1.154[e]		0.42[l]
	NNO	180	1.126/1.186[e]	14.6/13.7[i]	0.49[c]
	OCS	180	1.160/1.560	14.2/8.0[i]	0.37[i]
	CS_2	180	1.554	7.87[i]	0.237[i]
	NCCl	180	1.16/1.57[e]		
	BeF_2	180[g]	1.42[f]		
	MgF_2	158[g]	1.77[g]		
			2.07[e] (cryst)	2.80[i]	0.14[g]
	CaF_2	140[g]	2.10[g]		
			2.38[e] (cryst)	2.20[i]	0.089[g]
	SrF_2	108[g]	2.20[g]	1.96[i]	0.033[g]
	BaF_2	100[g]	2.32[g]	1.58[i]	0.02[g]
	SrI_2	180[g]			
	$CaCl_2$	180[g]			
17	NO_2	134.1	1.1934	10.84[i]	1.52,[i] 1.137[k]
				9.13[j]	0.40[l]
	FCO	135	1.34/1.18[h]	4.55/12.82[h]	0.94[h]
18	O_3	116.8	1.278	7.08[i]	1.28,[i] 0.816[k]
	SO_2	119.5	1.432	10.33[i]	0.820[k]
				9.97[j]	
	FNO	110	1.52/1.13		
	ClNO	116[e]	1.95/1.14		
	CF_2	105[g]	1.30[k]	6.0[k]	1.396[k]
	SiF_2	101	1.591	5.02[k]	0.440[k]
19	NF_2	104.2	(1.37)	4.84[k]	1.076[k]
	ClO_2	117.6	1.473	7.23[k]	0.626[k]
20	F_2O	103[e]	1.41[e]	3.97[k]	0.719,[k] 0.55[j]
				5.57[j]	0.69[k]
	Cl_2O	110.8[e]	1.70[e]	4.93[j]	0.41[j]
	Cl_2S	103[e]	2.0[e]		

[a] Equilibrium distances R_0 are given in Å, stretching (k_r) and bending force constants (k_δ/R_0^2) in mdyn/Å; values are taken from ref 133 unless stated otherwise. [b] Number of valence electrons. [c] Reference 180. [d] Estimated value by M. E. Jacox, D. E. Milligan, N. G. Moll, and W. E. Thompson, *J. Chem. Phys.*, **43**, 3734 (1965). [e] Reference 101. [f] Reference 44. [g] V. Calder, D. E. Mann, K. S. Seshadri, M. Allavena, and D. White, *J. Chem. Phys.*, **51**, 2093 (1969). [h] D. E. Milligan, M. E. Jacox, A. M. Bass, J. J. Corneford, and D. E. Mann, *ibid.*, **42**, 3187 (1965). [i] G. Simons, *ibid.*, **56**, 4310 (1972). [j] G. Herzberg, "Infrared and Raman Spectra", Van Nostrand, Princeton, N. J., 1966. [k] E. B. Wilson, J. C. Decius, and P. C. Cross, "Molecular Vibrations," McGraw-Hill, New York, N. Y., 1955. [l] J. A. Pople and G. A. Segal, *J. Chem. Phys.*, **44**, 3289 (1966).

tem, thereby causing this ionic species to actually prefer a linear nuclear arrangement.[49] In fact, it is quite generally found that the greater the ionic character in a given charge distribution the smaller the amount of bonding or antibonding characteristics exhibited in its corresponding orbital energy curves (because of the reduced possibilities for AO mixing).

The latter consideration also clearly suggests that the linear trend for alkali metal oxides M_2O (as exhibited by increasing magnitudes of bending force constants[50]) becomes stronger in the series lithium through cesium because of the progressively decreasing ability of the valence AO's of such atoms to bond with those of oxygen. This conclusion is reinforced by the fact that the net positive charge on the terminal atoms of these oxides increases toward higher atomic number,[7] thereby suggesting that the V_{ee} term in eq 12 for each of the later members of this series does not increase as fast with bending for an optimal (ionic) charge distribution as does V_{ee}^0 for a constrained distribution of the same system which is equivalent to that favored by the lithium member; consequently, the *additive potential term* $-\Delta V_{ee} \equiv (V_{ee}^0 - V_{ee})$ *increases with bending*[47] in eq 12 since while both V_{ee} and V_{ee}^0 are increasing the latter quantity does so more quickly. As a result it is seen that *both the orbital energy and the electron repulsion term* in the horizontal correction formula (eq 12) cause the *strength of the linear trend* in such systems to *increase with the atomic number* of the alkali metal. By contrast a comparison of Li_2S and Li_2O suggests that the former molecule quite likely prefers a bent geometry (although probably with a substantially larger equilibrium angle than that of water) because the Li AO's are better able to combine with those of sulfur (causing $\Sigma\epsilon_i$ to decrease faster with bending than $\Sigma\epsilon_i^0$ for an Li_2O-like charge distribution of Li_2S), and the total negative charge on the terminal atoms in the sulfide is also expected to be greater than in the corresponding oxide.[51]

Such an interpretation of eq 12 is also quite consistent with experimental observations regarding the equilibrium geometries of AB_2 molecules containing 16 valence electrons, such as CO_2 and BeF_2 (see Table I). First of all, it seems clear that the strength of interaction between the Be and F AO's is considerably less than between those of C and O and hence that $\Sigma\epsilon_i$ for BeF_2 itself does not favor a linear nuclear arrangement nearly so much as $\Sigma\epsilon_i^0$ for a CO_2-like charge distribution for the same system.[52] In addition, the fact that the terminal atoms in the fluoride undoubtedly possess a larger net negative charge than those of CO_2 implies strongly that V_{ee} for the former system *increases faster* with bending than does V_{ee}^0 for the comparative (CO_2-like) charge distribution. From eq 12 it is seen that *both* of the aforementioned effects indicate that BeF_2 should possess an angular potential curve which does not rise as steeply with molecular bending as that of CO_2, as indeed seems to be the case experimentally, at least based on the experience of *ab initio* SCF calculations for these systems.[53]

Perhaps more interestingly such an interpretation logically leads one to predict that the trend away from linear equilibrium geometry should continue as the electronegativity of the central atom decreases (thereby further decreasing the possibilities for AO mixing and also increasing the net charges on the fluorine atoms). Reference to Table I shows that, in fact, such a trend does exist experimentally in the series BeF_2, MgF_2, CaF_2, SrF_2, and BaF_2, whose equilibrium internuclear angles show a gradual decrease from the 180° value predicted generally for such 16-valence-electron systems on the basis of the MW model, all the way down to the 100° value observed for the barium member of this group of molecules. The analogous series of chlorides, bromides, and iodides show no such deviations from linearity, a trend which is unquestionably consistent with the smaller net negative charge (and relatively more diffuse charge distribution) expected for each of the other halogens in comparison to fluorine, as well as in the increased ability of their AO's to mix with those of the relatively electropositive central atoms in such molecules. The subject of the alkaline earth metal halides will be discussed further, including the role of d orbitals in the representation of such systems,[54] in connection with a more detailed survey of the geometries of triatomic AB_2 molecules in section III.C.1. Trends in the equilibrium internuclear angles of other types of systems will also be considered in light of eq 12 as they become pertinent (section III), particularly those found in the study of AH_2, AH_3, HAB, and AB_3 molecules.

Once it is noted that Koopmans' theorem can be used to predict relationships between bond angles of general molecular systems, however, it becomes clear, as noted in section II.B.2, that the same techniques are equally valid for the study of bond distances, despite the decided lack of emphasis on this general subject in the original papers[1,2] dealing with the MW model. Indeed, there is ample evidence from experimental investigations (see Table I, for example) that the same general relationship between equilibrium geometry and number of valence electrons holds quite satisfactorily for both types of structural quantities. Yet it is also true that such experimental data indicate some significant differences in the equilibrium distances of isovalent members of the same molecular family, just as have been noted above for the corresponding angular results. Again it seems clear that the basic reason for these *geometrical distinctions* is to be found in the differing amounts of covalent and ionic character in the respective charge distributions of such systems. If BeF_2 is compared to CO_2, for example, it is reasonable to conclude that $\Sigma\epsilon_i$ for this *ionic* system decreases *less rapidly* with approach of its nuclei than does the corresponding CO_2-like quantity $\Sigma\epsilon_i^0$ (eq 12) (because of the smaller amount of interaction between the Be and F AO's in the actual ionic system). At the same time, a simple point charge model indicates that the product of the *total* electronic charge of the Be and F atoms respectively is *less* for the *optimal* charge distribution of BeF_2 than for the CO_2-like distribution for the same system *in the same geometry*;[55] as a result, it seems quite likely that V_{ee} in eq 12 for the actual BeF_2 structure increases *less rapidly* with decreasing internuclear distance than does the V_{ee}^0 quantity for the corresponding (more covalent) CO_2-like model charge distribution. According to the basic assumption that the E_T^0 plotted curve for BeF_2 and the total energy curve of the reference system (CO_2) vary in an essentially parallel manner, it follows quite unambiguously (since $\Delta V_{ee} \equiv V_{ee} - V_{ee}^0$ is decreasing in this comparison and hence the additive repulsion term in eq 12 ($-\Delta V_{ee}$) as well as $\Delta\Sigma\epsilon_i$ is increasing with approach of the nuclei) that the actual BeF_2 stretching potential curve must have decidedly less bonding characteristics than its CO_2 counterpart,[47] in agreement with what is observed experimentally (see Table I).

From this point of view, it is also not at all surprising that molecules consisting only of first-row atoms and corresponding ones containing atoms of the second and following rows of the periodic table exhibit different bond lengths even though the number of valence electrons is the same (Table I). It is necessary to take account of the relatively diffuse nature of the constituent species in this case, since electron repulsion between two 3p AO's, for example, clearly does not increase as rapidly with diminishing bond distance as it does for orbitals of principal quantum number two. Hence, even though sulfur is less electronegative than oxygen and thus might be characterized by (slightly) greater interactive capabilities between its AO's and those of carbon, it still seems clear that the dominant effect (in terms of eq 12) in determining the difference in bond lengths between CS_2 and CO_2, respectively, is that of electron repulsion. Since V_{ee} for CS_2 varies much less *strongly* with R_{CS} than does V_{ee}^0 *for a CO_2-like charge distribution* of the same system, it follows, just as in the case of BeF_2 (but for somewhat different reasons), that the CO_2 bond distance is considerably shorter than in the system with which it is being compared (experimental R_{CS} in CS_2 is 1.554 Å). Similarly, one is led to the conclusion that MgF_2 should have a *larger* bond distance than BeF_2, this time because of the more diffuse charge distribution at the central atom of the former system. The increase in bond lengths for isovalent homonuclear diatomics as the electronegativity of the constituent atoms decreases is also easily explained in this manner, since once again increasing the diffuseness of the valence charge distribution clearly leads to a diminution in the rate at which both $\Sigma\epsilon_i$ decreases and V_{ee} increases with approach of the nuclei, and hence according to eq 12 results in a decided decrease in the *bonding* character of the associated stretching potential curves. In each of the latter cases the interpretation of eq 12 is seen to be virtually equivalent to what is expected based on the concept of mean atomic radii determining molecular bond distances,[7] but it is still interesting that such a relationship follows in such a straightforward manner from examination of a particular total energy expression (namely eq 2) of Hartree–Fock theory.

In summary then, the rule that the gross equilibrium geometry of molecules is determined for all practical purposes strictly on the basis of their *electronic configuration* is in general very successful in explaining structural trends in molecular systems. On the other hand, a correction must be applied to this simple model in order to understand certain exceptional cases, occurring primarily among ionically bonded systems. Attempts to describe the essential features of this (horizontal) correction in mathematical language have been based on the supplementary assumption that for *isovalent systems* (of the *same* electronic configuration) differences in equilibrium geometry result almost exclusively from distinctions in *electronic charge distribution.* Comparison of the total energy expression for two different charge distributions of a particular molecule, one of which is *optimal* for this system at a given geometry, the other of which is *equivalent*[46] to that of some reference system for the identical arrangement of nuclei, has led to eq 12.

In all examples given so far, unambiguous predictions on the basis of this equation have been possible since either one or the other of the two effects of $\Delta\Sigma\epsilon_i$ and ΔV_{ee}, respectively, has clearly been dominant or both have merely reinforced one another. It might well be anticipated, however, that this convenient state of affairs will not be present in every application undertaken, but experience with a wide range of systems undergoing various types of geometrical changes indicates strongly that the occurrence of such troublesome cases is actually quite infrequent. Numerous other applications of eq 12 will be discussed in section III.

The discussion of such *horizontal* corrections to the MW model has been restricted entirely to the study of SCF or Hartree–Fock theory and has pointedly omitted the consideration of so-called correlation effects, since experimental and theoretical evidence both indicate that such energy contributions *vary* in an essentially parallel manner (with changes in a given geometrical variable) for all *isovalent* systems within a given class. The same conclusion is *not* generally valid for comparisons of systems with differing numbers of valence electrons (such as for ions of the same vertical column of the schematic diagram in Figure 12), however, but at present there are not sufficient theoretical data available to evaluate the significance of this point; the success of the MW model in predicting geometrical distinctions (especially after a horizontal correction is applied) certainly suggests that effects of this nature play only a relatively minor role in such determinations, but it would be unwise to assume that they can be neglected if *quantitative* accuracy is desired. Basis set effects in SCF calculations have also not been considered but even this important question is not at all unrelated to the basic underlying premise of eq 12.

4. *Relationship of Canonical Orbital Energies to Hückel Theory*

Before moving to the consideration of specific *ab initio* calculations dealing with the MW model, it is worthwhile to consider a parallel development based on Hückel-type (semiempirical) treatments.[25,26,56-60] As mentioned earlier, it has been pointed out by Leclerc and Lorquet[25] and Allen and Russell[26] (and earlier by Boer, Newton, and Lipscomb[41]) that there is an inherent similarity between the calculative procedures involved in the Hückel and Hartree–Fock methods, respectively; in particular, it seems clear that the Hückel eigenvalues ϵ_i^H correspond at least *pro forma* to some type of SCF canonical orbital energy. Allen and Russell[26] and Allen[61,62] have drawn this analogy a step further and have identified the aforementioned semiempirical quantities with the *conventional* SCF canonical orbital energies ϵ_i.

On the basis of a comparison between the results of some extended Hückel[63] calculations for F_2O, FOH, and Li_2O (and other systems) and those of the nonempirical SCF treatments carried out by the present authors[23] for the same systems, it has been concluded[26,61-62] that the sum of the Hückel eigenvalues $\Sigma\epsilon_i^H$ will fail to produce the essential characteristics of SCF E_T potential curves in precisely the same cases for which $\Sigma\epsilon_i$ itself is insufficient for this purpose (see section II.B.1). In fact, however, the agreement actually found between the shapes of corresponding Hückel total energy ($\Sigma\epsilon_i^H$) and sum of conventional SCF canonical orbital energy ($\Sigma\epsilon_i$) curves appears to be quite rough (see schematic representation of the various curves in the inserts of Figures 3, 5, and 6); in the case of FOH (Figure 6), for example, the $\Sigma\epsilon_i^H$ and $\Sigma\epsilon_i$ curves cross at approximately a 45° angle, and in no instance can it accurately be stated that the shape of a given Hückel potential curve does not correspond more closely to the corresponding SCF total energy species than to that of $\Sigma\epsilon_i$ (indeed the Hückel curves do not resemble either of their *ab initio* SCF counterparts very convincingly in any of the three cases considered).

More recently Allen[61,62] has carried the supposed analogy between Hückel eigenvalues and the conventional SCF orbital energies still further by concluding that given the apparently universal failure of $\Sigma\epsilon_i$ data to satisfactorily represent the formation of equilibria in the bond stretching process, as demonstrated by the aforementioned *ab initio* study carried out by the present authors and Whitten,[44] it must follow that the extended Hückel method obtains its bond length predictions by means of what is described as a "physically incorrect process." The work of Davidson[40] (section II.A.3), however, suggests a different view of how such a semiempirical theory might be related to the Hartree–Fock formalism, namely by identifying the extended Hückel eigenvalues with a different type of SCF quantity *whose sum varies in an exactly parallel manner as the total energy* E_T.

In particular one can define a quantity ϵ_i' (which is distinct from but not totally unrelated to the ϵ^{ICSCF} quantities of Davidson discussed in section II.A.3) such that

$$\epsilon_i' = \epsilon_i + \Delta(V_{nn} - V_{ee})/N \qquad (13)$$

where ϵ_i is the conventional Koopmans' theorem-related canonical orbital energy, N is the total number of electrons in a given system, and $\Delta(V_{nn} - V_{ee})$ is the *change* in the nuclear-electronic repulsion difference *relative to its value at some fixed geometry.* It is readily seen from eq 2 that $\Sigma\epsilon_i'$ *must possess equal derivatives to those of the total energy* E_T *with respect to all possible geometrical variables,* regardless of the reference nuclear conformation chosen, since the two quantities differ by only an additive constant.[64] Furthermore, choosing the reference nuclear arrangement to be that corresponding to *equilibrium* for the molecule in question obviously *ensures that the* ϵ_i' *quantities satisfy Koopmans' theorem exactly at this important geometry.* Indeed, since the term $\Delta(V_{nn} - V_{ee})/N$ in eq 13 is quite generally found to be relatively small in absolute magnitude,[65] even for structures which differ greatly from the equilibrium nuclear arrangement, it follows that the discrepancies between corresponding ϵ_i' and ϵ_i results should never be particularly large in comparison with typical values observed experimentally for molecular ionization potentials.

Clearly, if the EHT calculations were able to produce good approximations to the ϵ_i' values of eq 13, the resulting potential curves and *vertical* ionization energies

would *necessarily be of equivalent accuracy* to the corresponding data derived from nonempirical SCF calculations, *even to the Hartree–Fock limit.* Of course, the results actually obtained with the EHT calculations of Allen and Russell[26] fall far short of reaching this goal, but the point is that such a set of ϵ_i' quantities *does exist* for any given system, and thus *in principle* it is possible by skillful parameterization to produce them through the solution of a Hückel-type secular equation. Such a conclusion runs contrary to that reached in the earlier critiques[61,62] of extended Hückel theory, which are now seen to be based on an overly narrow view of the definition of SCF canonical orbital energies.[40]

At the same time it is important not to overlook a fundamental difference between semiempirical models in general and those of the *ab initio* variety in making such comparisons, namely the lack of a well-defined wave function in the methodology of the former. The geometrical predictions of the semiempirical treatments are made first and foremost by *ad hoc parameterization*, whereas those of *ab initio* type generally (but not always)[66] seek this information much less directly by means of *systematic improvement of the wave function* on the basis of the variation principle. If only for this reason it is dangerous to draw very closely any analogy between semiempirical and *ab initio* theories.

It is theoretically impossible, for example, to include correlation effects in nonempirical treatments at the Hartree–Fock level (since a different form of the wave function is needed for this purpose) and thus potential curves generated by such calculations will often times be significantly different from those obtained experimentally (especially for bond-stretching or dissociation processes), but there is absolutely nothing *in principle* which prevents semiempirical investigations of the Hückel type from attaining perfect agreement with such an experimentally determined quantity *provided sufficient freedom is allowed in the parameterization scheme employed.* A good example for which the SCF or Hartree–Fock method is quite inadequate for representing a potential curve,[67,68] but for which a semiempirical treatment through *ad hoc* parameterization has been able to arrive at this goal,[69] may be found in connection with the study of the ground-state twisting barrier of ethylene (section III.B.5). In such cases, however, it is not at all realistic to argue that a Hückel-type population analysis necessarily provides an adequate representation of a given molecular charge distribution, *i.e.*, simply because an associated potential curve agrees well with that observed experimentally, since there is no guarantee in principle that the results of such parameterization schemes will be self-consistent for a wide range of physical observables.

C. Use of the Canonical ϵ_i's to Widen the Applicability of the Mulliken–Walsh Model

There has been a decided tendency in the years following the introduction of the Mulliken–Walsh geometrical model to identify it solely with its predictions of certain regularities in the *bond angles* of the *ground states* of molecules belonging to the same classes of systems discussed by Walsh in his original presentation.[2] But it is clear that if there is a sound theoretical basis for this empirical theory, as has been argued in the foregoing portion of this section, such a restrictive view of the applicability of this model fails to grasp the inherent versatility of its method. There should be no question that the goal of any attempt to give quantitative substance to the interpretations of Walsh's rules is to eventually *generalize its applicability to the study of virtually every molecule in any of its electronic states as it undergoes any and all types of geometrical changes.* How to proceed in accomplishing this task is the subject of the remaining part of this section.

1. Possible Extensions

a. Quantitative Reliability

The original presentation of the MW model[1,2] is necessarily qualitative in detail, particularly in its emphasis upon merely predicting an appropriate range for the equilibrium internuclear angle (particularly bent *vs.* linear) of a given system. Yet in many applications it is just as important to have a good idea of the *slope* or *curvature* of a given potential curve as well as of the location of its minima. Quantitative calculations should not only be able to predict details of this sort but also to answer basic questions about *why* distinctions in such results occur from one system to another. In particular the addition of a horizontal correction to the MW model in the form of eq 12 to predict relatively minor geometrical differences should be useful in this connection.

b. Generalized Geometrical Variations

Although the discussion in Walsh's series of papers[2] is well nigh confined to the predictions of changes in equilibrium *angles* for various tri- and tetratomic systems, it should be clear from section II.B.2 that such a limitation is by no means an intrinsic feature of this model. In particular, one can use the differential form of Koopmans' theorem (eq 9) to make quite useful predictions about equilibrium *bond lengths* of whole series of molecules based on the SCF results (total energy *and* canonical orbital energies) of only one such species. No bond-stretching correlation diagrams were included in any of the original writings[1,2] (although such geometrical changes were considered), but yet *ab initio* SCF calculations[44] indicate that the *same types of general features are observed* for the variation of canonical orbital energies with bond distance within large classes of systems as have been widely discussed in connection with *molecular bending motions.* Even more convincingly perhaps, examination of the pertinent experimental data indicates that trends in equilibrium bond lengths with changing numbers of electrons within a class of molecules are every bit as regular as those noted by Mulliken and Walsh for the internuclear angles of the same systems.

Nor in principle is it necessary to restrict application of the original model to such relatively simple geometrical changes as bond stretching or angle bending; a correlation diagram for *any geometrical path*, no matter how complicated, can be used to predict trends for analogous nuclear displacements *within complete series of molecules* and *not just for the system of immediate interest.* Thus it has been possible to relate the geometries of ethane, diborane,[22] and ammonia–borane[70] by means of a correlation diagram constructed from *ab initio* SCF results for only one of them and in a similar manner to study the barriers to dis- and conrotation for large groups of hydrocarbons.[71-73]

c. Molecules Containing Elements of the Second and Higher Rows of the Periodic Table

Mulliken and Walsh both noted the fact that the geometrical trends indicated in the various orbital energy correlation diagrams seem to be related almost exclusively to *valence electron* effects. Nevertheless, rather large differences in the equilibrium geometries of *isovalent* molecules containing elements of different rows of

the periodic table have obscured the basic accuracy of this aspect of the model. The discussion of section II.B.3 indicates, however, that most of the resulting confusion in this regard is intimately connected with the failure of the original model to account for differences in electronic charge distributions of isovalent systems possessing different numbers of filled inner shells. Once these effects have been taken into account, as, for example, by application of eq 12, it seems clear that the operation of the original model remains in tact, particularly as long as the systems being compared contain atoms which *center for center* belong to the same row of the periodic table (CS_2 and BCl_2^+, for example).

d. Determination of the Favored Arrangement of Nuclei in Polyatomic Systems

No mention seems to have been made in the original Mulliken–Walsh presentation of the possibility of using this geometrical model to predict the *order* of atoms preferred in a given polyatomic system, but examination of *ab initio* SCF results[74] for NNO and NON (both of which prefer linear geometries) suggests that this important question can also be resolved quite satisfactorily in a manner consistent with this simple theory (see also section III.C.2).

e. Geometries of Excited States

It is interesting that, despite the almost exclusive attention generally given to the geometrical predictions of the MW model for molecular *ground states*, the fact remains that in the original presentation of this theory[1,2] the *dominant consideration by far* is upon the shapes of systems in their electronically *excited states*. The main reason for the reluctance upon the part of many investigators to apply the results of *a priori* calculations to this important subject of the geometries of electronically excited molecules seems to be connected with some observations made concerning certain properties of *unoccupied* (or virtual) orbitals resulting from *ab initio* SCF calculations,[75-78] at least those in which large basis sets are employed. The problem with such orbitals is simply that they do not represent satisfactory approximations to upper-valence MO's which result from calculations in which these species are actually occupied; the virtual orbitals are generally much too diffuse for this purpose (unless of course a very restrictive basis is employed which does not contain diffuse species in the first place). There is a very simple solution to this dilemma, however, and that is simply to recall that in order for the original form of Koopmans' theorem to be useful it is extremely important that the *variational orbitals of the ion be represented quite faithfully by those of the corresponding neutral system*. In the present context this observation, coupled with the fact that *occupied* orbitals and particularly *the shapes of their orbital energy curves* retain their basic features to a very large extent regardless of the actual system for which they are calculated,[24,79] leads very easily to the conclusion that virtual orbitals need never be considered in applications of the MW model; instead it is merely necessary to construct the required correlation diagrams exclusively from *occupied* canonical orbital energy curves. Thus the examples of section II.B.2 show quite clearly that one can take such occupied orbital energy curves for 24-electron ozone[80] to make quite reasonable predictions about *both ground- and excited-state* potential curves of the 22-electron system N_3^-. More generally, if it is desired to construct a satisfactory correlation diagram for a given molecular family *from a series of SCF calculations for a single member*, it is only necessary to carry out the required computations for a *saturated* system of this type, *i.e.*, one for which all valence MO's are fully occupied (Rydberg orbitals can be ignored as usual since systems in which these species are occupied are treated quite satisfactorily as if they were positive ions). Nevertheless, as the aforementioned ozone–N_3^- example demonstrates, it is by no means necessary to restrict the calculation of generalized correlation diagrams in this manner since it is only the shapes (and not the spacing) of the orbital energy curves which are essential in making the geometrical predictions of the MW model; and this information can be obtained just as effectively in a piecemeal fashion from computations for several systems (in which one or the other of the higher lying orbitals is occupied in a given case) as it can if all the orbital energy curves are obtained for the same (saturated) system. In summary, the overwhelming weight of experience from *ab initio* calculations on this subject quite consistently supports the conclusion that as far as application of the differential form of Koopmans' theorem is concerned, it is really immaterial which set of canonical orbital energy curves is chosen, as long as each corresponds to an occupied molecular orbital in the state for which it is calculated.

At the same time, since the values of Coulomb and exchange integrals[81] are *generally* much less sensitive to geometrical changes than those of canonical orbital energies, there is considerable justification in removing the former quantities from consideration in such an idealized geometrical model. The success of this approximation may be judged from the comparison of various Koopmans' theorem and SCF total energy potential curves given in section II.B.2, for which cases *successive* applications of eq 9 are actually required.[82] On the other hand, it can certainly be anticipated that such a convenient state of affairs may not always exist in practice, in particular, that the *shapes* of potential curves for *different multiplets* of the *same electronic configuration* may differ significantly from one another. But again such deviations from ideality do not represent an extraneous feature introduced by the *use of SCF canonical orbital energies* in an attempt to obtain a *quantitative realization of the empirical theory* but rather the result of an *inherent deficiency in the original MW model itself* (and indeed in the more well-defined Hückel-type treatments of electronically excited states, which make no distinctions whatsoever between multiplets arising from the same electronic configuration).

f. More General Classes of Systems

It is obvious from the original presentation of the MW model that its applicability is not restricted to the same classes of systems for which correlation diagrams were explicitly given. The main problem with extending the utility of the model in this way seems to be the proliferation of molecular classes which occurs upon expanding the discussion to systems with greater and greater numbers of constituent nuclei. Examination of the early work of Mulliken[33] and Hund,[34] as well as of orbital charge densities resulting from *ab initio* SCF calculations, indicates rather clearly, however, that complications resulting from considerations of this type are alleviated greatly because of the peculiar characteristics exhibited by hydrogen atoms as they participate in molecular bonding, a subject which is discussed in the following subsection.

2. *Organizing Principle*

A fairly elementary analysis by means of standard group theoretical techniques[83] suggests that a quite

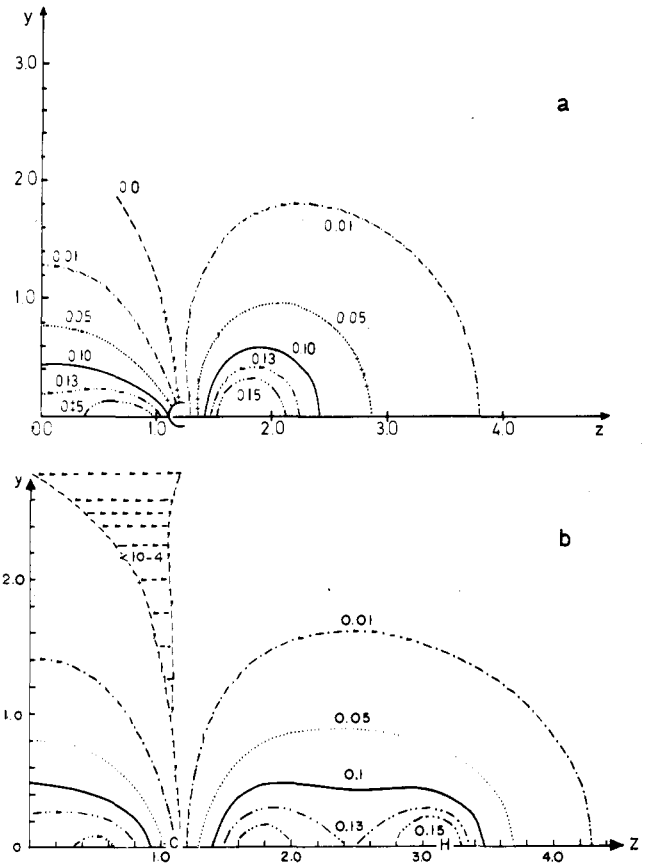

Figure 13. Charge density contours of the $3\sigma_g$ MO in C_2 (a) and in C_2H_2 (b), respectively.

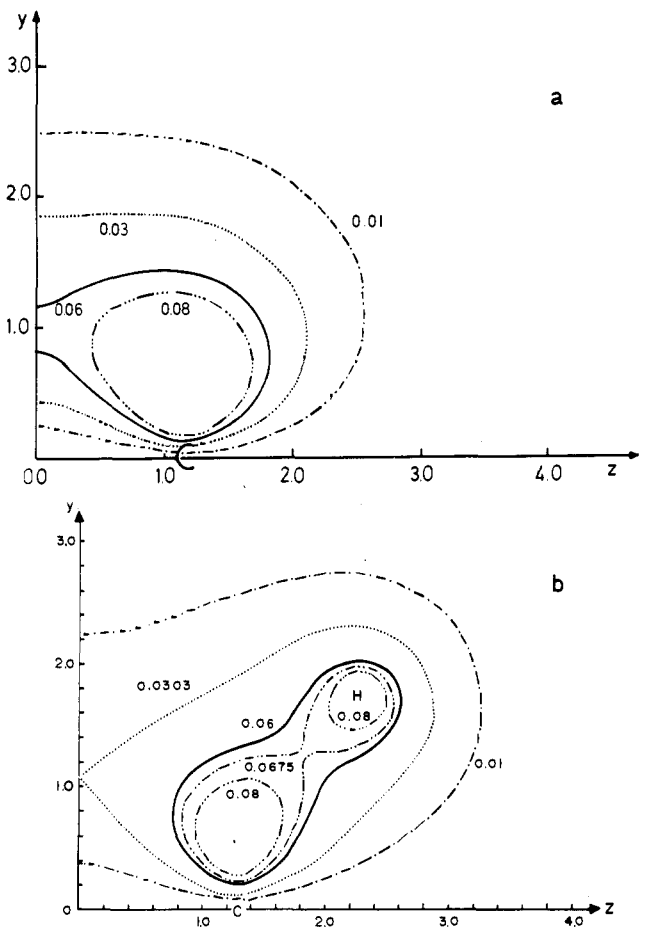

Figure 14. Charge density contours of the $1\pi_u$ MO in C_2 (a) and of the corresponding π_u-type ($1b_{2u}$) orbital in C_2H_4 (b).

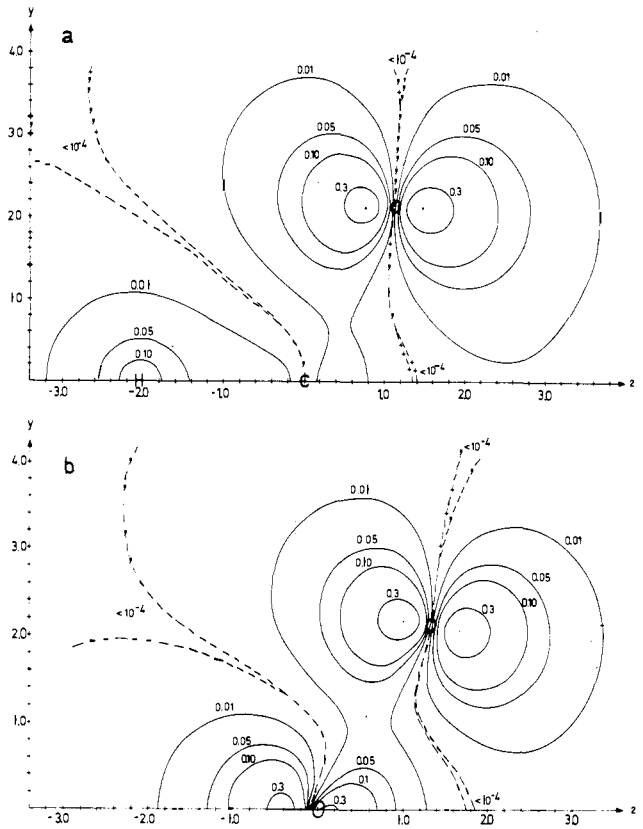

Figure 15. Charge density contours of the $6a_1$ MO in $HCOO^-$ (a) and in O_3 (b), respectively.

basic relationship exists between the molecular orbitals of simple diatomic molecules and those of related isoelectronic hydrogen-containing systems such as ethylene and diborane.[84] Comparison of pertinent orbital charge density diagrams has shown[85] that such similarities actually go far beyond the realm of pure theory, having their effect on the most basic details of the electronic structures of these molecules. The calculated charge densities for the $3\sigma_g$ MO's of C_2 and C_2H_2, shown in Figures 13a and 13b, respectively, provide a clear example which demonstrates this point; even though the effect of the constituent atoms is apparent in the C_2H_2 plot, it is clear that the basic character of both of these $3\sigma_g$ species is determined by a common element, namely the presence of the $p\sigma$ carbon AO's of each system. The π MO's of acetylene and C_2 are even more similar (as a result of the group theoretical consequences of *linear* C_2H_2 equilibrium ground-state geometry), but even in hydrogen-containing systems of lower nuclear symmetry it is easy to identify MO's of considerable π character (see Figure 14a,b). Furthermore, the similarity between corresponding MO's (for systems with and without hydrogens) heightens as the atomic number of the heavy atom increases, so much so, in fact, that in H_2O (see section III.A.1) th hydrogen nuclear positions are not even marked by maxima in the various orbital charge density plots. Similar relationships have been found between corresponding MO's containing three (or more) heavy atoms as, for example, in the case of comparison[86] of the $6a_1$ MO of ozone O_3 and that of the formate ion $HCOO^-$ (Figure 15a,b).

In a very real sense then, it becomes possible to interpret the results of calculations for systems containing hydrogen atoms in a very similar manner as for molecules with no constituent hydrogens but with a similar skeleton of heavy (nonhydrogenic) species. In this way it is possible to penetrate the rather superficial barriers placed be-

tween the studies of inorganic and organic molecules, respectively, in the original presentation of the MW model.[2] Specifically such a procedure[87] has succeeded in explaining the existence of such *cyclic* isomers as 16-valence-electron cyclopropene[88] and 18-valence-electron cyclopropane[89] in a manner which is *entirely consistent with the application of the original MW model* (without the use of any horizontal correction whatsoever), even though the latter theory implies strongly that the *ground states* of corresponding *isovalent* AB_2 molecules (such as N_3^- and O_3[24]) invariably possess equilibrium structures which are decidedly noncyclic.

Consequently, in the following section dealing with applications of the geometrical model discussed above, classification of the various molecular systems will be made according to the number of their constituent nonhydrogenic atoms. At the same time it will be important to keep in mind certain well-known relationships between classes of molecules with different numbers of heavy atoms, as exemplified by the well-known observation that fluoro-substituted systems invariably have the same general shape as their hydrogen-containing analogs (AH_2 *vs.* AF_2 systems, for example). In general a serious attempt will be made in what follows to define as carefully as possible the very real similarities that exist between various molecular classes (as defined by Walsh[2]) and thereby demonstrate that the methodology of the MW geometrical model can be summarized in terms of a much smaller set of orbital energy correlation diagrams than was originally claimed.

III. Applications

A. Molecules Containing One Nonhydrogenic Atom

1. AH_2 Systems

The original paper by Walsh[2] on the shapes of AH_2 molecules deals exclusively with the question of internuclear angles of such systems. In view of the discussion in the preceding section, however, it seems useful now to examine trends for both the bond distances and bond angles of this group of molecules.

a. AH Stretch. A General Study

The general conclusion emanating from the MW model is that molecular geometry depends first and foremost on electronic configuration, but examination of available experimental data for AH *bond lengths* in various AH_2 systems, as well as in other AH_n families, shows clearly that this simple principle is certainly not *dominant* in the study of these geometrical quantities (Table II). Note, for example, that the isoelectronic systems BH_2^- and NH_2^+ possess bond lengths which differ by at least 0.15 Å while the corresponding quantities for the *isovalent* pair water and H_2S differ by approximately 0.35 Å. In fact, a more general survey of the data in Table II (and also for systems containing second-row atoms) indicates that AH bond lengths are determined *first and foremost* by the *identity of the heavy atom* in such molecules, and only secondarily by the number of electrons (or electronic configuration).

To understand why such trends occur, it is quite useful to examine some orbital charge density contours[90] for various MO's of a typical AH_2 system such as water (given in Figure 16); these data should be compared with a fairly standard LCAO description of such orbitals, patterned after the original work of Walsh[2] (Figure 17). While the latter diagrams generally give the impression that the H_2O charge distribution consists of *three distinct maxima* corresponding to the various nuclear centers, the orbital and total charge densities actually calculated for this system seem better described in terms of a model of a *single central atom* with a *spherical* distribution of electrons which is only *slightly perturbed* by the presence of the off-center protons. The electronic charge distribution of such a molecule is apparently *not* altered greatly by the relative motion of the exterior protons, in distinct contrast to what might be expected on the basis of the usual LCAO description of such a process (Figure 17). This conclusion is, in fact, borne out quite well by the results of Hartree–Fock–Roothaan calculations[91] for NeH^+ dissociation, which show that the location of the *center of negative charge* for this system changes by only about 0.04 bohr (0.02 Å) as R_{NeH} is varied from 4.50 to 1.83 bohrs (the equilibrium bond distance of this system).

The accuracy of the foregoing description of AH bonding may be judged from the results of an empirical model given by Platt,[92] which has been very successful in predicting both internuclear distances and stretching force constants for *neutral* diatomic hydrides. In the Platt model the major premise is very simply that the electronic density of the *united atom* in such systems is not significantly affected by removal of a proton from the central nucleus, an assumption that is obviously in quite good agreement with the aforementioned NeH^+ result, as well as with the less specific information given by the H_2O orbital and total charge densities (Figure 16). Such a model for the electronic structure of these molecules clearly implies that all terms in the Hamiltonian, such as electron repulsions and kinetic energies, which *depend solely on the distribution of the electrons* in a given system, are *not significantly changed by variations in AH distances* (at least in the neighborhood of equilibrium).

TABLE II. AH Bond Lengths for a Number of Systems Containing a First-Row Central Atom[a]

No.[b]	Li	Be	B	C	N	O	F
2	LiH	BeH^+					
	1.595	1.312					
3		BeH	BH^+				
		1.343	1.215				
4		BeH_2	BH	CH^+			
		(1.34)	1.232	1.131			
			BH_2^+				
			(1.22)				
5			BH_2	CH	NH^-		
			1.18	1.120	1.084		
				CH_2^+			
				(1.12)[c]			
6		BeH_3^-	BH_2^-	CH_2	NH	OH^+	
		(1.34)	(1.24)	1.078[d]	1.038	1.029	
			BH_3	CH_3^-	NH_2^+		
			(1.19)	(1.08)	(1.07)		
7				CH_3	NH_2	OH	
				1.079	1.024	0.971	
8			BH_4^-	CH_3^-	NH_2^-	OH^-	HF
			1.25	(1.10)[e]	1.03	0.984	0.917
				CH_4	NH_3	H_2O	
				1.094	1.017	0.956	
					NH_4^+	H_3O^-	
					1.031	0.96	

[a] Experimental values are taken from ref 101, 133, and G. Herzberg, "Molecular Spectra and Molecular Structure," Vol. 1, Van Nostrand Princeton, N. J., 1966; values resulting from *ab initio* treatments (actually calculated or only estimated) are given in parentheses. All values are given in Å. [b] Number of valence electrons. [c] C. F. Bender and H. F. Schaefer, III, *J. Mol. Spectry.*, **37**, 423 (1971). [d] Reference 106. [e] R. E. Kari and I. G. Czismadia, *J. Chem. Phys.*, **50**, 1443 (1969).

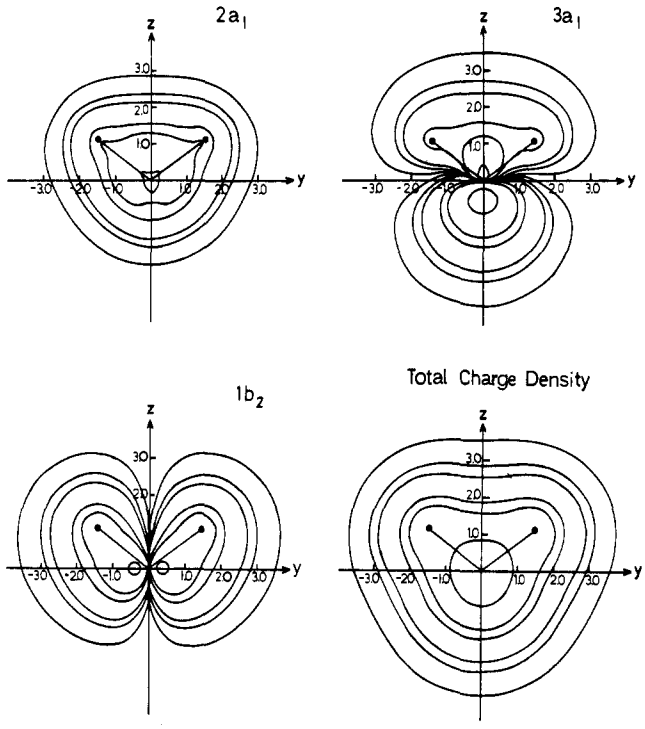

Figure 16. Total and various orbital charge density contours for H_2O in its ground-state equilibrium nuclear arrangement.

The nuclear attraction terms, on the other hand, should be much more sensitive to the approach of the exterior protons.

In terms of the horizontal correction to the MW model (eq 12), this conclusion suggests quite strongly that the orbital energy sum term (which contains nuclear attraction contributions; see eq 1) will be *more sensitive* to R_{AH} variation for a relatively *contracted* charge distribution than for one which is more diffuse. By contrast, since the electron repulsion term V_{ee} is relatively *independent* of R_{AH} *regardless of the nature of the* (roughly spherical) *charge distribution* favored by a given system, it is reasonable to expect that this quantity will *not* be a significant factor in determining differences in AH bond lengths between isovalent systems. From these observations one is led to expect that for an isovalent series $\Sigma\epsilon_i$ (which quite generally favors molecule formation[44]) *decreases faster with the approach of the protons* as the atomic number of the central atom *increases* across a *row* of the periodic table or as it *decreases* along a *column* (in both of which cases the valence charge distribution becomes progressively more contracted).

Such a conclusion is borne out quite clearly by the results of *ab initio* SCF calculations[44] for the isoelectronic systems NH_2^+ and BH_2^-, whose AH stretching correlation diagrams are shown in Figures 18a and 18b, respectively. From these results it is apparent that the NH_2^+ orbital energy curves all decrease sharply toward smaller internuclear separations while those of BH_2^- (with a less contracted charge distribution at the central atom) are much less sensitive to such geometrical variations. It is certainly not surprising then that the calculated[44] bond distance for NH_2^+ (1.07 Å) is considerably smaller than that for isoelectronic BH_2^- (1.296 Å).[93,94] *At the same time these results indicate quite clearly that geometrical changes which occur upon ionization of these two systems are quite different, since the aforementioned distinctions in the shapes of corresponding orbital energy curves become of direct physical significance as a consequence of the differential form of Koopmans' theorem* (eq 9). Removal of electrons from the $3a_1$ MO, for example, leads to a decided increase in bond length in the case of NH_2^+ (for which this species is strongly bonding) but to a *slight decrease* in the case of BH_2^- (for which the $3a_1$ is somewhat antibonding).

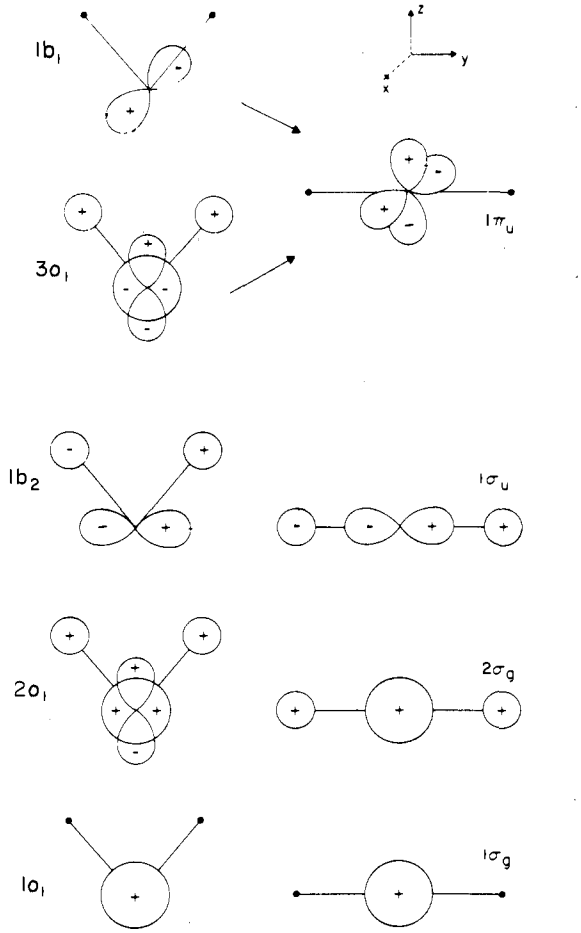

Figure 17. Schematic diagram representing the MO's of a linear and bent AH_2 molecule, respectively.[21]

From these considerations it is seen that neither the Platt[92] nor the MW (Koopmans' theorem) model is entirely successful in describing the essential nature of the bond length trends observed experimentally (see Table II) for AH_2 systems (and AH_n species generally). The more easily generalizable theory of Mulliken and Walsh is inadequate because it does not account for differences in nuclear attraction from one heavy-atom charge distribution to another, while that of Platt (at least in its original form[92,95]) is unsatisfactory for the prediction of bond length changes upon ionization. When both of these effects are taken into account (through application of eq 9 and 12, respectively), the somewhat unruly trends of Table II become much more understandable. The rather unusual relationships contained therein are seen to be based on a combination of two fortunately rare circumstances: the need for a large horizontal correction to the MW model as a result of the surprising constancy of the molecular charge distribution upon AH stretch (see Figure 16) and, secondly, the fact that the shapes of orbital energy curves for AH stretching are quite sensitive to the nature of the central atom (as in Figure 18a,b).

b. HAH Bending

Even though the original MW model is somewhat unsatisfactory for the description of *bond length trends* in the AH_2 family of molecules, it is much more successful in the prediction of the equilibrium angles of such sys-

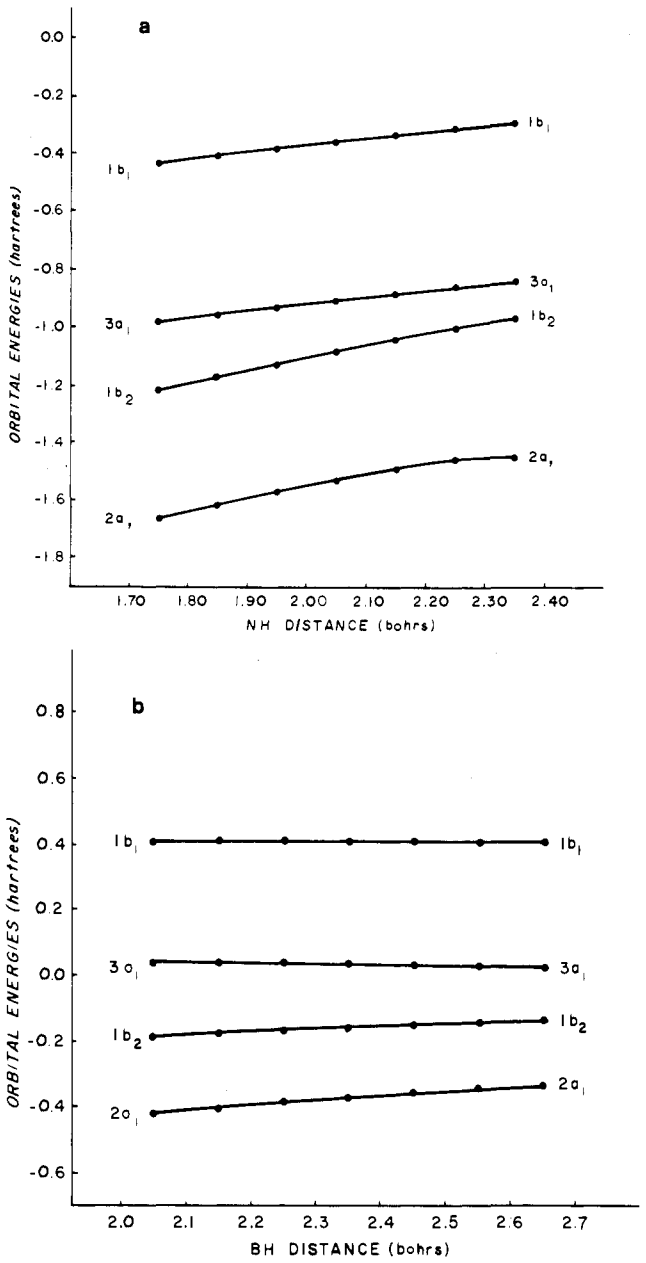

Figure 18. Calculated canonical orbital energies of the NH_2^+ (a) and BH_2^- (b) ground states, respectively, as a function of the corresponding AH bond distances.[21]

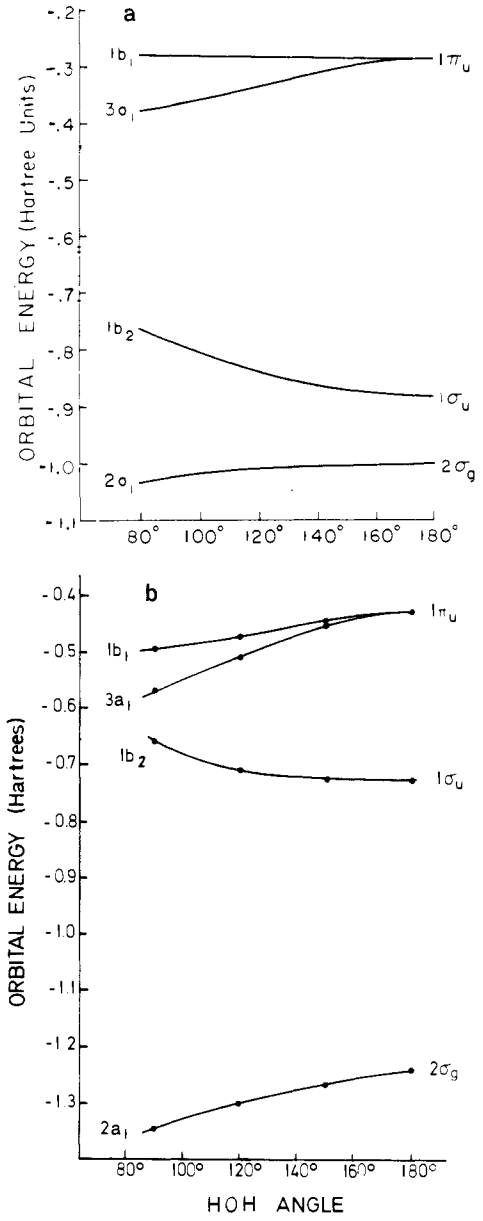

Figure 19. Calculated canonical orbital energies of the BH_2^+ (a) and H_2O (b) ground states, respectively, as a function of internuclear HAH angle.

tems, ultimately providing the often-mentioned rules[2] for relating the gross shapes of any given AH_2 member to its electronic configuration (systems with four valence electrons are linear in their ground states, while those with six to eight, respectively, are bent with roughly the same bond angle). As usual, *ab initio* SCF calculations have had no difficulty[21,94] in producing correlation diagrams (employing canonical orbital energies) which closely approximate that given empirically by Walsh[2] for general AH_2 systems (compare Figure 1a); the only real exception occurs in the case of the $2a_1$ species (see Figure 19a,b), whose orbital energy decreases with angle contrary to what Walsh has predicted in his diagram (Mulliken[96] had pointed out the error in Walsh's assumption in this case long before the above-mentioned SCF calculations were carried out). Furthermore, it is easily demonstrated that if one uses the SCF total *and orbital* energy results for virtually any member of this series in a given state, potential curves which are in complete agreement with the predictions of the MW model can be constructed by means of eq 9 for any other electronic configuration commonly exhibited by the AH_2 systems as a group.

Nevertheless, closer examination of the aforementioned SCF results[21,94] for a rather large series of AH_2 systems indicates that the MW model is not completely satisfactory for the prediction of all such bond angle trends, as must, of course, be expected from the fact that not all members of this family *possessing the same number of valence electrons* exhibit exactly the same internuclear angle in their respective ground states. Note, for example, the discrepancy between the shapes of the $1b_1$ (and also $1a_1$, not shown) orbital energy curves for BH_2^+ and H_2O, respectively, in Figure 19a,b; the curve in question has a definite downward slope in the case of H_2O, whereas for BH_2^+ the corresponding species remains very nearly constant with change in internuclear angle.[97] The original diagram of Walsh asserts that the $1b_1$ energy does remain constant for a general AH_2 system, and the argument given for this behavior is widely accepted:[59] the $1b_1$ is constructed *solely* from a $2p_x$ AO (perpendicular to the AH_2 plane) for *all* internuclear angles, and hence its binding energy should be independent

of said geometrical variable. The present authors have shown,[98] however, that this argument is *only* valid for the *kinetic* and *nuclear attraction* contributions to the $1b_1$ (or $1a_1$) orbital energy, that is, *for the terms which depend only on the charge distribution of this MO;* the average *electron repulsion* of such an orbital, however, *may vary with angle* since this quantity by definition (see eq 1, with the repulsion sum over occupied orbitals) depends not only on the charge distribution of the orbital *itself* but also quite obviously on *that of each of the other MO's of the system.* The calculated results for H_2O (but not for BH_2^+) show indeed that such variations in the $1b_1$ (and also $1a_1$) electron repulsion energy with $\angle$HAH bending can, in fact, be substantial.

From a correlation diagram constructed for BH_2^- (see Figure 1b of ref 21), it is apparent that the $1b_1$ and $1a_1$ orbital energies of this system also decrease with bending (although not as much as in H_2O); from these results it can be concluded that such behavior occurs *only if the* $3a_1$ *MO is occupied* in the system. This conclusion seems quite reasonable in light of the charge density contours of the $3a_1$ species (Figure 16) which show quite clearly that this orbital is not as symmetrically placed with respect to the $1b_1$ (or $1a_1$) for $\angle HAH = 105°$ as it is for linear geometry (in which case it is a pure $p\pi$ species). Furthermore, the fact that the $1b_1$ and $1a_1$ orbital energies decrease with $\angle$HAH whenever the $3a_1$ MO is occupied indicates unambiguously that the electron repulsion interaction between the former MO's and the latter is also *decreasing with internuclear angle.* The observation that this trend becomes increasingly stronger from BH_2^- to NH_2^+ (Figure 1a of ref 21) to H_2O indicates in addition that the effect depends significantly on the character of the central atom (see also the preceding discussion on AH stretch).

All this concern over some relatively minor change in the $1b_1$ and $1a_1$ orbital energies might be completely neglected were it not for the fact that changes of precisely the magnitudes under discussion do have an important effect on the interpretation of the molecular structure of AH_2 systems. Despite the fact that the two bent systems NH_2^+ and BH_2^- are isoelectronic, for example, actual SCF calculations[21] find that their bond angles differ by a relatively wide margin[99] ($\angle$HNH for NH_2^+ is 123°, $\angle$HAH for BH_2^- is 103°). Furthermore, the direction of such a discrepancy is the opposite of what would be expected on the basis of $\Sigma\epsilon_i$, which quantity clearly decreases faster toward smaller $\angle$HAH for NH_2^+ than for BH_2^-. Reference to eq 12 therefore shows unequivocally that this large difference in equilibrium angle must be attributed in the main to electron repulsion effects. From the above discussion it follows that V_{ee} for BH_2^- does *not decrease as fast* with bending as does the analogous quantity[100] for isoelectronic NH_2^+, and hence the additive potential term ($-\Delta V_{ee}$) is decreasing from NH_2^+ to BH_2^-, thereby causing the smaller equilibrium angle for the latter molecule.[47]

The electron repulsion effect also turns out to be the dominant factor in producing the well-known difference in bond angles between the isovalent pair H_2O ($\angle HOH = 104.52°$) and hydrogen sulfide, H_2S ($\angle HSH = 92.2°$).[101] Examination of *ab initio* SCF calculations for these two systems[99,102] shows that $\Sigma\epsilon_i$ for H_2O decreases *faster* with bending than the corresponding quantity for H_2S, so that an analysis based strictly on this quantity leads to the opposite (and clearly wrong) conclusion about which of the two systems is more bent. In the sense of eq 12 then, the reason that water has a larger equilibrium angle lies first and foremost in the fact that the electron repulsion V_{ee} *decreases faster* with diminishing HAH angle for this system (with its much more contracted valence charge distribution) than for H_2S (with a more diffuse electronic distribution); the parallel between the NH_2^+–BH_2^- comparison and the present one for H_2S and H_2O is quite apparent.

One of the interesting aspects of the foregoing calculations for H_2O and H_2S is the fact that inclusion of d-type orbitals in the basis set is found to have a much greater effect on the geometry of the system *with the first-row central atom* than for that containing the second-row species.[103] Such results clearly run contrary to heuristic speculations that the smaller H_2S angle comes about because the hybridization in this system is characterized by greater use of d AO's than that which is optimum for H_2O. In addition it is worth noting that while 3d functions can be used in producing a necessary change in calculated equilibrium angle to agree with that observed experimentally for H_2O, the same effect can be achieved by *substituting* s-type functions located *midway* between the respective pairs of O and H atoms.[90] Such results emphasize that the role of the d functions in the aforementioned H_2O calculation is not unique and hence is better described as a *polarization effect* rather than one of *hybridization;* the latter term would better be reserved for situations in which the population of d AO's is of the same magnitude as those of s and p type, a circumstance which is definitely *not* a characteristic of the electronic structure of *either* H_2O or H_2S.

The fact that the orbital energy of the $1b_1$ MO decreases with molecular bending (at least when the $3a_1$ is occupied) is more directly observable from several other experimental results. A Koopmans' theorem analysis based on the SCF results for water, for example, indicates that the $^2B_1$ ground state of H_2O^+ (obtained by ionization from the $1b_1$ MO) should possess a significantly larger equilibrium angle (by approximately 15°) than that of the un-ionized system. Studies of the various Rydberg series originating from the $1b_1$ in the electronic spectrum of H_2O, in fact, confirm this theoretical prediction. Since Walsh[2] assumed the $1b_1$ to be nonbonding, he had to rationalize this experimental finding by attributing *antibonding* character to the quite diffuse Rydberg MO. The present answer, namely that excitation (or ionization) from a *bonding* orbital ($1b_1$) occurs to the completely *nonbonding* Rydberg species, is clearly much more consistent with the expected diffuseness of the upper orbital in such transitions.

Similarly, it is found by means of a Koopmans' theorem analysis (eq 9) that a prototype AH_2 system with six valence electrons in a $^3B_1$ state (with $3a_1$ and $1b_1$ each singly occupied) possesses a bond angle of approximately 140°, in contrast to the 180° value assumed by Walsh[2] on the basis of his original correlation diagram. Again this disagreement is directly traceable to the fact that in the *ab initio* calculations the $1b_1$ orbital energy does decrease with bending whenever the $3a_1$ is also occupied, in contrast to the behavior indicated for this quantity in Walsh's early work. It is now believed[104-107] that the ground state of methylene CH_2 is a $^3B_1$ species with an equilibrium angle[108] of 134°, a result which is clearly more consistent with the present interpretation of the $1b_1$ orbital as favoring bent geometry.[109]

Despite the emphasis in the foregoing discussion on understanding the nature of certain anomalous features in the shapes of AH_2 systems it should not be overlooked that the simple MW model is remarkably successful in delineating the *basic trends* which occur among the equilibrium internuclear angles in this molecular family. It is

TABLE III. Bond Angle Trends in AH_2 Systems[a]

No.[b]	State	General MW trend	Behavior with bending $\Sigma\epsilon_i$	Behavior with bending V_{ee}	Horizontal correction (eq 12) for atoms A in Same row	Horizontal correction (eq 12) for atoms A in Same group	Examples
2	$2a_1^2$ $^1A_1$	Strongly bent ($2a_1$ occupied)	Decreases faster with more contracted charge density (bent trend)	Very little change	More bent with increasing atomic number ($\Sigma\epsilon_i$ dominant)	Less bent	LiH_2^+, very small angle
3	$2a_1^2 1b_2$ $^2B_2$	Very weakly linear ($1b_2$ singly occ)	Very little change		Quite small		LiH_2, BeH_2^+, BH_2^{2+}, all weakly linear
4	$2a_1^2 1b_2^2$ $^1A_1$	Linear ($1b_2$ doubly occ)	Increases somewhat faster with more contracted charge density (linear trend)	(bent trend)	Somewhat more strongly linear with increasing atomic number	Less	LiH_2^-, BeH_2, BH_2^+, MgH_2, all linear
5	$2a_1^2 1b_2^2 3a_1$ $^2A_1$	Bent (115-140) ($3a_1$ singly occ)	Decreases faster with more contracted charge density (bent trend)	(linear trend)	Less bent with increasing atomic number (V_{ee} dominant)	More bent	BeH_2^- (115-125), BH_2 (131), CH_2^+ (140), AlH_2 (119)
	$2a_1^2 1b_2^2 1b_1$ $^2B_1$	Linear ($1b_1$ energy independent of angle with $3a_1$ not occ)	Same as for $^1A_1$ with 4 valence electrons				BeH_2^-, BH_2, CH_2^+, AlH_2, all linear
6	$2a_1^2 1b_2^2 3a_1^2$ $^1A_1$	Strongly bent ($3a_1$ doubly occ)	Same as for $^2A_1$ with 5 electrons, except that effects are enhanced				BH_2^- (100), CH_2 (105), NH_2^+ (115-120), H_2O^{2+} (140-160), SiH_2 (90-95), H_2S^{2+} (95-100)
	$2a_1^2 1b_2^2 3a_1 1b_1$ $[^3B_1]$[c]	Weakly bent (125-180)	Decreases faster with more contracted charge density (bent trend)	(linear trend)	Same as for $^2A_1$ with 5 valence electrons		BH_2^- (125-130), CH_2 (134), NH_2^+ (145-155), H_2O^{2+} (160-180), SiH_2 (120-125), H_2S^{2+} (125-135)
7	$2a_1^2 1b_2^2 3a_1^2 1b_1$ $^2B_1$	Strongly bent ($1b_1$ has bent tendency)	Decreases faster with more contracted charge density (bent trend)	(linear trend)	Same as for $^2A_1$ with 5 valence electrons		CH_2^- (95-100), NH_2 (103), H_2O^+ (115-125), PH_2 (91), H_2S^+ (~95)
	$2a_1^2 1b_2^2 3a_1 1b_1^2$ $^2A_1$	Bent (120-160)	Same as for $^2B_1$ with 7 valence electrons but with less strongly bent trends				CH_2^- (120-125), NH_2 (135-145), H_2O^+ (145-160), PH_2 (123.1), H_2S^+ (120-130)
8	$2a_1^2 1b_2^2 3a_1^2 1b_1^2$ $^1A_1$	Very strongly bent (90-105)	Decreases faster with more contracted charge density (bent trend)	(linear trend)	Quite small ($\Sigma\epsilon_i$ trend enhanced because of $1b_1$ effect)	More bent with increasing atomic number (V_{ee} dominant)	NH_2^- (100-105), H_2O (104), H_2F^+ (~105), H_2S (92.2), H_2Se (91), H_2Te (90)

[a] Conclusions based on $\Sigma\epsilon_i$ and V_{ee} behavior are made with reference to eq 12 and existing experimental and calculated data. All angles are given in degrees. The notation for the electronic configurations is according to first-row members, *i.e.*, $2a_1$ is the first valence MO. [b] Number of valence electrons. [c] Similar trends are quite likely for the corresponding $^1B_1$ state.

only when one looks at *subtle differences* which occur between isovalent systems in this class that the need arises to look for modifications of the original model. In this way it is found that (a) orbital energy curves do vary from one system to another, particularly that of the $1b_1$ (and also $1a_1$) species, and (b) the electron repulsion term V_{ee} also varies somewhat differently with angle depending on the nature of the system.

Both effects become *more important the more contracted the valence charge distribution,* with the V_{ee} term (because $(-\Delta V_{ee})$ is dominant in eq 12) controlling geometrical distinctions between isovalent systems, but with the orbital energies alone controlling geometrical changes upon ionization (as always because of eq 9). As a result a new set of *supplementary* rules can be developed to explain such *secondary* effects in the geometries of AH_2 systems, with these being summarized in terms of a series of predicted equilibrium angles for a fairly large group of such molecules with first-row central atoms, as given in Table III. In preparing this table the authors have relied heavily on the aforementioned SCF calculations for the $^1A_1$ states of certain systems with six valence electrons in order to estimate the magnitude of geometrical differences between isoelectronic members of this family; supplementary calculations for BeH_2 and H_2O together with eq 9 have made many of the other predictions for ions of any given neutral system possible. (In particular it has been assumed that the $1b_1$ orbital energy decreases progressively faster with diminishing angle as the atomic number of the central nucleus is increased.) A similar table can be prepared for AH_2 systems with central atoms from higher rows of the periodic table by simply taking account of the general tendency of such molecules to possess smaller equilibrium angles than their first-row counterparts, as discussed above in connection with the H_2O–H_2S comparison.

2. AH_3 Systems

On the basis of the perturbed sphere model discussed in the preceding section, the interpretation of the geometry of AH_3 molecules is expected to closely parallel that

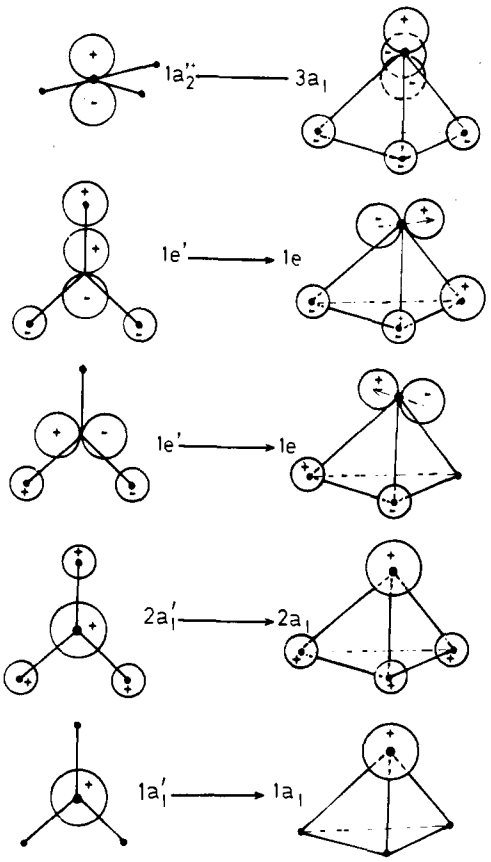

Figure 20. Schematic diagram representing the MO's of pyramidal and planar AH_3 molecules, respectively.

of AH_2 systems, since the presence of an additional hydrogen atom would not seem to change the general bonding characteristics in any significant manner. Such expectations are, in fact, borne out in actual calculations, with orbital charge density diagrams of a typical AH_3 system showing very much the same features as those discussed above for H_2O (Figure 16); a schematic representation of the AH_3 orbitals in terms of an LCAO expansion is given in Figure 20. The only real difference between the constitution of the MO's in these two classes of systems occurs in the fact that there is no orbital for the AH_3 molecules which remains essentially unchanged with ∠HAH variation, *i.e.*, one which is completely analogous to the $1b_1$ MO for AH_2 species. Indeed *both* p_x and p_y AO's of the central atom are involved in AH bonding (*via* the 1e degenerate MO of AH_3 systems) and not just the p_y orbital (as is the case for AH_2 molecules). Otherwise, there is an obvious resemblance between the $1a_1$, $2a_1$, and $3a_1$ MO's of a molecule such as NH_3 and the corresponding species (with the identical symmetry labels) in H_2O.

a. AH Stretch

The interpretation of the behavior of AH_3 systems upon AH stretch is virtually identical with that given for the analogous geometrical changes in AH_2 molecules; thus the bond lengths in AH_3 systems are observed to follow very nearly the same patterns that they do in corresponding AH and AH_2 molecules with the *same central atom and the same number of electrons* (see Table II). Thus the bond distance in ammonia (1.017 Å) is very similar to that in NH_2^- (1.03 Å) but not especially close to that of either H_2O (0.957 Å) or HF (0.917 Å), and the CH distances in CH_3^+ and CH_2 are almost identical (approximately 1.08 Å in each case), while the analogous quantity in isoelectronic BeH_3^- appears to be much larger (1.34 Å).[21,101] Indeed the view of discussing the origin of bond distance trends in such systems in terms of a perturbed-sphere model is also consistent with the fact that Joshi[110] has been able to obtain quite satisfactory bond distances for various numbers of the AH_3 family strictly on the basis of one-center calculations, that is, SCF treatments which include no hydrogenic basis functions whatsoever. In the case of NH_3, for example, his calculated value for the NH bond length of 0.984 Å is only slightly worse than the recent near Hartree–Fock result of Rauk, Clementi, and Allen[111] for the same quantity (1.000 Å *vs.* the experimental value of 1.017 Å).

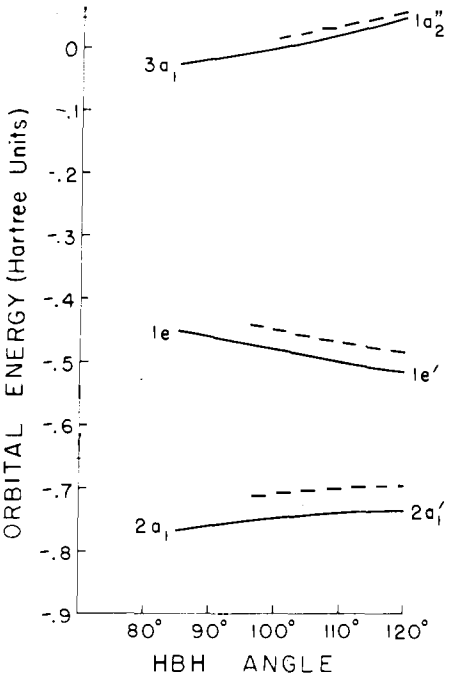

Figure 21. Calculated canonical orbital energies of BH_3 as a function of the HBH angle.[21] (Dashed lines refer to an SCF treatment with a more flexible basis set.)

b. ∠ *HAH Bending*

The comparison between ∠HAH bending characteristics in AH_2 and AH_3 molecules does not run quite as parallel as in the case of the AH stretch, mainly because the basic features of the angular orbital energy curves for each component of the 1e MO of AH_3 molecules are quite different from those of the $1b_1$ species for systems of the AH_2 class (see Figure 21). The situation is also changed somewhat because the $3a_1$ species (lone-pair orbital) in AH_3 systems is everywhere less stable than any of its valence counterparts, whereas the corresponding ($3a_1$) MO in AH_2 molecules is the *second least stable* orbital of this type (except for linear geometry, in which it is, of course, degenerate with the $1b_1$ species). As a result AH_3 systems with six valence electrons do not occupy the $3a_1$ MO ($1a_2''$ in planar symmetry) in their ground states, whereas AH_2 systems with the same number of electrons do occupy their $3a_1$ species at least once (see previous section).

This observation coupled with the knowledge of the shape of the 1e orbital energy curve (see Figure 21) led Walsh[2] to predict that all six-valence-electron AH_3 molecules are planar in their ground states. *Ab initio* SCF calculations[21] for BeH_3^-, BH_3, and CH_3^+ find that this supposition is, in fact, correct, with only small differences in the bending force constants of these systems being noted. Nevertheless the fact that the $2a_1$ orbital energy

decreases with bending (Figure 21) vitiates Walsh's more general conclusion that AH_3 systems with four or less valence electrons will also be planar. In fact, calculations by the authors[112] for BeH_3^+ (four valence electrons) suggest that this system is already distinctly nonplanar,[113] and there is no question that this trend away from planar structures is merely reinforced by the removal of still more valence electrons. On the other hand, the aforementioned calculations do find (with the help of eq 9) that each of the five-valence-electron species BeH_3, BH_3^+, and CH_3^{2+} is planar, in agreement with Walsh's original predictions.

For systems with more than six valence electrons, the lone-pair orbital $3a_1$-$1a_2''$ becomes occupied, and its increased stability away from the planar conformation (Figure 21) implies a strong trend toward pyramidal (or bent) equilibrium geometries for such molecules. It is, of course, well known that systems in this class with eight valence electrons such as NH_3, H_3O^+, and PH_3 do, *in fact*, possess nonplanar structures, but the magnitude of the bond angle in a given case varies significantly ($\angle HNH = 107.2°$, $\angle HOH = 117°$ and $\angle HPH = 93.5°$, respectively[101]).

The fact that the highest occupied orbital in these systems is so easily identifiable with a lone-pair species suggests rather clearly that the foregoing explanation for the change in geometry which occurs upon its occupation is very closely related to that given for the same phenomenon in terms of the *valence bond type of analysis used in the VSEPR structural model*[29] (which emphasizes the increased stability of the lone-pair orbital in pyramidal relative to planar nuclear arrangements as a result of diminished repulsion with the corresponding bond-pair species). The same type of comparison between these structural models can be made with regard to their treatment of the *shapes* of AH_2 molecules and, in fact, Bartell and Thompson[114] have shown on the basis of a more general analysis in terms of the localized orbitals of Ruedenberg and Edminston[115-117] that such a close relationship should be found quite generally.

Nevertheless the VSEPR model appears to hold a definite advantage over the simple MW model in this discussion since it has been used to rationalize the *differences* in the equilibrium geometries of NH_3, H_3O^+, and PH_3, respectively, whereas its MO counterpart can only assume (at least in its original form) that the shapes of these systems are *identical as a result of their equivalent electronic configurations*. From the discussion of the analogous question in the study of AH_2 systems, however, it is clear how this shortcoming of the MO model can be overcome, that is, by taking advantage of eq 12.

In fact, as should be expected on the basis of the perturbed-sphere model discussed above, it is found that the horizontal correction (in the sense of Figure 12) which must be applied to the MW model to account for such distinctions in the shapes of isovalent AH_3 species is dependent on very much the same factors as have been observed in the case of AH_2 systems. *Ab initio* SCF calculations by Shih[118] for NH_3 and PH_3, respectively, indicate once again that it is the electronic repulsion term which is dominant in determining *differences* in the shapes of such isovalent systems, with V_{ee} for PH_3 *increasing faster* with bending than the corresponding quantity for NH_3 (V_{ee} increases still less quickly in H_3O^+). Examination of eq 12 shows clearly that this fact tends to make PH_3 more bent[47] than NH_3 (and H_3O^+ less bent than either of the two). The $\Sigma\epsilon_i$ term produces a counteracting tendency, since it *decreases* increasingly faster with bending in the order $H_3O^+ > NH_3 > PH_3$, thereby tending to reduce the magnitude of the structural differences brought about by the V_{ee} term; just as before for the H_2O–H_2S and BH_2^-–NH_2^+ comparisons, however, this effect is found to be weaker than that caused by the electron repulsion term.

An interesting observation which emerges from this study is that the foregoing explanation is obviously based on the assumption (and the calculated finding[100,118]) that the (total) electron repulsion *increases at a faster rate* with bending for a system such as PH_3 than it does for a more contracted system such as NH_3. The VSEPR model, on the other hand, explains the *same set of geometrical distinctions* by assuming that certain orbital repulsion terms *decrease at a faster rate* with bending for the identical comparison.[119] While these two assumptions are not completely contradictory, they are also not obviously consistent with one another either, and thus there would appear to be considerable merit in examining the results of *ab initio* SCF calculations for the molecules under discussion in terms of both the canonical and the localized orbital representations to see how this seemingly paradoxical situation can actually be resolved.[120]

Before closing the discussion of AH_3 geometrical trends, it is well to consider a remaining group of systems in this family, namely those with seven valence electrons. According to Walsh's original presentation,[2] systems of this type should be nonplanar, although not as strongly so as their counterparts with eight valence electrons. If, on the other hand, advantage is taken of calculated canonical orbital energy correlation diagrams for systems with both six[21] and eight[118] valence electrons, the opposite behavior is predicted (on the basis of the differential form of Koopmans' theorem) for almost all such seven-valence-electron systems containing a first-row central atom; in fact, it is found that the trend toward planarity increases gradually as the electronegativity of the central atom increases, as might well be expected in light of experience with AH_3 systems containing eight valence electrons. Experimentally CH_3 is generally believed to be a weakly planar system,[101] and the foregoing analysis in terms of eq 9 predicts that NH_3^+ is also planar with a significantly *greater* curvature in its out-of-plane bending potential curve. On the other hand, such calculations suggest that BH_3^- is even less strongly planar than CH_3 (and, in fact, is probably slightly pyramidal), while the doubly negative species BeH_3^{2-} is indicated to be almost surely nonplanar.

Since PH_3 has a significantly smaller bond angle than ammonia, it follows that eight-valence electron AH_3 species composed of second (or higher) row atoms are much less likely to become planar upon ionization (at least out of the $3a_1$ MO). Thus PH_3^+ is predicted to be nonplanar in its ground state, although with a larger bond angle than its un-ionized counterpart; the trend toward nonplanarity should increase toward the left of the second row so that SiH_3 is predicted to be pyramidal in its ground state with an even smaller internuclear angle than PH_3^+. If ionization occurs from the 1e MO, the situation will clearly be altered since the orbital energy curve of this species shows the opposite behavior with bending as the $3a_1$ (see Figure 21). Thus the ^2E state of PH_3^+ undoubtedly possesses an even smaller equilibrium angle than PH_3 itself. Despite the fact that the analogous state for CH_3 is reported[121] to possess a planar geometry, there are strong reasons for believing that such a species is actually even more strongly bent than the ground state of CH_3^-, which in turn should be characterized by an internuclear angle of no more than 100° based on the Koopmans' theorem analysis given above. These and

TABLE IV. Bond Angle Trends in AH_3 Systems[a]

No.[b]	State	General MW trend	Behavior with bending $\Sigma\epsilon_i$	Behavior with bending V_{ee}	Horizontal correction (eq 12) for atoms A in Same row	Horizontal correction (eq 12) for atoms A in Same group	Examples
4	$2a_1^2 1e^2$ $^3A_2$	Bent ($2a_1$ trend apparently stronger than that of 1e)					LiH_3, BeH_3^+ (<90), Y-shaped
5	$2a_1^2 1e^3$ ^2E	Weakly planar (1e triply occ)	Increases somewhat less quickly[c] with more contracted charge density (planar trend)	Increases more contracted charge density (bent trend)	More strongly planar with increasing atomic number		BeH_3, BH_3^+, CH_3^{2+}, weakly planar, force const increases from Be to C
6	$2a_1^2 1e^4$ $^1A_1$	Strongly planar	Same as for ^2E with 5 valence electrons				BeH_3^-, BH_3, CH_3^+ planar, force const increases from Be to C
	$2a_1^2 1e^3 3a_1$ ^3E	Bent (more than 4-electron species)	Decreases faster[c] with more contracted charge density (bent trend)	Less strongly bent with increasing atomic number (V_{ee} dominant) (planar trend)	Somewhat More		BeH_3^- (90–100), BH_3 (100–110), CH_3^+ (110–120), AlH_3 (90–100)
7	$2a_1^2 1e^4 3a_1$ $^2A_1$	Slightly nonplanar to weakly planar ($3a_1$ occ)	Decreases faster with more contracted charge density (bent trend)	More strongly planar with increasing atomic number (V_{ee} dominant) (planar trend)	Somewhat Less		BeH_3^{2-} (105–115), BH_3^- (110–115), CH_3 (115–120), NH_3^+ (120), SiH_3 (105–115), PH_3^+ (110–120)
	$2a_1^2 1e^3 3a_1^2$ ^2E	Strongly bent ($3a_1$ doubly occ)	Decreases faster with more contracted charge density (bent trend)	Less strongly bent with increasing atomic number (V_{ee} dominant) (planar trend)	Somewhat More		BeH_3^{2-} ($\leq$85), BH_3^- (85–90), CH_3 (90–95), NH_3^+ (95–100), PH_3^+ (85–90)
8	$2a_1^2 1e^4 3a_1^2$ $^1A_1$	Bent ($3a_1$ doubly occ)	Same as for ^2E state with 7 valence electrons				H_3O^+ (118), NH_3 (107), CH_3^- (105),[d] PH_3 (93), AsH_3 (91.8)

[a] Conclusions based on $\Sigma\epsilon_i$ and V_{ee} behavior are made with reference to eq 12 and existing experimental data. All angles are given in degrees. The notation for the electronic configurations is similar to that in Table III; i.e., $2a_1$ is the first valence MO. [b] Number of valence electrons. [c] In general, the expression "decreases faster" is equivalent to "increases slower" or "less quickly". Furthermore, if, for example, the term "decreases faster" is used, it does not always mean that the quantity actually does decrease with the geometrical change, since in some cases the behavior depends on the specific system under consideration; V_{ee} decreases with bending in NH_3, for example, but it increases in PH_3. Thus it is only the *relative* behavior which is really important. [d] Footnote e of Table II.

other trends in the geometries of AH_3 systems are summarized in Table IV.

3. AH_4 Systems

No *ab initio* canonical orbital energy correlation diagrams have yet been reported for AH_4 systems, but Saturno[14] has given what appears to be a quite reasonable substitute on the basis of his united atom calculations.[11-13] What is seen from Saturno's diagram is that the triply degenerate t_2 MO of tetrahedral AH_4 systems is split apart into nondegenerate a_{2u} and doubly degenerate e_u species, respectively, upon continuous distortion into a square-planar geometry. The most interesting result of the study is the finding that the aforementioned nondegenerate species becomes *less stable* upon distortion out of the tetrahedral geometry while the companion degenerate MO is made more stable by such geometrical changes.

Removal of electrons from the a_{2u} species has thus been interpreted by Saturno[14] as resulting in a change from the tetrahedral geometry favored by such eight-valence-electron systems as CH_4 and NH_4^+. More recently Arents and Allen[122] have reported *ab initio* calculations for CH_4^+ and have, in fact, found that this system is distorted; these authors have related this result directly to the Jahn–Teller effect, but it is clear that it is also quite consistent with Saturno's observations in terms of the MW structural model. Saturno[14] has further predicted that six-valence-electron systems in this class (such as CH_4^{2+} or BH_4^+) should possess square-planar geometries, but there is apparently no experimental evidence or *ab initio* SCF calculations either to confirm or deny this supposition. In view of experience with the differential Koopmans' theorem discussed in section II.B.2, however, one might reasonably expect that an analysis of the aforementioned SCF results for CH_4^+ in terms of eq 9 should be capable of producing a reliable answer to this question. More recently, Gimarc[59] has reached many of the same conclusions as Saturno, based on the results of semiempirical (EHT) calculations.

B. Molecules Containing Two Nonhydrogenic Atoms

1. Simple Diatomics and Related Hydrogen-Containing Systems

In the previous section it has been emphasized that to a quite good approximation the MO's of AH_2, AH_3, and AH_4 systems can be described in terms of slightly perturbed atomic orbitals of the central A atom. An analogous relationship is also apparent between the orbitals of various hydrogen-containing systems with two heavy atoms and members of the family of simple (nonhydride) diatomics. In order to better characterize the nature of

TABLE V. Bond Distance Trends in Diatomic Molecules

No.[b]	State	General MW trend	Behavior with approach of nuclei $\Sigma\epsilon_i$	Behavior with approach of nuclei V_{ee}	Horizontal correction (eq 12) for atoms in Same row	Horizontal correction (eq 12) for atoms in Same group	Examples[a]
4	$2\sigma_g^2 2\sigma_u^2$ $^1\Sigma_g^+$	Very large distance (equal occupation of bonding and antibonding MO's)	Decreases faster with smaller difference in electronegativity between atoms (bonding trend)	Increases faster with smaller difference in electronegativity or less diffuse charge density (bonding trend)	Less bonding with greater difference in electronegativity (V_{ee} dominant)	Less bonding with greater diffuseness	BLi probably not bound, Be_2 ($\approx$4.0), Mg_2, even larger distance, if bound
6	$2\sigma_g^2 2\sigma_u^2 \pi_u^2$ $^3\Sigma_g^-$	Relatively large distance (only π_u bonding)					B_2 (1.59), BeC larger, Al_2 significantly larger
8	$2\sigma_g^2 2\sigma_u^2 \pi_u^4$ $1\Sigma_g^+$	Intermediate distance (two "extra" bonding MO's: π_u	Same as above		Same as above		C_2 (1.2422), BN (1.281), Si_2 larger
	$2\sigma_g^2 2\sigma_u^2 \pi_u^2 3\sigma_g^2$ $^3\Sigma_g^-$	and $3\sigma_g$, the latter more bonding)					
10	$2\sigma_g^2 2\sigma_u^2 3\sigma_g^2 \pi_u^4$ $^1\Sigma_g^+$	Small distance (three "extra" bonding MO's: $3\sigma_g$, π_u)	Same as above		Same as above		N_2 (1.094), CO (1.128), BF (1.262), P_2 (1.894), SiS (1.928)
	$2\sigma_g^2 2\sigma_u^2 3\sigma_g \pi_u^4 \pi_g$ $^{3,1}\Pi_g$	Somewhat larger distance (π_g antibonding)					N_2 ($^1\Pi_g$, 1.213)
12	$2\sigma_g^2 2\sigma_u^2 3\sigma_g^2 \pi_u^4 \pi_g^2$ $^3\Sigma_g^-$	Intermediate distance (two "extra" bonding MO's, since π_g antibonding)	Same as above		Same as above		O_2 (1.207), FN larger than O_2, S_2 (1.889)
14	$2\sigma_g^2 2\sigma_u^2 3\sigma_g^2 \pi_u^4 \pi_g^4$ $^1\Sigma_g^+$	Relatively large distance (only one "extra" bonding MO: $3\sigma_g$)	Same as above		Same as above		F_2 (1.435), Cl_2 (1.988)

[a] Values are given in Å and are in general taken from G. Herzberg, "Spectra of Diatomic Molecules," Van Nostrand, Princeton, N. J., 1966. [b] Number of valence electrons. The notation for the electronic configurations is according to first-row members; *i.e.*, $2\sigma_g$ is the first valence MO.

this relationship, the essential features of the electronic structure of simple diatomics, as first described by Mulliken,[33] are summarized in the following paragraph.

The valence MO's of a homonuclear diatomic molecule composed of first-row atoms are denoted as $2\sigma_g$, $2\sigma_u$, $3\sigma_g$, $1\pi_u$, $1\pi_g$, and $3\sigma_u$, respectively; the stability order of these orbitals is generally the same as written above, although in certain cases the $3\sigma_g$ and $1\pi_u$ species are interchanged.[123,124] All the σ_g and π_u species (in-phase overlap) are *bonding* and their occupation invariably leads to *increased binding* and *decreased bond distances;* the opposite behavior is found for each of the σ_u and π_g (antibonding) species. Each of these trends can be derived mathematically *via* the differential form of Koopmans' theorem (eq 9), as discussed in connection with the study of general bond distance relationships in section II.B.2. *Differences* in the bond lengths of *isovalent systems* are usually not adequately predicted by this simple principle, and hence a horizontal correction in terms of the two additive potential terms $\Delta\Sigma\epsilon_i$ and $(-\Delta V_{ee})$ of eq 12 must be applied in such cases. The magnitude and direction of such horizontal corrections are very nearly the same as for those described previously in connection with a study of bond length trends in simple triatomic (all heavy atoms) systems (section II.B.3). The electronegativity difference of the constituent atoms is again an important consideration and an equivalent pattern is observed as before when going from first- to second-row atoms,[125,126] as can be seen, for example, from Table V.

The foregoing analysis of the molecular orbitals of a diatomic molecule can easily be extended to the study of systems containing one or more hydrogen atoms in addition to the two nonhydrogenic species. This point is illustrated, for example, by means of a diagram (Figure 22) correlating the orbital energies of the C_2H_{2n} series of molecules,[85] beginning with the homonuclear diatomic C_2 and continuing with the more well-known hydrocarbon species acetylene (C_2H_2), ethylene (C_2H_4), and ethane (C_2H_6), respectively; the correlation scheme used therein is completely unambiguous because of group theoretical considerations. All of the orbital energy changes which occur from one system to the other in this figure are easily understandable, and in particular it is possible to distinguish two distinct effects in interpreting such results by which the presence of the hydrogenic species manifests itself.

The first of these, which is generally the only one actually considered, concerns changes in orbital stability caused *directly by altering the constitution of the MO itself.* The charge density contours of Figure 14a,b, for example, show quite clearly that hydrogen AO mixing is a very important factor in the composition of the $1b_{2u}$ MO of ethylene as compared with the corresponding π_u

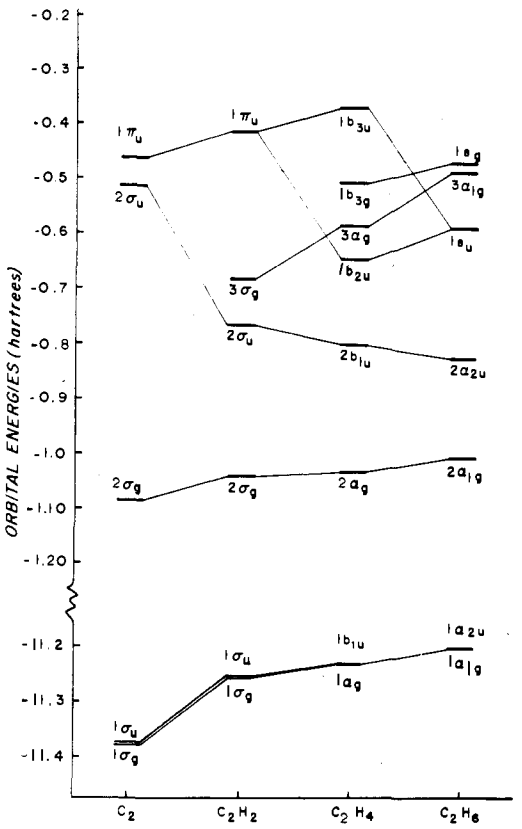

Figure 22. Correlation diagram for corresponding orbital energies in C_2, C_2H_2, C_2H_4, and C_2H_6, respectively, obtained from SCF calculations.[85]

species of the simple diatomic C_2, and as a consequence the orbital energy of the ethylene species is by far the lower (see Figure 22). A similar explanation can be given for increased stability of the $3\sigma_g$ MO of C_2H_2 (see Figure 13a,b) relative to the corresponding C_2 orbital (not occupied in the $^1\Sigma_g^+$ ground state of C_2, and hence not shown on the correlation diagram of Figure 22).

The second of these effects can be observed from calculated trends for *inner-shell orbital energies* ($1\sigma_g$-$1a_{1g}$ and $1\sigma_u$-$1a_{2u}$ species in Figure 22). This behavior obviously cannot be explained on the basis of *mixing* between hydrogen AO's and carbon 1s orbitals since charge density contours demonstrate that the *inner-shell orbitals themselves* are virtually identical for each member of the C_2H_{2n} series. In this case the changes in orbital energy are clearly not caused by distinctions in the composition of *their respective MO's* but rather by differences in the *external environment* of each heavy nucleus (as reflected in the magnitude of the electron repulsion term in eq 1) introduced as a result of the successive hydrogenation across the C_2H_{2n} series. In other words, the *primary* reason why the $1\sigma_g$ and $1\sigma_u$ orbital energies in acetylene are substantially higher than their counterparts in C_2 is the fact that the increase in electron repulsion which occurs for these MO's upon hydrogen addition significantly outweighs the corresponding increase in nuclear attraction which accompanies this process; such an effect is clearly consistent with the fact that only a relatively small amount of diamagnetic shielding is observed for acetylenic protons in nmr studies.[85] The same explanation has been given in connection with the study of certain orbital energy trends observed for AH_2 (and other AH_n) systems, again pertaining to MO's whose actual compositions are not significantly affected by relative motion of the constituent nuclei (see section III.A.1). Nor do the inner-shell MO's represent the only case in which such a shielding effect can be observed for the present C_2H_{2n} series; the results of Figure 22 also show that the $1\pi_u$ MO (for which H AO mixing is forbidden by symmetry) is likewise characterized by an increase in orbital energy from C_2 to C_2H_2 and finally to C_2H_4 (where it is denoted as $1b_{3u}$). Note also, however, that the corresponding orbital energy abruptly *decreases* from C_2H_4 to C_2H_6 ($1e_u$) as bonding with hydrogen AO's does become symmetry-allowed for the latter molecule (an effect of the first type). Because of Koopmans' theorem, the calculated orbital energy trends of Figure 22 are of *direct physical significance*, with these results running parallel to those observed experimentally for the *corresponding ionization potentials* for this group of molecules.[85]

Just as in the case of simple diatomic molecules, bond length trends can also be explained for ABH_n species, provided the effect of hydrogen addition upon the individual MO's of such systems (as discussed above) is taken into account. The analogy to the bond length changes in C_2, N_2, O_2, and F_2 is clear: the bond length of C_2H_2 (1.208 Å) is smaller than that of C_2 as a result of occupation of the *bonding* $3\sigma_g$ MO, whereas the corresponding quantity in ethylene (1.35 Å) and ethane (1.54 Å) becomes *progressively larger* as a result of differential occupation of the *antibonding* $1\pi_g$-type species.

On the other hand, a rather large horizontal correction must be made to account for *differences* in the bond lengths of isoelectronic A_2 and A_2H_2 counterparts; this fact is apparent from the observation that in N_2 the equilibrium separation is 0.10 Å less than R_{CC} in C_2H_2 while that of F_2 is 0.12 Å smaller than R_{CC} for the isoelectronic counterpart (C_2H_6). Such geometrical distinctions are not at all surprising, however, since (a) bonding with H AO's decreases the CC bonding (or antibonding) character of the C_2H_{2n} systems relative to that in a simple diatomic (see Figure 6 of ref 85) and (b) the charge distributions at the carbon atoms are much more diffuse in the hydrogenic systems than for the corresponding heavy atoms in isoelectronic diatomics not containing hydrogen atoms. As a result $\Sigma\epsilon_i$ in ethylene, for example, *decreases less strongly with approach of the heavy atoms* than the analogous quantity for isoelectronic O_2; at the same time V_{ee} for the hydrocarbon *increases less rapidly* with decreasing R_{CC} than it does for the analogous geometrical change in the isoelectronic diatomic. From eq 12 it is clear that both of these effects produce a trend toward larger bond lengths in the C_2H_{2n} systems relative to those in the corresponding series of homonuclear diatomics.[47,127] The fact that R_{CH} increases slightly[101] with successive addition of hydrogen in the C_2H_{2n} series is consistent with the general trends observed for AH bond lengths (see Table II) and is again understandable in terms of eq 12 because of the slight expansion of the charge distribution[85] of the carbon atom which occurs in going from C_2H_2 to C_2H_6.

The finding that hydrogen addition results in significant changes in orbital stabilities relative to what is observed for some parent diatomic molecule of the same number of electrons (especially as it pertains to the question of a possible *reordering* of orbital energies from one system to another) is also of great importance in the discussion of electronically excited states. Since spectral term values depend to a good approximation on the relative spacing of the (canonical) orbital energies, the results discussed above imply that some drastic changes in electronic transition energies to various excited states will be observed when certain hydrogenic systems are compared to isovalent diatomic species not containing hydrogen. Both Mulliken[84] and Walsh[2] have frequently made use of such orbital energy effects in interpreting molecular spectra on

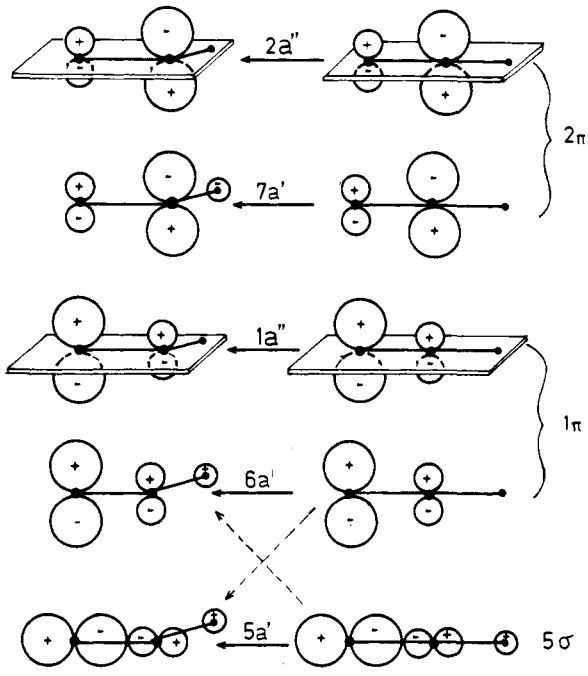

Figure 23. Schematic diagram representing the upper valence MO's of a linear and bent HAB molecule, respectively. (The relative stability of the 5σ and 1π MO's determines whether 5σ-5a' or 5σ-6a' is the correct correlation; see also ref 23.)

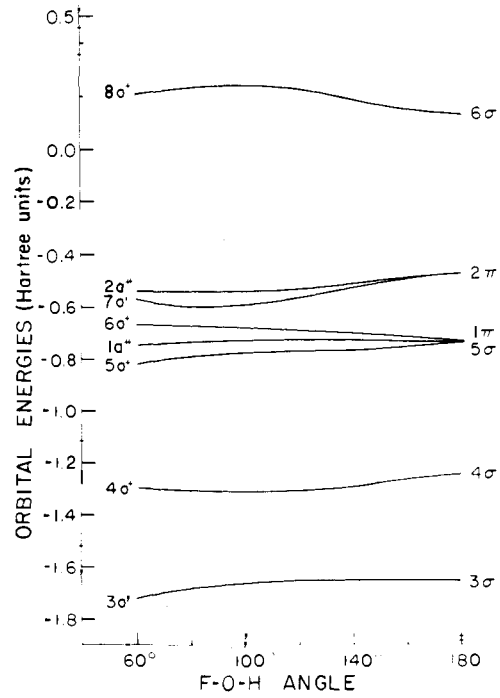

Figure 24. Calculated canonical orbital energies of FOH as a function of internuclear angle.[23]

a qualitative basis and, because of the foregoing analysis in terms of Koopmans' theorem (section II.B.2), it now seems clear that such a procedure can also be employed in considering such phenomena more quantitatively in terms of *ab initio* SCF (and CI) calculations.

2. *HAB Systems*

The simplest class of hydrogen-containing systems with a nonhydrogenic skeleton is, of course, the HAB family of molecules. Stable systems of this type are known which possess as few as 8 valence electrons (LiOH) to as many as 14 (FOH). The hydrogen atom in such systems invariably prefers the position adjacent to the more electropositive of the constituent atoms even though it is well known that stronger AH bonds can be formed with the more electronegative species (section III.A.1.a). Because of the electron transfer which occurs in the parent heteronuclear diatomic, however, the situation is clearly reversed relative to that which occurs when only one such heavy atom is present, and instead the depleted charge cloud of the less electronegative species is better able to effect stabilization *via* bonding with the quite polarizable hydrogen atom.[128] The same general trend also carries over to H_2AB systems, to be discussed in section III.B.4.

As usual the MO's of this family of molecules are clearly related to those of nonhydrogenic systems with the same heavy-atom skeleton, as can be judged from Figure 23; a description of each of these MO's, particularly as it relates to the behavior of its respective angular orbital energy curve, may be found in ref 23. Not surprisingly, this similarity is carried over into the study of the geometries of HAB systems, with trends in AB distances following much the same pattern as that discussed in the previous section for simple diatomics (see Table V). Generally speaking such distances are greater for HAB systems than for isoelectronic nonhydrogenic diatomics [for example, R_{CN} in HCN is significantly greater (1.156 Å) than R_{NN} (1.094 Å)] as long as the electronegativity difference between A and B is roughly the same in both systems.[129] As mentioned in section III.B.1, however, this tendency for added hydrogen atoms to lead to a lengthening in AB bonds relative to isoelectronic diatomics is somewhat dependent on the manner in which the H AO's contribute to the MO's of the hydrogenic system (see footnote 127); if, for example, such participation occurs almost exclusively through AB *antibonding* MO's as is the case in HNO (for which the H AO's mix quite strongly with π_g-type species in bent nuclear conformations), this trend becomes much less significant (R_{NO} in HNO is 1.21–1.24 Å as compared to R_{OO} in O_2 of 1.207 Å). Of course, it is to be expected that any effect which depends strongly on the number of hydrogens in a system will be of relatively minor significance for members of the HAB family, with only one such atom per molecule. The AH bond distances observed for these systems depend almost exclusively on the character of the attached heavy atom (see Table II); for example, R_{CH} values in HCN (1.064 Å) and in HCP (1.067 Å), respectively, are quite typical for triply bonded carbon atoms.

The third type of nuclear motion possible in such systems is HAB bending. A correlation diagram for this molecular family has been obtained[23] for FOH and is given in Figure 24; the same general trends in orbital stability are reproduced in the HCN diagram obtained by Pan and Allen,[43] although generally speaking they are less pronounced than in the FOH case. It should be noted that if the 5σ MO lies just slightly below the 1π for a linear conformation (as in FOH, for example; see Figure 24) it necessarily has to be correlated with a π-type species for the bent molecule, as can be seen from the actual calculated orbital charge densities for FOH (given in Figures 17–20 of ref 23); at the same time the in-plane component of the 1π MO must be correlated with a σ-type (a') species in the bent geometry. Hence an alternative correlation has been given for these MO's in the schematic diagram of Figure 23 (the decreased symmetry of the bent configuration and application of the noncrossing rule require such a correlation).

It is worth pointing out, however, that even if the 5σ and 1π MO's are separated by a great enough margin at

TABLE VI. Bond Angle Trends in HAB Systems[a]

No.[b]	State	General MW trend	Behavior with bending $\Sigma\epsilon_i$	Behavior with bending V_{ee}	Horizontal correction (eq 12) for central atom[c] In same row	Horizontal correction (eq 12) for central atom[c] In same group	Examples
8	$3\sigma^2 4\sigma^2 1\pi^4$ $^1\Sigma^+$	Weakly bent (5σ not yet occupied)[d]	Decreases faster with more concentrated charge density at central atom (bent trend)	(linear trend)	Less bent with increasing atomic number of central atom[c] (V_{ee} dominant)[e]	More	HCN^{2+} (bent), LiOH (weakly linear)
10	$3\sigma^2 4\sigma^2 1\pi^4 5\sigma^2$ $^1\Sigma^+$	Linear (5σ occupied)	Same as above		More strongly linear with increasing charge concentration at central atom		HCN (linear), FOH^{4+} (more strongly linear, Figure 11), HNN^+, HCO^+ (linear)
11	$3a'^2 4a'^2 1a''^2 5a'^2 6a'^2 7a'$ $^2A'$	Weakly bent (2π–$7a'$ singly occupied)	Same as above		Less bent with increasing charge concentration at central atom		HCO (119.5), HNN (bent)
12	$\ldots 7a'^2$ $^1A'$	Bent ($7a'$ doubly occupied)	Same as above		Same as above		HCF (101.6), HCCl (103.4)[f], HNO (108.6), HSiCl (102.8), HPO (104.7)
13	$\ldots 7a'^2 2a''$ $^2A''$	Bent ($2a''$ occupied)	Same as above		Same as above		HOO (106, calcd)[g]
14	$\ldots 7a'^2 2a''^2$ $^1A'$	Strongly bent ($7a'$, $2a''$ both doubly occupied)	Same as above		Same as above		HOF (97.2),[h] HOCl (113)[i,j]

[a] Conclusions drawn in the same manner as in Tables III and IV. Internuclear angles are given in degrees. [b] Number of valence electrons. [c] The terminal atom is also important as it withdraws or donates charge toward the central atom. [d] The alternative correlation (Figures 23 and 24) is assumed, in which case the 5σ in C_s symmetry favors linear geometry. [e] The trends discussed are based on the assumption that V_{ee} is dominant; they would be reversed if it were opposite, i.e., if $\Sigma\epsilon_i$ were dominant. [f] The charge at the central atom is more contracted than in HCF since F is withdrawing more charge than Cl. [g] D. H. Liskow, H. F. Schaefer, III, and C. F. Bender, *J. Amer. Chem. Soc.*, **93**, 6734 (1971); calculated value. [h] H, Kim, E. F. Pearson, and E. H. Appelman, *J. Chem. Phys.*, **56**, 1 (1972). [i] Charge at central atom more contracted than in HOF. [j] K. Hedberg and R. M. Badger, *J. Chem. Phys.*, **19**, 508 (1951).

180° so that σ and π character is preserved for these orbitals throughout the bending process, there still is a major difference between the calculated SCF correlation diagrams and that given empirically by Walsh[2] with respect to the shapes of the orbital energy curves of the first π-type MO. Walsh has explained the linear geometry of an HAB system with ten valence electrons (such as HCN) on the basis of a correlation diagram in which *both* the 5σ and 1π (in-plane component) become *less stable with bending* whereas the calculated SCF correlation diagram of Figure 24 actually shows that only *one* of these orbitals is in this category. The $p\sigma$ MO does become *less stable* with bending because of *decreased interaction* with the hydrogen AO's (Figure 24 and discussion in ref 23), but the in-plane component obviously becomes *more stable* as a result of *increased overlap* with the hydrogen AO's. Calculations based on Koopmans' theorem (eq 9) are successful in predicting the correct (linear) structure for a ten-valence-electron system (see Figure 11 and the discussion in section II.B.2) on the basis of a correlation diagram such as that obtained for FOH (Figure 24), thereby clearly demonstrating that Walsh's assumption of a *1π orbital energy which favors a linear nuclear arrangement is unnecessary* to explain the basic geometrical trends observed for this family of molecules.

The behavior of the 2π-$7a'$ orbital energy curve in the original diagram agrees qualitatively with the calculated behavior; occupation of this MO (and also that of the 2π-$2a''$ component) produces a trend toward bent structures as is observed in the change from linear HCN to the bent systems HNO and FOH, respectively (Figure 11).

As usual, however, closer examination of existing experimental (and calculated) results for the bond angles of HAB molecules shows that the broad qualitative predictions of the MW model need some refining in order to explain significant quantitative differences in the shapes of isovalent systems in this class (see Table VI). For example, there is apparently a spread of at least 7° in the ground-state equilibrium angles of known HAB systems with 12 valence electrons, with reported values varying from 101.6° in HCF to 108.6° in HNO; in addition the Koopmans' theorem analysis of the FOH SCF calculation[23] indicates (see Figure 11 for the curve marked "HNO")[130] that FOH^{2+} has a larger angle than any of the other isovalent HAB systems (about 120°).

In order to explain results of this type, it is necessary to derive a horizontal correction to the MW model by means of eq 12 (again with the aid of existing *ab initio* SCF calculations), and when this is done it is found that the situation is actually quite similar to that found in the study of AH_2 equilibrium angles. The $(-\Delta V_{ee})$ term in eq 12 appears to be the dominant factor in causing distinctions in the bond angles of HAB systems, particularly when the 2π-$7a'$ MO is occupied (recall the similar role played by the 1π-$3a_1$ species for the AH_2 molecular family), with this quantity *increasing with bending as the electronic distribution at the central atom A becomes more concentrated;* again the other term in eq 12 ($\Delta\Sigma\epsilon_i$) shows the opposite behavior but is apparently always a less significant factor than the electron repulsion difference referred to above. Consequently, applying this correction to the original form of the MW model leads one to conclude[47] that the *bond angles* for a given group of isovalent systems (at least as long as the 2π-$7a'$ species is occupied) *should increase as the charge distribution at the central atom becomes more concentrated* (compare also the discussion of the horizontal corrections for AH_2 and AH_3 molecules in their bending modes in section III.A.1,2).

Reference to Table VI shows that, in fact, this pattern is actually what is observed experimentally. For example, the charge concentration at the central atom is increased in HCCl relative to HCF and also in HOCl relative to HOF

(because of the change in the electronegativity at the end atom), and in both comparisons it is the first member which possesses the larger equilibrium angle. A similar change occurs from HSiCl to HCCl, with the concentration of (valence) electronic charge increasing from Si to C, again causing the bond angle to open up (see Table VI). Furthermore, HNO clearly possesses a more concentrated central atom charge distribution than either of its aforementioned isovalent counterparts HOCl or HCF, and thus again because of the dominance of the electron repulsion term in eq 12 is expected to have a larger bond angle than each of these systems, as, in fact, is observed; the fact that the central atom in FOH^{2+} possesses a still more concentrated electronic charge distribution is also consistent with this general trend, at least on the basis of Koopmans' theorem results discussed earlier (see Figure 11).

The general techniques of the MW model are also quite satisfactory for the prediction of the gross shapes of HAB systems *in their excited states.* Once again application of eq 9 using the results of SCF calculations for a typical HAB system is able to reproduce the general conclusions of the MW model as they pertain to the geometry of excited states; for example, $^{3,1}A''$ ($7a' \rightarrow 2a''$) states of 12-valence-electron HAB species are predicted to be uniformly less bent than the corresponding ground states as a result of the transfer of an electron to an MO with decreased tendency toward bent geometry (see Figure 24). Similarly, one can use this theoretical procedure to explain the fact that the lowest excited states of ten-valence-electron HAB molecules (such as HCN, for example) are characterized[131] by bent nuclear structures in contrast to what is observed for their respective ground states; in this case, as Walsh has pointed out in his original work, the reason for the change in geometry is the excitation of an electron from an orbital which is more stable for a linear conformation (1π-$6a'$) to one with the opposite characteristic (2π-$7a'$).

At present there are still some experimental results which do not seem to be so easily explained according to the foregoing model, however, such as the finding that the equilibrium angle of HNO in its $^1A''$ excited state is considerably smaller than that for the corresponding HCF species[132,133] (with a less concentrated electron distribution at its central atom) and also the conclusion that the ground-state bond angle of HCO is somewhat less[133] than 120° (see Table VI) despite the fact that in this electronic configuration the 2π-$7a'$ MO is only singly occupied (11 valence electrons). Both of these points are being studied at the present time by means of *ab initio* SCF and CI calculations.[134] But even granting these exceptional cases, it seems safe to say that the MW model, especially as corrected by means of eq 12, is quite capable of giving an accurate description of the geometrical relationships that exist within the HAB family, as well as of pointing up certain striking similarities between such systems and those of AH_2 type. The various trends in HAB bond angles which have emerged from the foregoing study are summarized in Table VI, and these in turn should be compared with the analogous results given earlier for the AH_2 family of molecules (Table III).

3. A_2H_2 Systems

There are two distinct ways in which two hydrogen atoms can be bonded to the skeleton of a simple AB diatomic molecule: both at the same heavy atom or one at each of them. The empirical finding is that molecules of the type HABH are favored only if the parent diatomic is of the *homonuclear* variety, as, for example, in acetylene (C_2H_2), diimide (N_2H_2), and hydrogen peroxide (O_2H_2).

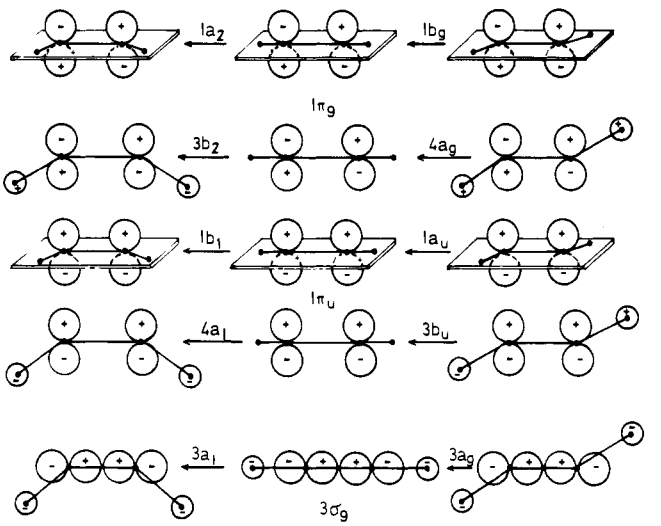

Figure 25. Schematic diagram representing the upper valence MO's in cis and trans A_2H_2 molecules and in the corresponding linear conformer, respectively.

In a situation in which there are two *different* atoms to choose from, both of the hydrogen species apparently prefer bonding at the same site. Furthermore, the fact that the diimide isomer $H_2N^+N^-$, in which both hydrogens are bound to the same heavy atom of an N_2 skeleton, is apparently only slightly less stable than diimide itself[135] suggests rather strongly that there is virtually never any *strong* preference for the formation of symmetric A_2H_2 systems.

One reason for the observed paucity of systems in this molecular family might be the fact that the presence of the hydrogen atoms invariably reduces the bond strengths between the nonhydrogenic species in such molecules, as compared to those found to exist for isoelectronic simple diatomics.[85] Thus C_2H_2, N_2H_2, and O_2H_2 all have somewhat greater R_{AA} values than the corresponding isovalent diatomic systems N_2, O_2, and F_2, respectively; this rather general diminution in AA bonding upon hydrogenation coupled with a simultaneous reduction in the rate of change of the total electronic repulsion has been discussed earlier with reference to eq 12 (section III.B.1). It is not surprising then that systems such as B_2H_2 or Be_2H_2 are apparently not bound with respect to dissociation into two AH fragments since the bonds in the corresponding isoelectronic diatomics C_2 and B_2 are already rather weak. Similarly the considerably reduced binding energies of simple diatomics[125] containing atoms in the second and higher rows of the periodic table are likewise quite consistent with the failure to observe stable HAAH systems composed of other than first-row heavy atoms; the system Si_2H_2, for example, is unstable with respect to dissociation into two SiH radicals.

Rotation of the AH bonds in such systems relative to a linear nuclear arrangement leads to a number of possible structures of which the cis, trans, and skewed conformations will be discussed below. The higher lying valence MO's of A_2H_2 systems are shown in Figure 25 for the cis, linear, and trans conformations, respectively, and are seen to be quite similar to the analogous species in HAB molecules (see Figure 23). Nevertheless, these similarities are not carried over entirely into the appearance of the angular correlation diagrams of both types of systems, as can be seen by comparing the calculated C_2H_2 and Si_2H_2 results[136-140] in Figure 26a,b with analogous data for FOH (Figure 24). In the case of trans distortions, most of the discrepancies (if not all of them) are found to stem from the fact that the $3a_g$ and $3b_u$ MO's retain their

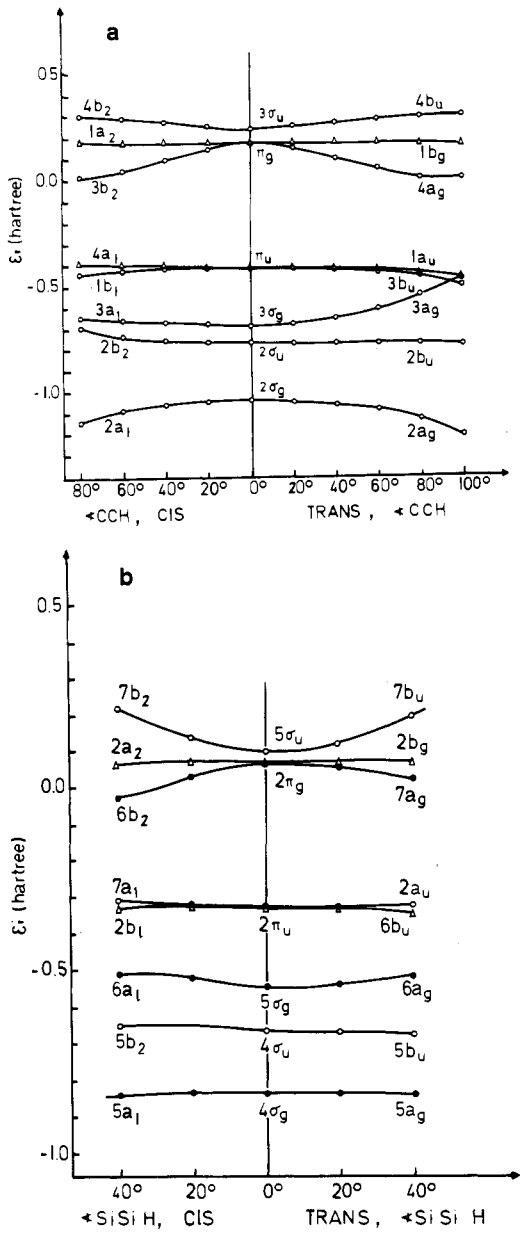

Figure 26. Calculated correlation diagram for the valence MO's in *cis*- and *trans*-acetylene,[137] C_2H_2 (a), and *cis*- and *trans*-Si_2H_2 (b).[139,140]

identity throughout the entire bending process for the A_2H_2 systems, whereas as discussed before the analogous species for HAB molecules are generally transformed into one another[141] (section III.B.2).

Again it is found that the lowest π-type MO (in-plane component $3b_u$) becomes *more* stable as the internuclear angle decreases (Figure 26a,b), contrary to what is shown in Walsh's generalized A_2H_2 diagram; the same distinction has been found to exist between calculated and empirical HAB correlation diagrams. Interestingly enough, however, the same MO ($4a_1$) becomes *less* stable on bending into the cis conformation (see Figure 26a,b), a result which has been interpreted by Gimarc[60] as resulting from the operation of the noncrossing rule (since $p\sigma$ and in-plane $p\pi$ MO's belong to the same symmetry species in cis but not trans geometries). Examination of the pertinent SCF results[137] indicates that the charge distribution of the $3a_1$ and $4a_1$ MO's, respectively, are increasingly confined to the same region of space upon cis bending, and thus that increased electronic repulsion[142] causes the destabilization of the $4a_1$ species for this type of geometrical motion; the change of hybridization for the corresponding MO's ($3a_g$ and $3b_{3u}$, respectively) in the trans bending mode produces the opposite behavior (see Figure A9–A13 in ref 137), thereby avoiding this destabilizing effect to a great extent. The behavior of the second π-type orbital energy is much more readily understood, just as in the case of the HAB correlation diagram; the fact that the in-plane component of this MO becomes much more stable on bending (into either the cis or trans nuclear arrangements; Figure 26a,b) is again the key in the MW model for the explanation of the nonlinear equilibrium geometries in the ground states of all such systems in this class with more than ten valence electrons.

The orbital energy trends discussed above can be used in the usual manner to rationalize and/or predict equilibrium structures for members of the A_2H_2 family, including many such systems not discussed in Walsh's original presentation.[2] For example, if ionization in acetylene takes place from the $1\pi_u$ MO (producing the $^2\Pi_u$ ground state of $C_2H_2^+$), a Koopmans' theorem analysis of Kammer's acetylene results[138] indicates that the resulting species is even more strongly linear than the neutral ground state (see Figure 26a,b); if the electron is lost from the $3\sigma_g$, however, application of eq 9 finds that the acetylene ion in the resulting $^2\Sigma_g^+$ state actually prefers a bent (trans) geometry. The CC bond length of the positive ion in the $^2\Pi_u$ state is also expected to be substantially larger than in acetylene itself, while the corresponding change is probably relatively small if ionization occurs from the $3\sigma_g$ species (see Figure 6 of ref 85 for the pertinent R_{CC}-stretching correlation diagram).

Just as with the class of HAB systems, it is found that all systems of A_2H_2 type possessing ten valence electrons (with all valence MO's except the $2\pi_u$ fully occupied) prefer linear geometries. The same type of horizontal correction to the MW model must be applied as before in order to account for distinctions in the strength of this linear trend for isovalent A_2H_2 systems, *i.e.*, it is again the electron repulsion term which is dominant in such corrections (see eq 12), with the usual result that the linear trend weakens as the electronic charge distribution at the central atom becomes less concentrated (see Table VII). Thus it is found, for example, that the Si_2H_2 ground state angular potential curve[140] shows less curvature in the neighborhood of the linear geometry than does its C_2H_2 counterpart.[138]

Systems with 11 valence electrons, as, for example, $C_2H_2^-$ and $N_2H_2^+$, are found to prefer bent geometries in their ground states, as a result of occupation of the in-plane component of the π_g MO (see Figure 26a,b). A Koopmans' theorem analysis of C_2H_2 and N_2H_2 SCF results indicates that $N_2H_2^+$ has a somewhat stronger bent trend than $C_2H_2^-$, thereby suggesting that in this case it is the $\Delta\Sigma\epsilon_i$ term which is dominant in eq 12 for comparison of these systems (see Table VII), although explicit SCF calculations would have to be carried out to be certain on this point. Both of these systems have larger AA bond lengths than that of ground-state acetylene because of occupation of the $1\pi_g$ MO, with its strong antibonding character[68] (see Table V).

Molecules in this class with 12 valence electrons doubly occupy the π_g MO in their ground states and are thus more strongly bent than either $C_2H_2^-$ or $N_2H_2^+$. In the case of diimide (N_2H_2) the major question has been whether a cis or a trans nuclear conformation is preferred; consideration of the various calculated correlation diagrams indicates that a definite prediction (based on orbital energy behavior alone) as to which of the two

TABLE VII. Bond Angle Trends in A_2H_2 Systems[a]

No.[b]	State	General MW trend	Behavior with bending $\Sigma\epsilon_i$	Behavior with bending V_{ee}	Horizontal correction (eq 12) for atoms A in Same row	Horizontal correction (eq 12) for atoms A in Same group	Examples
8	$\ldots 3\sigma_g^2 1\pi_u^2$ $^3\Sigma_g^-$	Strongly linear (π_u only half occupied)	Increases faster with more contracted charge density at central atoms (linear trend)	Decreases (linear trend)	More strongly linear with increasing atomic number of A	Less strongly	B_2H_2 (should be linear)
9	$\ldots 3\sigma_g^2 1\pi_u^3$ $^2\pi_u$	Linear (π_u triply occ)	Same as above		Same as above		$B_2H_2^-$, $C_2H_2^+$ (more strongly linear)
	$\ldots 3\sigma_g 1\pi_u^4$ $^2\Sigma_g^+$	Bent (π_u fully occ while $3\sigma_g$ only singly occ	Decreases faster with more contracted charge density at central atoms A (bent trend)	Increases (linear trend)	Less strongly bent with increasing atomic number of A (V_{ee} dominant in horizontal correct.)	More strongly	$C_2H_2^+$ (weakly bent, 10-30, cis), $Si_2H_2^+$ (25-55)
10	$\ldots 3\sigma_g^2 1\pi_u^4$ $^1\Sigma_g^+$	Linear	Increases faster with more contracted charge density at central atoms A (bent trend)	Decreases (linear trend)	More strongly linear with increasing atomic number of A	Less strongly	C_2H_2 linear, Si_2H_2 linear (smaller bending force const), $N_2H_2^{2+}$ linear
	$\ldots 3\sigma_g^2 1\pi_u^3 1\pi_g$ $^3\Sigma_u^+(^3B_u, ^3B_2)$	Bent (π_g occupied, in-plane component)	Decreases faster with more contracted charge density at central atoms (bent trend)	Increases (linear trend)	More strongly bent with increasing atomic number of A ($\Sigma\epsilon_i$ dominant)	Less strongly	C_2H_2 (40-50, trans), Si_2H_2 (30-40, presumably cis)
11	$\ldots 3\sigma_g^2 1\pi_u^4 1\pi_g$ $^2\pi_g$ (^2A_g, $^2B_2$)	Bent (in-plane π_g component occ)	Same as above		Same as above		$C_2H_2^-$ (45-55, trans), $N_2H_2^+$ (50-60, trans)
12	$\ldots 3\sigma_g^2 1\pi_u^4 1\pi_g^2$ ^1A_g, $^1A_1$	Bent (π_g doubly occ)	Same as above		Same as above		N_2H_2 (70, trans)
14	$\ldots 3\sigma_g^2 1\pi_u^4 1\pi_g^4$ ^1A	Bent (skewed)	Same as above		Same as above		H_2O_2 (83, trans, 112 skewed), H_2S_2

[a] Conclusions are drawn in a similar manner as in corresponding previous tables. Internuclear angles are given in degrees; 0° corresponds to a linear nuclear arrangement in this case. [b] Number of valence electrons. The notation for the electronic configurations is according to first-row members; *i.e.*, $2\sigma_g$ is the first valence MO.

N_2H_2 isomers is the more stable is not really possible. In spectroscopic studies it has sometimes been assumed[143] that the ground state of this system is a triplet just as it is for isoelectronic O_2, but there seems little question now that it is in reality a singlet species,[135,144-145] analogous to that of isoelectronic[134] HNO. Alster and Burnelle[146] have determined *via* semiempirical calculations that cis-trans isomerization of diimide occurs most easily *via* a geometrical path in which *only one of the NH bonds* is rotated in the molecular plane to the opposite side of the NN bond, a finding which clearly emphasizes the importance of NH bonding in producing molecular stability for this system since such a path provides for the minimal loss in H AO mixing for this process. Recent *ab initio* SCF calculations[135,144] have indicated that it is the trans isomer which is favored, and a more recent CI study[145] has reached the same conclusion.[147]

Addition of more electrons to the π_g-type MO of A_2H_2 systems not only enhances the trend toward bent geometry and increased central bond lengths but also produces a tendency toward skewed structures such as in the case of hydrogen peroxide H_2O_2 (14 valence electrons). Such additional distortions are again consistent with the tendency to relieve the unfavorable situation which develops from greater and greater occupation of the π_g species (with its nodal plane between the heavy nuclei), as discussed earlier in connection with a more general study of geometrical trends in hydrogen-containing systems possessing a diatomic skeleton.[68] Nevertheless, the rotational barrier restricting this system to a nonplanar geometry is relatively small, and thus again it is questionable whether the simple MW model is really adequate for making the fine distinctions required to determine the gross molecular shapes in this case.

As usual details of the geometry of excited states in this molecular family are also forthcoming from the MW model, with the most well-known applications occurring for the spectrum of acetylene. The lowest excited states of this system result from a $1\pi_u \rightarrow 1\pi_g$ excitation, and a straightforward analysis of the SCF results for either the acetylene[137,138] or the diimide[145] ground state by means of the differential form of Koopmans' theorem leads quite unambiguously to the conclusion that all such species should prefer a bent nuclear arrangement, again in qualitative agreement with the predictions of the simple MW model. Experimental measurements[148,149] have confirmed that the lowest lying singlet species of this type does prefer a bent (trans) geometry, but fairly extended CI calculations by Kammer[138] have indicated quite strongly that not all multiplets resulting from such a $\pi_u^3\pi_g$ configuration favor the same structure (see Figure 27). The lowest triplet of this type ($^3\Sigma_u^+$-$^3B_2$), for example, is calculated to prefer a cis nuclear conformation, while the two spatial components of the next triplet ($^3\Delta_u$) are found to prefer bent trans and nearly linear geometries, respectively; the least stable triplet of this type ($^3\Sigma_u^-$) is also calculated[138] to prefer a nearly linear geometry (Figure 27). In these cases the MW model can still be used to predict at least some of the geometrical distinctions on the basis of *which components of the* $1\pi_u$ *and* $1\pi_g$ *species* are actually involved in a specific transition, but to proceed further it is necessary to have at least a rough idea of the form of the multideterminantal wave function for each of these species.

Certainly one interesting feature concerning the multiplets of the $\pi_u^3\pi_g$ configuration of acetylene is the finding that the order of its singlets is exactly inverted relative to that of the triplets of this type (Figure 27). This observation was first made by Ross on the basis of some semiempirical calculations[150] and was later reaffirmed by means of *ab initio* CI calculations[151] (and again *via* Kammer's more recent CI study[138]). According to these cal-

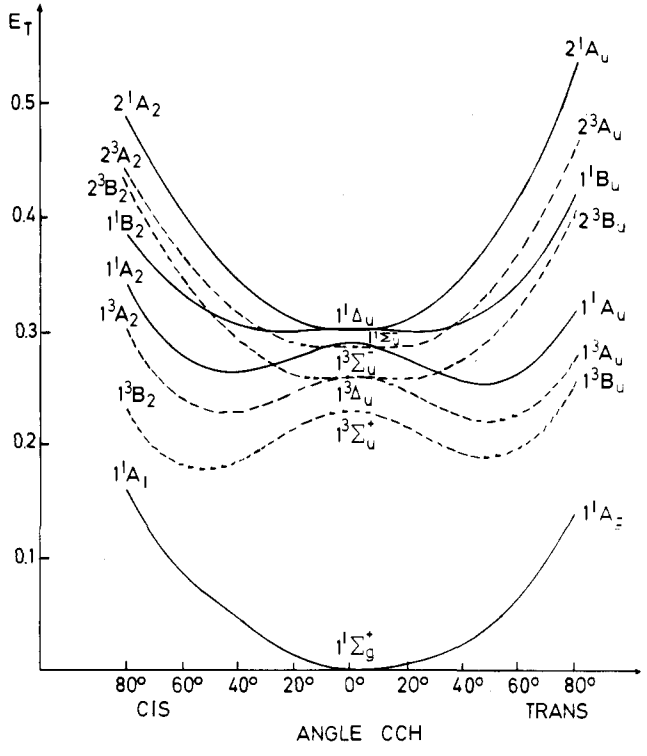

Figure 27. Calculated angular potential curves for various states of *cis*- and *trans*-acetylene, obtained from a limited CI treatment.[138]

culations the most stable singlet state of this type is a $^1\Sigma_u^-$ species rather than the $^1\Delta_u$ multiplet assumed by Walsh in his early interpretation of the acetylene electronic spectrum. A comparative study of the excited states of the isovalent silicon analog[140] has led to similar findings for the spectrum of this (unstable) system.

The electronic spectrum of diimide is not as accessible to experimental study as is that of acetylene. The most stable configuration of this system in *linear* geometry clearly is π_g^2, the same as that of isoelectronic O_2 and HNO in analogous nuclear arrangements. The presence of the hydrogen atoms in both HNO and N_2H_2 leads to a splitting of the π_g MO in bent geometries, however, and not at all surprisingly it is found[134,135] that this effect is significantly stronger for A_2H_2 systems than for the monohydrogenic HAB species discussed in section III.B.2. In trans geometry the order of multiplets in N_2H_2 is a_g^2 ^1A_g, $a_g b_g$ $^{3,1}B_g$, and b_g^2 ^1A_g, which, of course, is different from the order in the linear structures, for which the most stable state is a triplet (just as for isoelectronic O_2). The tendency toward bent geometry in these states weakens as the electrons are removed from the more stable a_g species (see Figure 26a,b) and placed instead in the out-of-plane b_g MO; thus according to the calculations[145] the a_g^2 ground state of N_2H_2 favors a 70° trans conformation, while the higher energy b_g^2 species is actually weakly linear.[152]

The effect of the additional hydrogen atom in A_2H_2 systems as compared to those of HAB type can be judged by the greater size of the ^1A_g–^3B_g splitting calculated for diimide in its ground-state equilibrium geometry[145] *vis-à-vis* the analogous singlet–triplet separation for isoelectronic[134] HNO. The gradual changeover from a triplet ground state in O_2 to a singlet species in N_2H_2 is quite apparent in this comparison, with HNO representing an obvious intermediate situation between these two extremes having a quite small singlet–triplet energy splitting. All of these relationships are clearly consistent with the general considerations of the MW model, especially if

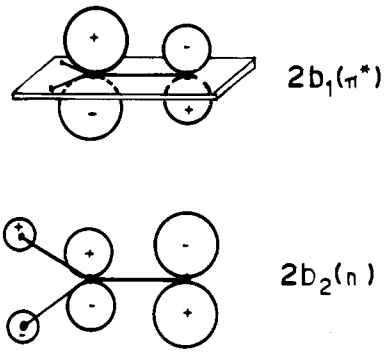

Figure 28. Schematic diagram representing the n and π^* orbitals of an H_2AB molecule.

one looks at the three systems O_2, HNO, and N_2H_2 as fundamentally heavy-atom diatomics with differing degrees of perturbation effected by the various numbers of hydrogen atoms in the molecules of this series (see section III.B.1). A summary of experimental and calculated trends in the shapes of A_2H_2 systems is contained in Table VII and this should be compared with the very similar results discussed earlier for members of the HAB family of molecules (Table VI).

4. H_2AB Systems

As mentioned in the previous subsection systems consisting of two *different* heavy atoms and a pair of hydrogenic species invariably prefer an H_2AB structure (both H atoms on the same side of the molecule). The AB bond lengths in such systems again follow a pattern similar to that noted above for the family of simple diatomics (Table V), but some clear distinctions do arise as a result of the fact that the π_g-type orbitals (generally denoted as n and π^*, respectively; see Figure 28) *are not equivalent* in the reduced symmetry of the molecules in this category. Although both of these species possess nodal planes between the constituent heavy nuclei, that of the π^* is considerably more pronounced since the n orbital is *localized* to a large extent at the B atom of such systems; consequently, while the π^* is a normal *antibonding* MO in this case, the n is generally considered to be *nonbonding* (although, in fact, it too is somewhat antibonding).

Consequently, a Koopmans' theorem analysis of an H_2AB prototype system (such as formaldehyde, H_2CO) shows that addition of electrons to the π^* is marked by a lengthening of the AB bond of about the same magnitude as is observed for the analogous population of π_g MO's in homonuclear diatomics (Table V), but that occupation of the n orbital leads to a *much smaller increase* in R_{AB}. Translated into practical terms for the ground states of H_2AB molecules, this finding indicates that there is a gradual increase in R_{AB} from 10- to 12-valence-electron systems (for which the n orbital is successively populated), followed by a much more pronounced increase in going from systems with 12 to those with 14 valence electrons. Indeed the same type of behavior can be seen in the bond lengths of HAB systems, with R_{AB} increasing by only about 0.05 Å from HCN to HNO (10 to 12 valence electrons) but by nearly 0.20 Å from HNO to FOH (12 to 14 valence electrons; see Table VI) and is also apparent from the analogous data for A_2H_2 species, with R_{OO} in H_2O_2 being much larger than R_{NN} in N_2H_2 but with much less difference between the heavy-atom bond lengths of N_2H_2 and C_2H_2, respectively (see Table VII).[153]

The main interest in the shapes of H_2AB molecules

has generally centered around the question of whether such systems are planar or nonplanar; all known species with 12 or less valence electrons (H_2CN, H_2CO, H_2CS, for example) are believed to be planar, whereas those with 13 or 14 (the maximum number normally observed) are thought to be nonplanar (H_2CF, H_2NF, H_2NCl). As mentioned above, the MO's which are differentially occupied in the ground states of this series of molecules are the n and π^* species, respectively (see Figure 28). The original Walsh diagram[2] for this class of systems shows the π orbital energy to decrease with out-of-plane bending but the corresponding quantity for the n MO to be independent of $\angle$HAB; more recently Gimarc[60] (on the basis of semiempirical calculations) has reported the same type of orbital energy trends for the H_2AB family. The results of *ab initio* calculations[154] are in essential agreement with the foregoing analysis as it regards the π^* species but, nevertheless, find that the n orbital actually becomes somewhat *less stable* as bending out of the molecular plane proceeds (see Figure 29a,b), apparently because for this species the H and B AO's approach each other through a nodal plane (see Figure 6a,b of ref 154 as well as Figure 28 of the present work). As a result because of the foregoing orbital energy trends, it follows quite easily by means of Koopmans' theorem analysis of the aforementioned SCF results of H_2CO that systems with *12 valence electrons* are in their ground state the *most strongly planar* of all members of the H_2AB family with from 10 to 14 valence electrons; not only do those with 13 and 14 valence electrons become *nonplanar* as a result of the *occupation of the π^* MO* but also those with 10 and 11, respectively, become *less strongly planar* compared to those with 12 upon removal of electrons from the n species.

From a more general point of view it is important to note that the orbital energy trends found in Figure 29a,b are essentially equivalent, despite the fact they are obtained for two different closed-shell states (the ground and $n^2 \rightarrow \pi^{*2}$ species, respectively) of the same system (H_2CO). In fact, the same behavior is observed for the orbital energy results of *open-shell SCF treatments* for various singly excited states of formaldehyde (such as the $^{3,1}A_2$-$^{3,1}A''$, $n \rightarrow \pi^*$ species, for which both n and π^* are occupied). These findings emphasize that in the great majority of cases the shapes of orbital energy curves are determined to a major extent by the *nodal structure of the corresponding MO's* and are not greatly affected by the nature of the *electronic state* for which they are calculated. This result *does not imply*, however, that the *charge distributions of the orbitals themselves* do not vary greatly from state to state; quite the opposite behavior is often observed, in fact, as, for example, in the case of the $1b_1$ (π) species obtained for the aforementioned closed-shell states of H_2CO (see Figure 30a,b for the pertinent charge density contours; note the great similarity in the corresponding orbital energy curves given in Figure 29a,b).

The main point of interest in the spectra of H_2AB molecules has been the so-called $n \rightarrow \pi^*$ excited states of systems with 12 electrons. Walsh's prediction that such species would be nonplanar because of the effect of exchanging n for π^* population relative to the electronic configuration of the (planar) ground state has been verified by subsequent experimental investigations[155,156] of both the singlet and triplet, and it has also been shown to be in accord with the results of *ab initio* (both SCF and CI) calculations.[154] The inversion barriers for both states (0.096 eV for the triplet and 0.044 eV for the singlet[156]) are quite small, however, thereby emphasizing that there is no strong preference for the nonplanar structures; it is

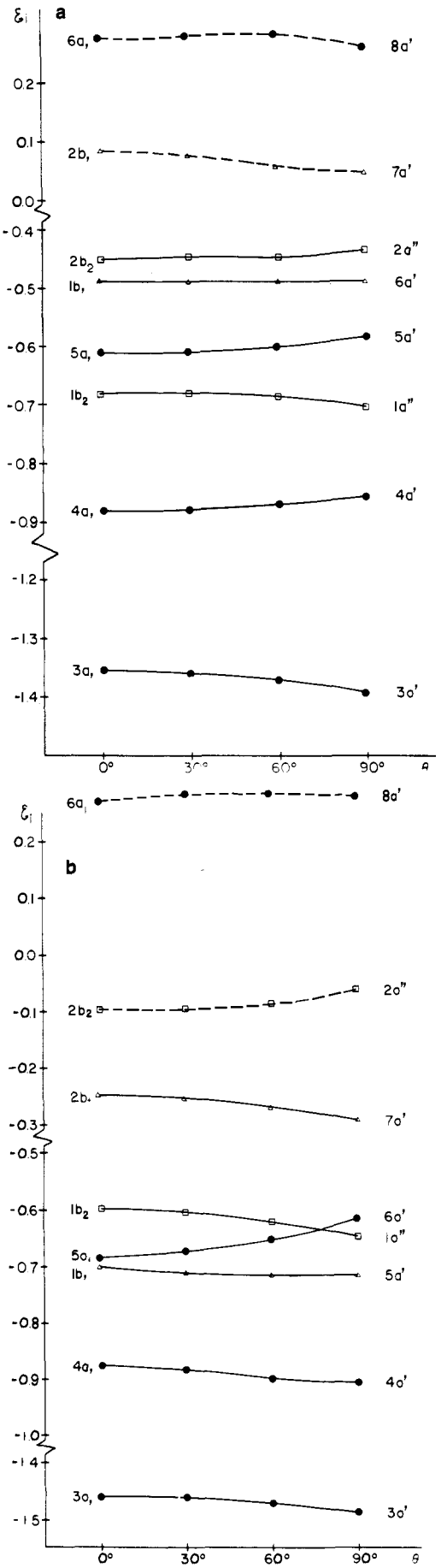

Figure 29. Calculated canonical orbital energies[154] of H_2CO as a function of the out-of-plane bending angle for the ground state (a) and the doubly excited $n^2 \rightarrow \pi^{*2}$ ($2b_2^2 \rightarrow 2b_1^2$) state (b).

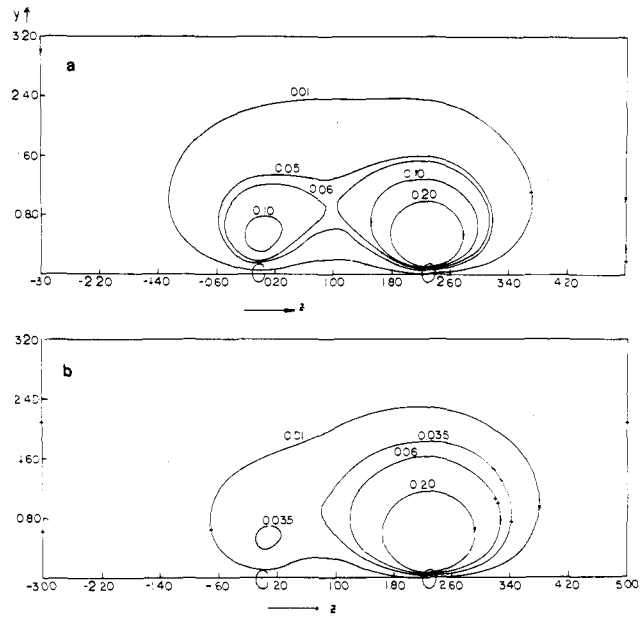

Figure 30. Calculated charge density contours[154] of the $\pi(1b_1)$ orbital in H_2CO in the ground state (a) and in the doubly excited $n^2 \rightarrow \pi^{*2}$ state (b).

probably more realistic to say that the MW model (and also a Koopmans' theorem analysis of the aforementioned SCF results) merely predicts a *strong trend away from the planar geometry of the H_2CO ground state*, without being able to give a clear-cut decision as to what the actual equilibrium conformations are for these excited species.

The observation[157] that the transition energies to the n $\rightarrow \pi^*$ states are substantially *lower* for thioformaldehyde H_2CS than for H_2CO itself is easily understood in light of the composition of the n orbital in these two systems (Figure 28); in both cases this orbital is more or less localized at the B atom, but because of the greater electronegativity of the oxygen atom relative to that of sulfur, this fact implies it is more stable (corresponds to a higher ionization potential) in formaldehyde than in thioformaldehyde. By contrast the π^* MO's of both systems are practically equivalent since they are composed mainly of C AO's (see Figure 28), and hence the orbital energy difference between the n and π^* species is considerably smaller for H_2CS.[158]

Finally, although the $\pi \rightarrow \pi^*$ *triplet* has been calculated to be a *valence* state in the aforementioned SCF–CI treatment,[154] all indications are that the corresponding *singlet* has a considerably more *diffuse* composition and is not in fact responsible for the rather strong absorption in the H_2CO spectrum at 8.0 eV, as originally thought. The aforementioned distinction between the $\pi \rightarrow \pi^*$ triplet and singlet states appears to be an example of a more general phenomenon, not accounted for in the original presentation of the MW model. This point will be taken up again in the next subsection in connection with the discussion of the electronic spectrum of ethylene.

5. H_2ABH_2 Systems

Although the molecular orbitals and spectrum of ethylene were discussed in Walsh's original presentation, no general correlation diagram was given for this class of (H_2ABH_2) molecules. The MO's of all such systems can again be classified according to σ or π character, just as for the other types of molecules discussed earlier which contain a heavy-atom diatomic skeleton. Figure 22 shows, for example. that the $1b_{3u}$ and $1b_{2u}$ of ethylene

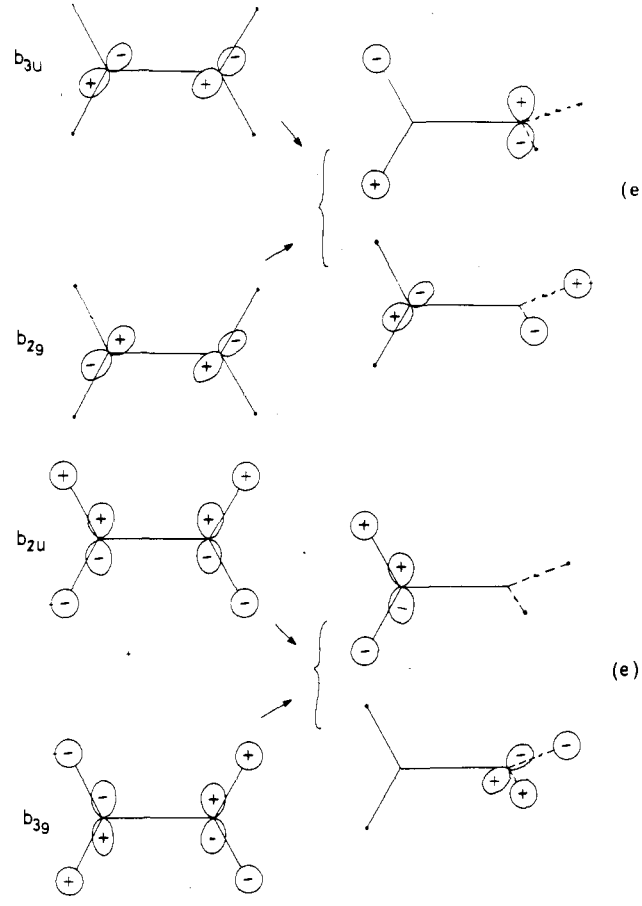

Figure 31. Schematic diagram depicting the transition between corresponding MO's of planar and perpendicular conformations of A_2H_4 systems.

stem from a π_u-type orbital of C_2, with only the latter being affected heavily by hydrogen AO mixing and hence being considerably more stable than the $1b_{3u}$ (π) species; similarly the $1b_{3g}$ and $1b_{2g}$ (π^*) MO's are clearly related to the π_g orbital of isoelectronic O_2. Consequently the interpretation of the various orbital energy trends for H_2ABH_2 systems can be based on the same principles as have been used previously for the HAB, HAAH, and H_2AB systems (section III.B.2–4). The AB bond lengths in this family are in general considerably larger than for their isoelectronic homonuclear diatomic counterparts, mainly because hydrogen AO mixing depletes the strengths of the *bonding* MO's $3a_g$ ($3\sigma_g$) and $1b_{2u}$ (π_u) more than it lessens the opposite character in the antibonding orbitals (such as $1b_{3g}$). As a result one finds only a few bound systems in this class, just as in the HAAH family, with members containing second- or higher row atoms or even such weakly binding first-row species as beryllium or boron[159] still unknown.[160]

The geometrical motion of most interest for H_2ABH_2 systems is that of relative rotation (or torsion) of the AH_2 groups; a schematic diagram for the behavior of the important π-type MO's for such structural changes is given in Figure 31. Torsion is strongly favored for the antibonding π_g-type species (b_{3g} and b_{2g}) but strongly resisted by their bonding counterparts (see Figure 32a,b).[68] By contrast the orbital energies of the σ-type MO's are seen to be relatively unaffected by such nuclear motion, and closer investigation shows that even the small changes which do occur are caused *almost entirely by variation in σ–π repulsion*, that is, *not by the direct effect of the σ MO's themselves*. In fact, it has been found (see Table III or ref 68) that only a little more than 5% of the total

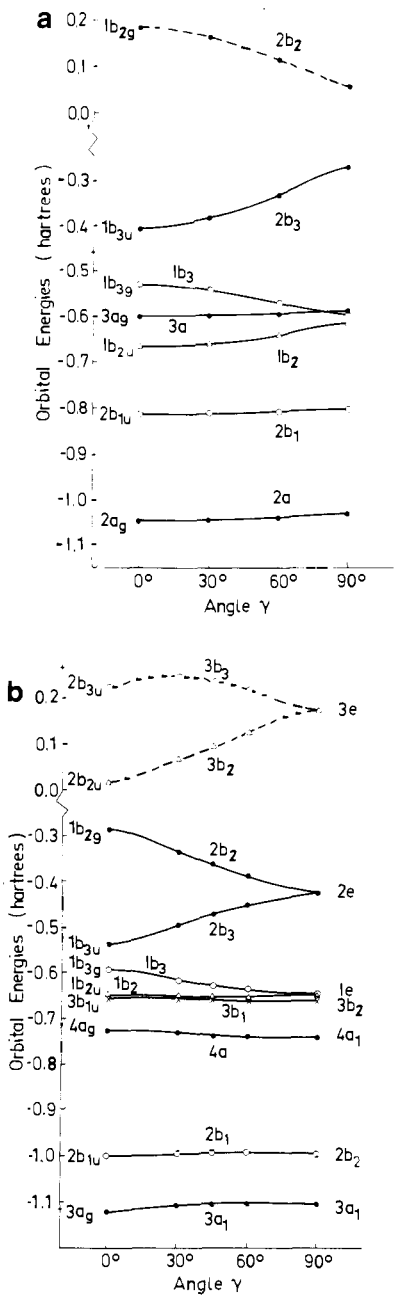

Figure 32. Calculated canonical orbital energies[68] as a function of the CH_2 twisting angle γ(γ = 0° planar and γ = 90° perpendicular CH_2 groups) in ethylene C_2H_4 (a) and in allene C_3H_4 (b).

barriers to internal rotation in these molecules is caused by what could be described as *pure σ-orbital effects*. In addition it is found that the effect of a given antibonding π_g-type MO generally significantly outweighs that of a bonding π_u species, so that *planar* $H_2A_2H_2$ species are only possible if the *number of electrons in* π_u *MO's exceeds that in the* π_g *species by at least two*, as of course it does in the ethylene ground state (12 valence electrons) but not in any of the other low-lying states of such molecules (note that the SCF method is not adequate for a quantitative description of this rotational potential surface,[67,68] as can be seen from Figure 33, and thus CI effects should be taken into account in applying the MW model in this case). Thus a Koopmans' theorem analysis of SCF results[68] for C_2H_4 shows that both the positive and the negative ions of this species are slightly nonplanar (by about 20° in each case) in their equilibrium nuclear arrangements, as a result of either the removal of an electron from the π ($1b_{3u}$) MO or the addition of same to the π^* ($1b_{2g}$) species relative to the unionized ground state; such behavior contrasts sharply with that of other systems discussed up to this point (including H_2AB systems), for which planar (or linear) ground-state geometries have been seen to be possible for more than just a single number of electrons.

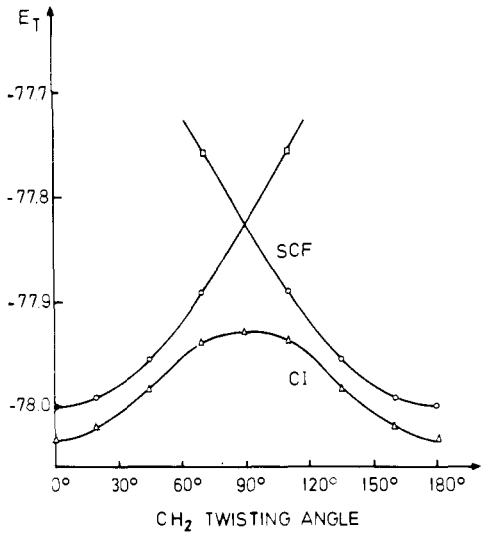

Figure 33. Calculated SCF and CI twisting potential curves of ethylene (planar 0°, perpendicular 90°).

The hydrazine ion $N_2H_4^+$ is also believed to be slightly nonplanar since it is isoelectronic with $C_2H_2^-$, while hydrazine itself prefers a *strongly* rotated geometry in which, just as in H_2O_2, there is a skewed arrangement of the AH bonds; this fact again illustrates that occupation of (antibonding) π_g MO's produces a much more decisive geometrical effect than that of the (bonding) π_u-type species. The same type of analysis[68] is also possible for the larger system C_3H_4 allene (Figure 32b) which, as N_2H_4, has equal occupation of π_u-type (π) and π_g-type (π^*) MO's in its ground-state configuration and is known to prefer an *antiplanar arrangement of* CH_2 *groups*. In this case the nodal planes in the π_g-type MO's are located further away from the charge density maxima, and thus the aforementioned tendency toward skewed geometry is not dominant in the electronic structure of this system; hence a relatively symmetric (D_{2d}) nuclear configuration (at least compared to that of N_2H_4) is believed to be optimum. This distinction is apparently also responsible for the fact that while hydrazine has a considerably larger AA bond length than ethylene as a result of differential occupation of the antibonding π^* ($1b_{2g}$) MO, the analogous bond distance in allene is actually somewhat smaller than that of C_2H_4 (see also section III.C.3).

The MW model has also been used with great success[2,84] in interpreting details of the electronic spectra of A_2H_4 systems, particularly for the prediction of the gross shapes of the rotational potential curves of ethylene in its interesting $\pi \rightarrow \pi^*$ triplet (T) and singlet (V) excited states. According to the rule discussed earlier in this section, both of these states should favor antiplanar geometry because of their equal occupation of the π and π^* MO's, respectively. This expectation is, in fact, borne out by *ab initio* SCF and CI calculations[67,68,161] for the T state, with a quite deep potential minimum found for the antiplanar arrangement of CH_2 groups, but considerable controversy has arisen over the analogous calculations for the corresponding singlet (V) state. The major point of discussion in this case has concerned the very large difference in the charge distributions calculated for the

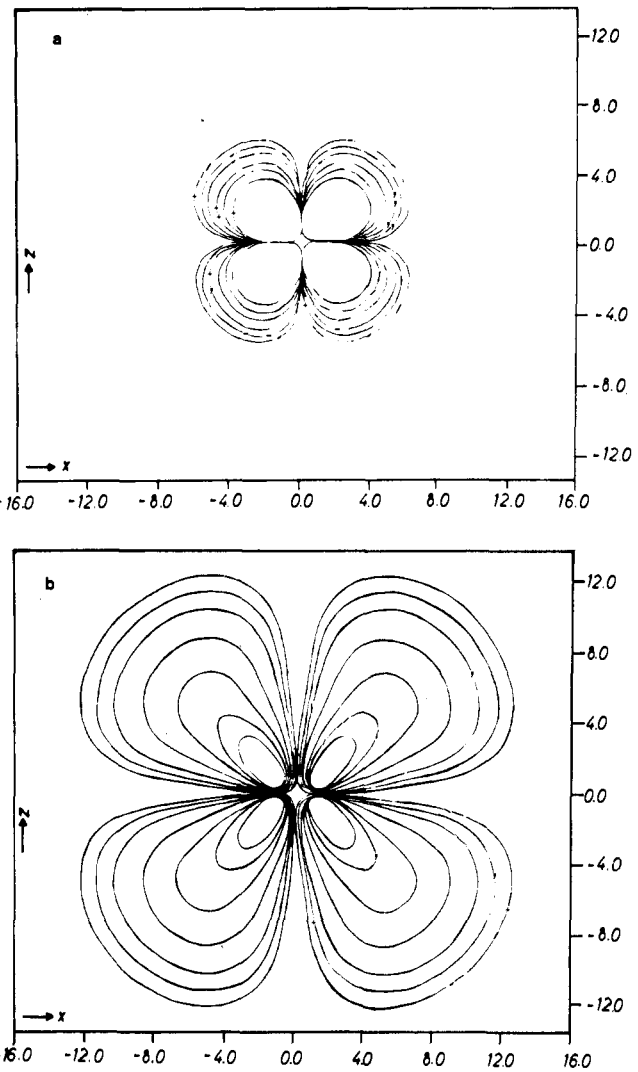

Figure 34. Calculated charge density contours of the π^* MO in the $\pi \rightarrow \pi^*$ triplet state of ethylene (a) and in the corresponding $\pi \rightarrow \pi^*$ singlet (b).

respective π^* MO's of each state (Figure 34a,b), with this MO in the singlet species quite generally found to be considerably more diffuse[162-164] than that in the T state.

Basch and McKoy[163] have suggested that this difference might be only an artifact of the SCF method, and more recently Mulliken[165] has also speculated that such distinctions can most probably be corrected *via* (extremely) accurate CI treatments. On the other hand, from at least one point of view the calculated results seem quite reasonable as they stand. To begin with it should be recalled[81] that the total energies of corresponding triplet and singlet states of this type differ by exactly twice the exchange integral K_{ab} between the two singly occupied MO's a and b in the identical electronic configuration

$$E_T(^3A) = E_T(^1A) + 2K_{ab} \qquad K_{ab} > 0 \qquad (14)$$

provided the *same* set of MO's is used for both states; this approximation is the same as that used in the derivation of Koopmans' theorem (eq 9). In *ab initio* SCF calculations,[166] however, the MO's are *individually optimized for each excited state*, and it is certainly not surprising in view of eq 14 that the energy minimization process leads to particularly significant differences in the corresponding MO's of triplet and singlet, respectively, whenever K_{ab} is large, as is the case for the *valence-type* π and π^* MO's in ethylene and more generally for so-called in-plane excitations;[167] if K_{ab} is small, clearly less adjustment need be made to obtain the singlet wave function from that of the corresponding triplet. A general effect of this type is obviously quite closely related to the Pauli principle, and in light of these considerations it is easy to understand why the upper orbital of the singlet wave function in such a case is calculated to be relatively diffuse since such composition clearly allows for a decreased value for K_{ab}.

Once it is seen that the diffuseness of the π^* MO in the ethylene V state results directly as a consequence of *removing the restriction* that both triplet and singlet species make use of *the same* set of orbitals, it is clear that this situation is not greatly different from that arising more generally in comparing the results of *ab initio* SCF calculations with the conclusions of the MW model (with its close relationship to Koopmans' theorem). Systems with the *same electronic configuration* are quite generally assumed to prefer the *same net charge distribution* and hence the same types of structural potential curves in the latter model (see sections II.B.2-3), while for *quantitative results such an assumption is never entirely justified.* In essence it is necessary to apply a correction to the MW model wherever significant differences in charge distribution occur for systems with the same electron configuration; in this case the correction is somewhat different from that of eq 12. Stated in qualitative terms the simple rule suggested by these calculations is as follows: as the amount of exchange energy increases through a series of multiplets arising from the same electronic configuration, so also does the diffuseness of the associated electronic charge distribution, and with it the tendency for states of this type to exhibit geometrical characteristics approaching those of positive ions (or Rydberg-type species). If such a rule is actually operative, it is clear that in-plane excitations[167] such as $\pi \rightarrow \pi^*$ transitions in ethylene and formaldehyde (see also section III.B.4) and other π-electron systems should be very much affected by this principle, whereas out-of-plane species such as $n \rightarrow \pi^*$, $\sigma \rightarrow \pi^*$, or $\pi \rightarrow \sigma^*$ and especially Rydberg transitions should be influenced much less by it. Perhaps a principle of this kind offers the true explanation as to why the T-V energy separation is very much overestimated[84] by eq 14 *unless a much smaller value of* $K(\pi\pi^*)$ *is assumed than that calculated using typical valence representations of the initial and final orbitals in such transitions.*

6, H_3ABH_3 Systems

There are essentially two distinct nuclear geometries favored by systems containing six hydrogen atoms and a parent diatomic skeleton, namely the umbrella structure of ethane (C_2H_6) or the bridged structure of diborane (B_2H_6). Quite obviously it is possible to define a geometrical path[168] by which a general system in this class is transformed in a continuous manner from one of the limiting structures into the other, and hence an analysis of geometrical trends for these molecules can be carried out in a manner completely analogous to that used previously in discussing more conventional types of structural changes, despite the fact that such an application was not actually considered in the original presentation of the MW model.

The constitution of the upper valence MO's of a general system of this type is again closely related to that of the corresponding orbitals for a simple diatomic (see Figure 35 for a schematic diagram). Calculations for diborane and ethane[22] have demonstrated, for example, that the most stable unoccupied valence MO of 12-valence-electron diborane in its equilibrium bridged structure is of

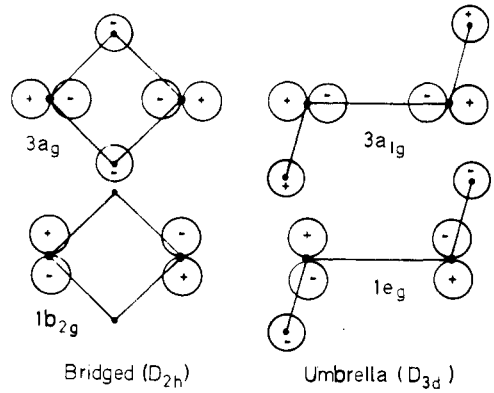

Figure 35. Schematic diagram representing two MO's of importance in the transition from an umbrella to a bridged structure of an A_2H_6 molecule.

π^* type ($1b_{2g}$), quite similar to the π^* MO in ethylene or the π_g in O_2. Calculated orbital energy diagrams show very simply (Figure 36) that this MO ($1b_{2g}$-$4a_g$-$3a_{1g}$) is more stable in an ethane-like umbrella nuclear arrangement, mainly because of the possibility of significant interaction with the hydrogen AO's in such geometries (Figure 35).[169] In ethane, with 14 valence electrons, the corresponding MO is occupied, thereby producing a strong tendency toward the umbrella geometry, whereas in diborane, in which it is not occupied, the opposite trend is observed. The usual analysis thus predicts that members of the H_3ABH_3 family favor umbrella geometries if they possess 14 valence electrons, such as ethane, ammonia-borane[70] (BNH_6) and silane[139] (Si_2H_6) but that systems of this type with a smaller number of electrons, such as diborane, prefer less conventional nuclear arrangements in which two of the hydrogen atoms are bent back toward the center of the molecule.

Closer investigation of these geometrical trends[70] has shown, however, that an important horizontal correction must be applied to the MW model in this case to account for the significantly different bonding characteristics of carbon and boron AO's, respectively. Just as for AH_2 and AH_3 bending, it is found that the electron repulsion term V_{ee} is the dominant factor in this correction (eq 12), *decreasing faster* with distortion into a bridged geometry for the *more contracted charge distribution* of carbon compounds than for that of boron-containing systems. This fact then makes the less contracted system more inclined[47] to favor compact nuclear geometries (in this case the bridged nuclear arrangement), as is observed. Explicit SCF calculations[70] for $C_2H_6^{2+}$, for example, have found that while this species favors a strongly distorted geometry relative to that of neutral ethane, it does not possess an energy minimum for a completely bridged-type structure; thus the tendency to distort from the umbrella configuration is unquestionably present for this system, but the aforementioned electron repulsion effect prevents this trend toward bridged structures from being fully realized in this case.

Another important distinction between boron and carbon compounds in the H_3ABH_3 class concerns their respective behavior toward stretching of the central bond. In the *umbrella* nuclear conformation, the $p\sigma$ ($3a_{1g}$) MO is much stronger for ethane than for either isoelectronic $B_2H_6^{2-}$ or for diborane itself;[169] as a result it appears that *neither* of the aforementioned two boron compounds is stable in an umbrella geometry, whereas, of course, at least one of the corresponding carbon-containing substances is definitely bound with respect to dissociation into two CH_3 radicals in this D_{3d} arrangement. Furthermore, in a *bridged* geometry, for which the strengths of

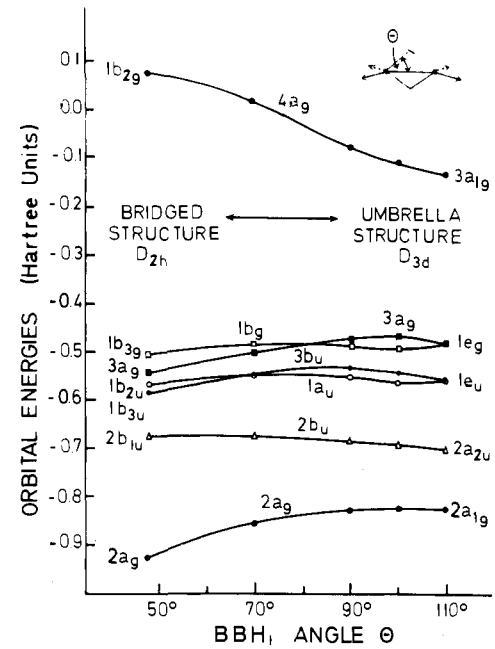

Figure 36. Correlation diagram for the transition between an umbrella and bridged structure of an A_2H_6 molecule (calculated for B_2H_6).[22]

the AH bonds are a more important factor than $p\sigma$ bonding, the situation is completely reversed, with both C_2H_6 and $C_2H_6^{2+}$ potential curves being repulsive with respect to CC stretch (Figure 2 of ref 70) while diborane is known to be bound in such a nuclear arrangement (although by only a relatively small margin[22]). Apparently the presence of the bridged hydrogen atoms lessens the strength of $p\sigma$ bonding between carbon atoms while somehow improving it in the case of the boron compounds. The conclusion from these investigations is that for this molecular family bridged structures are only possible if bonding between the $p\sigma$ AO's of the heavy atoms is relatively weak. A similar analysis accounts for the existence of bridged A_2H_4 compounds of either beryllium or boron.

The other type of geometrical motion in H_3ABH_3 systems of great interest is that of internal rotation from eclipsed to staggered nuclear conformations within an umbrella nuclear framework. If this type of motion is analyzed according to the methodology of the MW model, or more specifically in terms of changes in π orbital energies and repulsions,[68] the only safe conclusion seems to be that such a qualitative approach is simply not sufficiently precise to make a definite prediction one way or another as to which of the aforementioned nuclear conformations is the most stable; the situation is wholly similar to that discussed earlier in connection with attempts to predict the relative stability of the cis and trans isomers of diimide (section III.B.3).

Nevertheless, Fink and Allen[170] have claimed that certain invariants do exist among the components of the total energy of ethane upon rotation. Similarly, Lowe[171] has asserted that the ethane barrier arises exclusively from the behavior of (extended Hückel) e_u and e_g pairs of orbital energies (Figure 22) during the course of the rotation process, again an explanation which would appear to bear a close relationship to the techniques of the MW model. On the basis of a comparison of two different *ab initio* SCF treatments,[172,173] however, Epstein and Lipscomb[174] have pointed out that neither the Fink-Allen nor the Lowe explanations for the occurrence of the ethane rotational barrier are supported by the results of calculations *which optimize all geometrical parameters for*

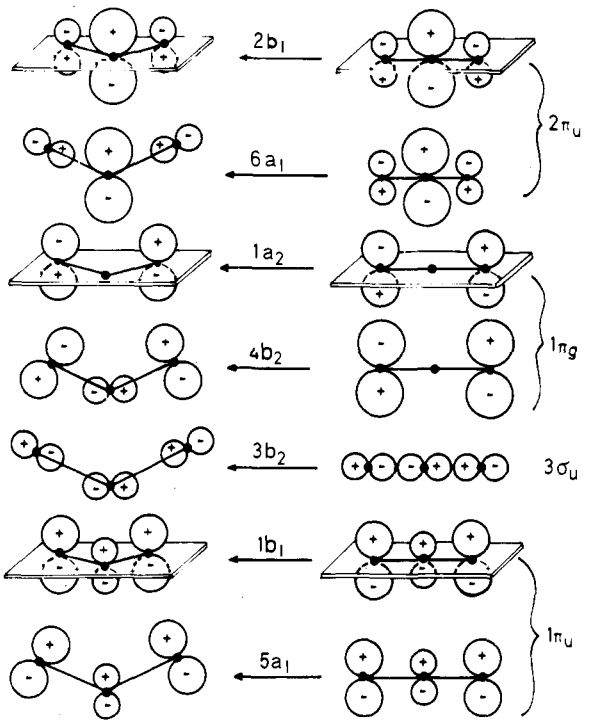

Figure 37. Schematic diagram representing the most important upper valence MO's in a linear and bent AB_2 molecule, respectively.

each stage of the internal rotation process. Such refinements in the theoretical treatment do not result in significant changes in the shape of the rotational potential curve itself, but they do greatly affect the variations exhibited by *individual energy components.* It is precisely because in the great majority of cases orbital energy trends are *practically unaffected* by changes in auxiliary geometrical variables and/or AO basis set that such a simple geometrical model as that given by Mulliken and Walsh has proven to be so generally successful; the ethane rotational barrier results merely underscore the limitations of analyses of this type, especially in situations for which the total energy varies relatively little from one conformation to the other.

C. Molecules Containing Three Nonhydrogenic Atoms

1. Symmetric AB_2 Systems

The discussion of geometrical trends for symmetric triatomic molecules constitutes the *largest single portion* of Walsh's original series of papers,[2] and indeed forms the sole basis of Mulliken's initial presentation[1] of this structural model. This observation, coupled with the fact that a very high percentage of the *early attempts* to obtain a quantitative realization of the MW model *were not at all* successful in representing the essential features of AB_2 correlation diagrams (see the discussion in section II.A.2), emphasizes that the class of triatomic molecules represents a very important testing ground for any theoretical construct designed to give mathematical justification to the methodology of such an empirical model. It is precisely in this pursuit that the use of canonical SCF orbital energies has succeeded as being the most physically consistent means for constructing the MW diagrams strictly on the basis of quantitative calculations, *at least as long as the concept of equating total energy potential curves with corresponding* $\Sigma\epsilon_i$ *species is abandoned and instead the differential form of Koopmans' theorem (eq 9) is used* to obtain the geometrical relationships which constitute the primary objective of empirical models of this type (see the discussion in section II.B.1-2).

a. Bond Angle Trends

The very first angular correlation diagram for an AB_2 system constructed from a*b initio* SCF canonical orbital energies was obtained[23] for F_2O (see Figure 2 of ref 23), and this work was followed shortly thereafter with 20 more such correlation diagrams for a series of ground and excited states[24] of the systems O_3 and N_3^- (Figures 2-3 of ref 24), NO_2^+ and NO_2^-,[175] and also symmetric NON,[74] all of which agree in essential detail (particularly in the behavior of the upper valence orbital energy curves) with that calculated for F_2O and indeed with that given empirically by Walsh for a generalized AB_2 system; a representative calculated diagram of this type has already been introduced in Figure 2a. Subsequently, still other AB_2 correlation diagrams have been reported for NO_2 (Burnelle[176]), $NO_2\pm$ (Pfeiffer and Allen[177]), CF_2 (Sachs, Geller, and Kaufman[178]), and C_3 (Liskow, Bender, and Schaefer[179]), all of which show the same familiar canonical orbital energy trends for molecular bending.

As usual a schematic diagram showing the approximate constitution of the valence MO's of an AB_2 system (Figure 37) is helpful in understanding the behavior of the corresponding orbital energy curves; for the great majority of applications only the $3\sigma_u$, $1\pi_g$, and $2\pi_u$ MO's need be considered. The $3\sigma_u$ and both components of the $1\pi_g$ ($4b_2$ and $1a_2$ in the bent system) possess orbital energy curves which rise with decreasing internuclear angle (Figure 2a), a behavior which is explained quite simply on the basis of the common nodal plane through the central atom which characterizes each of these species (Figure 37); the opposite trends are exhibited by the $2\pi_u$ ($6a_1$ and $2b_1$ for bent systems) orbital energy curves. From Figure 2a it is seen that the aforementioned tendencies are stronger in the case of the $1\pi_g$-$4b_2$ and $2\pi_u$-$6a_1$ species, whose charge density contour diagrams are given in Figures 38a,b and 39a,b, respectively, for both linear and bent geometries.[23] For the $4b_2$ MO end atom p functions strike the nodal plane more or less head-on, thereby enhancing the geometrical trends much more than in orbitals whose p functions approach each other laterally upon bending ($1\pi_g$-$1a_2$ or $3\sigma_u$-$3b_2$).

Similarly it is clear that the orbital energy trend for the $2\pi_u$-$6a_1$ MO is much more pronounced than that of the $2\pi_u$-$2b_1$ species because in the case of the former pσ bonding between the central and end atoms becomes an increasingly significant factor as bending proceeds (Figure 39a,b), whereas the analogous development cannot occur for the $2b_1$ species (see Figure 37). A much more detailed description of the angular dependence of the MO's of symmetric triatomics, complete with charge density diagrams for all valence species, may be found elsewhere.[23]

Because the MO's which stem from the linear $2\pi_u$ species and favor a bent nuclear arrangement are invariably less stable than any of their $3\sigma_u$ or $1\pi_g$ counterparts with the opposite angular behavior, it follows easily that *AB_2 systems with 16 valence electrons* (hence occupying all MO's except for the $2\pi_u$) *possess the most strongly linear ground states observed for the entire AB_2 family* (see Table I; CO_2, N_3^-, NO_2^+, for example); this conclusion is in fact borne out by experimental force constant measurements.[50,180] Adding electrons to the $2\pi_u$-$6a_1$ MO reverses this tendency completely, so that AB_2 systems with 17 valence electrons (such as NO_2) are actually nonlinear in their ground states. Further addition of

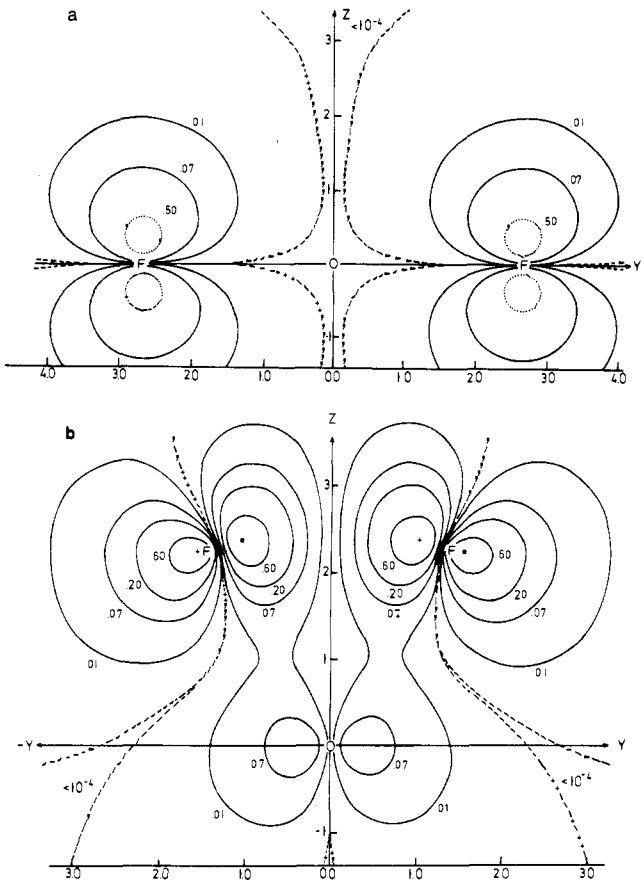

Figure 38. Calculated charge density contours for the $1\pi_g$-$4b_2$ MO of F_2O in the linear nuclear arrangement (a) and for a bent structure with $\angle FOF = 60°$ (b).

electrons up to a total of 20 of valence type enhances this trend away from linear structures, with F_2O possessing a quite small internuclear angle of about 100° (Table I).

Proceeding downward from 16 valence electrons implies depopulation of the π_g MO, and hence a trend toward less strongly linear molecules is expected; the 12-valence electron molecule C_3 is still believed to be linear but to be characterized by an extremely weak bending force constant,[179,180] in obvious agreement with what must be concluded on the basis of the MW model (and also eq 9). For systems with less than 12 valence electrons, such as C_3^+, one can further predict that depopulation of the $3\sigma_u$-$3b_2$ MO weakens the trend toward linear equilibrium geometry still more, in fact, producing bent systems again. If the electrons are removed from either component of the $1\pi_u$, however, which shows the opposite orbital energy behavior as the $3\sigma_u$ species, the trend toward linearity should be somewhat enhanced relative to the case of the C_3 ground state; thus on the basis of the differential form of Koopmans' theorem the $^2\Pi_u$ multiplet of C_3^+ (which is apparently the ground state of this system)[179] is predicted to be definitely linear. Systems with more than 20 valence electrons would also be predicted to be linear on the basis of Figure 2a because of the strongly linear trend in the $5\sigma_g$-$7a_1$ MO, next to be occupied after the $2\pi_u$-($6a_1$, $2b_1$) species; in fact, complex ions with 22 valence electrons such as I_3^- are believed[2] to be linear. All of these trends are obviously predicted in a straightforward manner on the basis of a Koopmans' theorem analysis (eq 9) of the *total and orbital SCF energies of any of the triatomic systems* for which calculations are available; specific applications using the O_3 and N_3^- results are found in section II.B.2. (A summary of

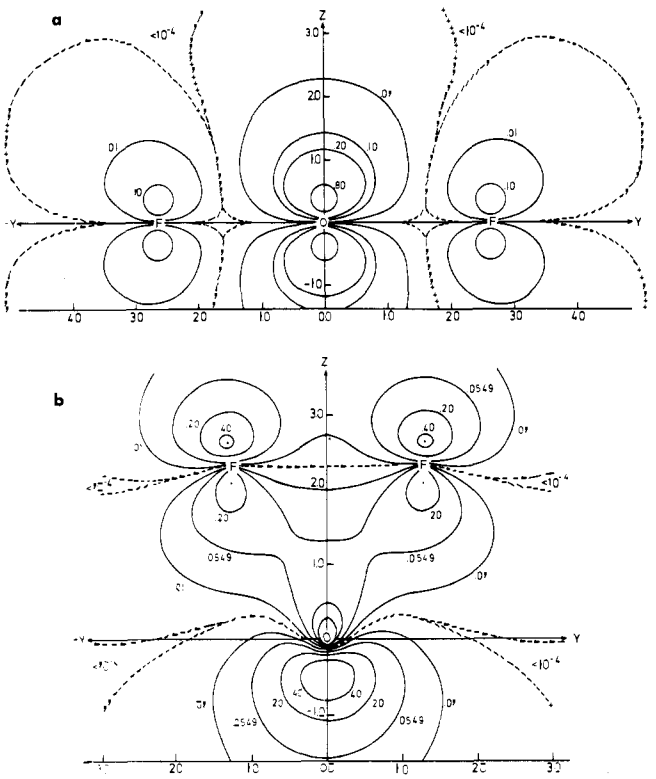

Figure 39. Calculated charge density contours for the $2\pi_u$-$6a_1$ MO of F_2O in the linear nuclear arrangement (a) and for a bent structure with $\angle FOF = 60°$ (b).

the trends in internuclear angles of AB_2 molecules is given in Table VIII.)

Nevertheless in certain well-defined cases a rather large horizontal correction (in the sense of eq 12) must be applied to the MW model in order to satisfactorily account for observed geometrical distinctions between isovalent members of this important class of molecules; for example, it was noted in section II.B.3 that ionic systems of this type generally possess quite different angular potential curves from species of much more *covalent* character containing the same number of valence electrons. Thus Li_2O is linear whereas water is strongly bent, and the whole group of alkaline earth metal fluorides becomes progressively more bent as the row number of the central atom increases, despite the fact that isovalent (and much less ionic) CO_2 is strongly linear (see Table VIII). In all these cases decreased interaction between central- and end-atom AO's for the ionic species coupled with quite understandable alterations in the rate of change of electron repulsion V_{ee} as bending proceeds (see section II.B.3) has a decided effect on the angular potential curves of such systems, even though the *underlying postulates of the MW model* (and Koopmans' theorem) *do not distinguish between members of the same family on this basis.*

From a technical point of view it should be emphasized that such geometrical trends are reproduced to a high degree *without the aid of d functions* or other polarization species in the AO basis set.[53] This statement must be qualified somewhat, however, if the *potential curves of interest possess extremely shallow minima.* Thus Hayes[54] has noted that d functions are important to obtain quantitatively reliable bond angles in the series of alkaline earth metal fluorides and has based the explanation of this result on a symmetry argument which stresses the fact that *more* d AO's can interact with the MO's of such AB_2 systems in *bent* than in linear geometries. Similar arguments have been given by Body, McClure, and Clementi[181] for

TABLE VIII. Bond Angle Trends in ABC (and H_nABC) Systems[a]

No.[b]	State	General MW trend	Behavior with bending $\Sigma\epsilon_i$	Behavior with bending V_{ee}	Horizontal correction (eq 12) for central atom B In Same row	Horizontal correction (eq 12) for central atom B In Same group	Examples
12	$\ldots 4\sigma_g^2 3\sigma_u^2 1\pi_u^4$ $^1\Sigma_g^+$	Very weakly linear	Increases slower with increased electronegativity difference between central and terminal atoms (linear trend)	Increases faster with increased electronic charge at terminal atoms (bent trend)	More strongly linear with increased atomic number of central atom (V_{ee} dominant in determining horizontal correction)	Less strongly	C_3 (180), SiC_2 (180)
14	$\ldots 1\pi_u^4 1\pi_g^2$ $^3\Sigma_g^-$	Weakly linear (π_g doubly occ)	Increases faster with increased charge at terminal atoms (linear trend)	Same as above	Same as above		NCN (180), CCO (180)
16	$\ldots 1\pi_u^4 1\pi_g^4$ $^1\Sigma_g^+$	Linear (π_g fully occ)	Same as above	Same as above	Same as above		CO_2, N_3^-, NO_2^+ (linear), BeF_2 (weakly linear), SrF_2 (108)[d]
17	$\ldots 1\pi_u^4 1\pi_g^4 2\pi_u$ or $1a_2^2 4b_2^2 6a_1$ $^2A_1$	Weakly bent ($6a_1$ singly occ)	Decreases slower with increased electronegativity difference between terminal and central atoms (bent trend)	Same as above	Less strongly bent with increased atomic number of central atom	More strongly	NO_2 (134.1), FCO (135), BF_2 (<134)
18	$\ldots 1a_2^2 4b_2^2 6a_1^2$ $^1A_1$	Bent ($6a_1$ doubly occ)		Same as above	Same as above		O_3 (116.8), FNO (110), CF_2 (105), SiF_2 (101)
19	$\ldots 1a_2^2 4b_2^2 6a_1^2 2b_1$ $^2B_1$	Bent		Same as above	Same as above		NF_2 (104.2), FOO (bent)
20	$\ldots 6a_1^2 2b_1^2$ $^1A_1$	Strongly bent ($6a_1$ and $2b_1$ doubly occ)		Same as above	Same as above		F_2O (103), Cl_2O (110.8),[c] Cl_2S (103)
22	$\ldots 6a_1^2 2b_1^2 7a_1^2$	Linear	Increases slower with increased electronegativity difference (linear trend)	Same as above	More strongly linear with increased atomic number of central atom	Less strongly	I_3^- (180), XeF_2 (180) [ClF_2 with 21 electrons: 135]

[a] Conclusions are drawn in a similar manner as in previous tables. Internuclear angles are given in degrees. [b] Number of valence electrons. [c] The net charge at the terminal atoms is smaller in Cl_2O than in F_2O, and therefore the "effective" atomic number of A is larger in Cl_2O than in F_2O; hence according to eq 12 the larger angle occurs in Cl_2O. [d] See section II. B. 3.

d-orbital effects in NH_3 and also more recently by Liskow, Bender, and Schaefer[179] in their discussion of SCF calculations for C_3. Nevertheless it is significant that in such exceptional cases other polarization functions, particularly off-center s and p species,[118] can be just as effective as d AO's in obtaining the desired quantitative geometrical behavior for a system, thereby emphasizing the fact that inclusion of d functions is *not conceptually* important. Furthermore, on the basis of existing SCF calculations there are strong reasons to conclude that it is the *polarity of the AB bonds in triatomic systems and not the proclivity of their constituent atoms to make use of polarization functions* which is mainly responsible for the observed fact that isovalent members of this molecular family can possess widely different angular potential curves (see also section II.B.3).

b. Bond Length Trends

Characteristic geometrical trends can also be distinguished in surveying experimental results for bond lengths of AB_2 molecules, and as usual it is possible to rationalize these general patterns on the basis of appropriate (AB stretching) orbital energy correlation diagrams, such as those given in Figure 40a,b for CO_2 and BeF_2, respectively.[44] In both of these cases, for example, it is found that among the most important valence orbitals the $1\pi_u$, $3\sigma_u$, and even the $1\pi_g$ are AB bonding, while the $2\pi_u$ is AB antibonding.[182] Each of these trends seems quite reasonable in light of the constitution of the corresponding MO (see Figure 37), with the apparent exception of the AB *bonding* nature of the $1\pi_g$; by analogy to the π_g orbital in simple diatomics, this orbital might be expected to be *antibonding* because of the nodal plane present in its charge density. Experimental evidence, however, does support the calculated finding of distinctly bonding characteristics for this species since CO_2^+ in its $^2\Pi g$ ground state (obtained by removing one electron from the $1\pi_g$ MO) is observed to possess a *larger* CO bond length than CO_2 itself in its ground state, thereby indicating according to Koopmans' theorem (eq 11a) that ionization has indeed occurred from an orbital of bonding type. Mulliken[1] has pointed out that a $d\pi$ function located at the A atom in such systems has the proper symmetry to be bonding with both $p\pi$ AO's at the terminal atoms and thus might be expected to play an important role in producing the aforementioned behavior, but the fact remains that the actual SCF calculations[44] find the $1\pi_g$ to be bonding *without the use of any d functions whatsoever.*

The real explanation for the $1\pi_g$ orbital energy trend for AB stretch appears to lie in the fact that the central A atom in triatomic molecules, particularly in CO_2 and BeF_2, has a *large net positive charge*, thereby producing a strong attraction for the electronic charge of the orbital in question, localized as it is at the terminal (B) atoms of such systems. This statement is clearly supported by the results of a study of changes in the character of H_2 orbital energy curves whenever a *positive or negative charge is placed at the inversion center of the molecule.* If a negative charge is placed between the two nuclei, the

normally bonding σ_g MO of H_2 eventually is converted into an *antibonding species* as the magnitude of the central charge is increased; if, on the other hand, a positive charge is used for this purpose, the *normally antibonding* σ_u species gradually becomes a *bonding* orbital (the conversion is complete when the magnitude of the extraneous charge has increased to about 1.0). These findings emphasize, just as the results for the 1s orbital energy variations discussed earier in sections III.A.1–2 and III.B.1, the basic weakness of the conventional MW model in attempting to explain *all* orbital energy changes *entirely* in terms of the AO constitution of the specific MO involved, thereby completely ignoring the very real and oftentimes more important consequences of the presence of large unscreened positive or negative charges at the various atomic centers.

As a result of the bonding character of the $1\pi_g$ MO in AB_2 systems, it is found that the bond lengths in such molecules reach their *minima* (within a class of similarly covalent species containing atoms of the same row of the periodic table) for species such as CO_2 and N_3^- for which the $1\pi_g$ becomes fully occupied (16 valence electrons). By Koopmans' theorem either *addition* or *subtraction* of electrons from such systems produces a trend toward *larger* AB bond lengths (see Table I). Thus C_3 with 12 valence electrons has a fairly large bond length of 1.277 Å, NCN (14 valence electrons) a somewhat smaller value (1.23 Å), CO_2 and N_3^- still smaller (16 valence electrons) at 1.16 and 1.12 Å, respectively, while further addition of electrons (occupying the $2\pi_u$ MO) reverses this trend, with AB bond distances increasing progressively through NO_2 and O_3 (17 and 18 electrons, respectively) to F_2O (20 valence electrons), with values of 1.193, 1.278, and 1.41 Å, respectively, having been reported. (For more examples see Table I of the present work or Table IX of ref 44). These general trends in the bond distances of triatomic molecules are summarized in Table IX.

Nevertheless, a sizable horizontal correction must be applied to the original MW model to account for quite large bond distance discrepancies which exist between isovalent systems of *different covalency* in this family. In general, bond lengths will increase as the electronegativity difference between A and B becomes larger and/or as the row number of the constituent atoms increases. Both effects are quite understandable in terms of eq 12, as has been pointed out above in connection with a general discussion of this expression, and the reader is thus referred to section II.B.3 for more details on this subject.

c. Geometry of Excited States

The geometrical trends indicated by the MW model hold equally well for *valence excited states* of systems as for the corresponding *ground states*, and thus the structure of a molecule in an excited valence state[183] can also be predicted by making use of the calculated orbital energy correlation diagrams given earlier. It has been shown in section II.B.2 that the differential form of Koopmans' theorem (or successive application thereof) can be used to give even quantitative substance to such relationships between ground and excited state potential curves (see, for example, the various AB_2 angular potential curves in Figures 8 and 9 which have been constructed *via* eq 9 from SCF data for a given state of a *single* molecule of this type).

Thus CO_2, N_3^-, and other isovalent systems are expected to prefer bent geometries in their excited states (despite the opposite characteristic noted for their respective ground states) whenever the $6a_1$ MO is populated in such species (see Figures 2a, 37, and 39a,b) since this orbital is well known to be much more stable in strongly bent than in linear nuclear arrangements. It is also clear from this model that AB_2 systems with 18 valence electrons, such as SO_2 and O_3, are *less strongly bent* in their lowest excited states than in their respective ground states as a

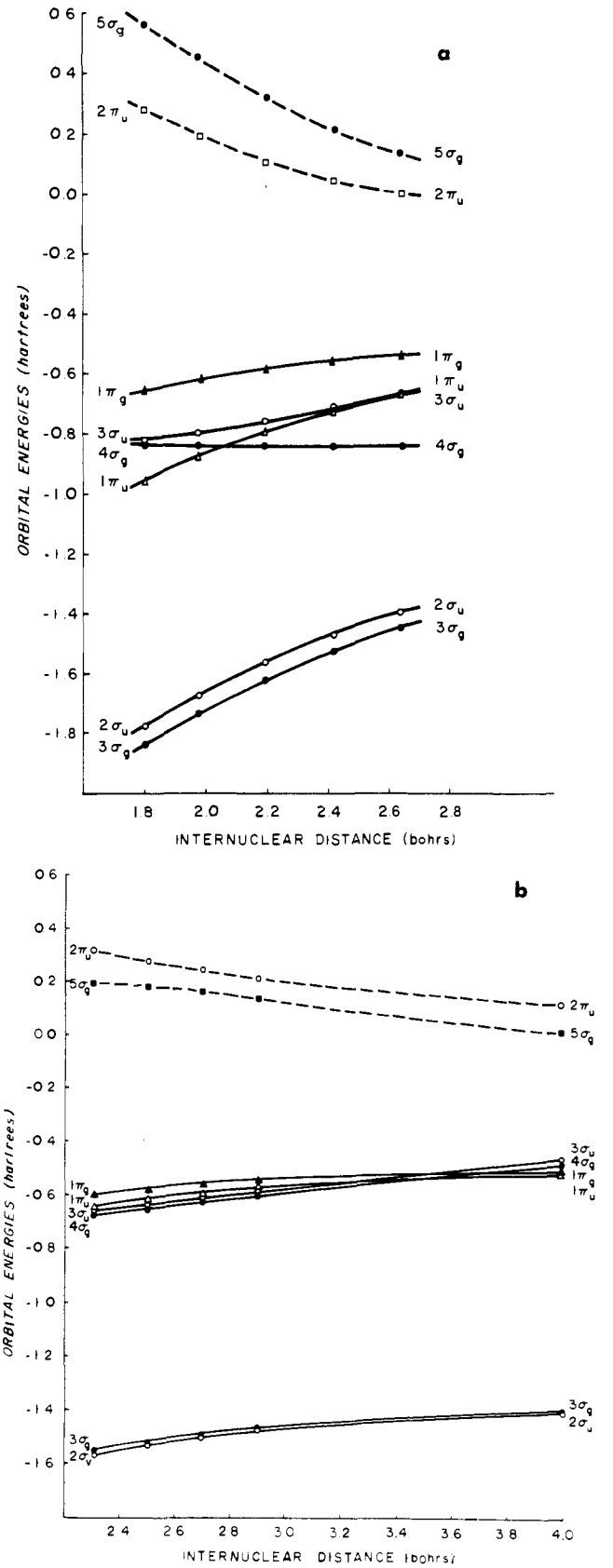

Figure 40. Calculated canonical orbital energies as a function of internuclear distance[44] for CO_2 (a) and for BeF_2 (b).

TABLE IX. Bond Distance Trends in ABC Molecules[a]

No.[b]	State	General MW trend[c]	Behavior with approach of nuclei $\Sigma\epsilon_i$	Behavior with approach of nuclei V_{ee}	Horizontal correction (eq 12) for atoms in Same row	Horizontal correction (eq 12) for atoms in Same group	Examples
12	$3\sigma_g^2 2\sigma_u^2 4\sigma_g^2 3\sigma_u^2 1\pi_u^4$ $1\Sigma_g^+$	1.25-1.30	Decreases more slowly	Increases more slowly	In general greater internuclear distance with		C_3 (1.277)
13	$\ldots 1\pi_u^4 1\pi_g$ $^2\Pi_g$	Somewhat smaller than above ($1\pi_g$ bonding)	with increased difference in electronegativity between neighbor atoms		increased difference in electronegativity	increased atomic number of either atom	CCN, CNC (1.245)
14	$\ldots 1\pi_u^4 1\pi_g^2$ $^3\Sigma_g^-$	1.20-1.25 smaller than above ($1\pi_g$ doubly occ)	(Trends valid throughout entire table)		(Trends valid throughout entire table)		NCN (1.232)
15	$\ldots 1\pi_u^4 1\pi_g^3$ $^2\Pi_g$	Somewhat smaller than above					N_3 (1.1815),[d] NNO^+ (1.155/1.185),[e] CO_2^+ (1.177), NCO ($\Sigma \leqslant$ 2.408), BO_2 (1.265), CS_2^+ (1.564)
16	$\ldots 1\pi_u^4 1\pi_g^4$ $^1\Sigma_g^+$	1.12-1.16, small ($1\pi_g$ fully occ)					N_3^- (1.12), CO_2 (1.16), NNO (1.126/1.186),[e] OCS (1.16/1.56)[e], CS_2 (1.554), BeF_2 (1.42)
17	$(\ldots 1\pi_u^4 1\pi_g^4 2\pi_u)$ $\ldots 6a_1$ $^2A_1$	Somewhat larger than above ($2\pi_u$ antibonding)					NO_2 (1.1934), FCO (1.34/1.18)[e]
18	$\ldots 6a_1^2$ $^1A_1$	1.25-1.30 larger than above ($2\pi_u$ doubly occ)					O_3 (1.278), CF_2 (1.30), FNO (1.52/1.13),[e] SO_2 (1.432), SiF_2 (1.591), ClNO (1.95/1.14)
19	$\ldots 6a_1^2 2b_1$ $^2B_1$	Somewhat larger than above					NF_2 (1.35 or 1.37)
20	$\ldots 6a_1^2 2b_1^2$ $^1A_1$	1.40-1.45 relatively large ($2\pi_u \equiv 6a_1 + 2b_1$ fully occupied)					F_2O (1.41), Cl_2O (1.68), Cl_2S (2.0)

[a] All value are given in Å. [b] Number of valence electrons. The notation for the electronic configurations is according to first-row members. [c] The values given in this column refer to first-row members only. [d] Calculations (ref 182) find that the two bonds are not equal in N_3, indicating an electronegativity difference between the atoms in the molecular environment (they find equal bond lengths in N_3^-). [e] The prediction as to which one of the two bond lengths in asymmetric triatomics is the large one is obvious, whereas the magnitude of each depends heavily on the charge transfer which occurs.

result of (single) occupation of the $2b_1$ MO in place of the $6a_1$. Such argumentation also explains the fact that NO_2 in its first excited state ($^2B_1$) is weakly linear, while in its $^2A_1$ ground state it is bent, again because occupation of the $2b_1$ in the excited state is less effective in reversing the trend toward linear geometry of systems with one less valence electron. More examples can be found in the existing calculated angular potential curves for various states[24] of O_3 and N_3^- and also for the odd-electron system[176,184] NO_2 (see Figures 8 and 9 of the present work and Figure 1 of ref 176, for example). The underlying basis which produces such a simple and concise relationship between ground and valence excited state potential curves for all molecules in a given family is clearly the fact that orbital energy trends are largely unaffected by the nature of either the system or the electronic state in a given case (at least as long as the corresponding MO's are actually occupied in the calculations being considered, which is of course the only situation of any real interest; see section II.C.1.e).

2. *Asymmetric Triatomics*

a. Role of Symmetry

Although the analysis in the preceding section has been based to a very large extent on symmetric members of the triatomic family, it must be emphasized that the general geometrical trends discussed therein are also observed for systems of lower nuclear symmetry; for example, the shapes (*i.e.*, bond angles and bond distances) of NNO, FCO, FOO, OCN, and many others appear to be determined basically by the number of valence electrons they contain. In order to study the relation between symmetric and asymmetric triatomics, it is useful to consider the results of *ab initio* SCF calculations carried out[74] for nitrous oxide in both symmetric NON and equilibrium NNO nuclear arrangements, in each case for a large series of internuclear angles. The most fundamental result stemming from these calculations is the great similarity they show to exist between the MO's of symmetric and asymmetric conformations, respectively. This result is particularly apparent in the comparison of the $1\pi_g$ charge density of NON with that of the 2π of NNO (Figure 41a,b); furthermore, practically the same degree of similarity is found to exist between the other valence MO's for these two nuclear arrangements (see Figures 4 and 5 of ref 74, for example). There is, to be sure, some central AO mixing present in the π_g-type species of the asymmetric structure which, of course, cannot occur in the corresponding MO of the symmetric NON conformation because of group theoretical restrictions, but this eventuality can be looked upon as merely a form of perturbation.

A comparison of the NNO ground state angular correlation diagrams (Figure 42) shows not surprisingly that this similarity between MO's of asymmetric and symmetric triatomics is carried over into the variation of their corresponding orbital energies (see Figure 2a). The only

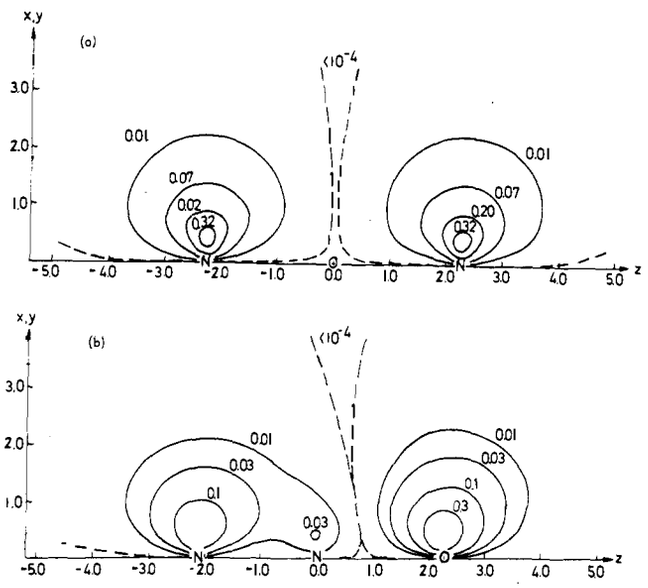

Figure 41. Calculated charge density contours for the $1\pi_g$ (2π) MO in the hypothetical molecule NON (a) and in NNO (b).

apparent discrepancies occur for angles beyond 100°, for which the $2\pi_u$-type in-plane orbital energy (10a) begins to rise while the corresponding π_g-type species (9a) starts to decrease with bending, but such distinctions are easily explained in terms of the lower symmetry of nitrous oxide and the effect of the noncrossing rule, with the π_g (2π) species correlating with the $6a_1$ MO at small angles rather than with the usual $4b_2$, and the opposite trend occurring for the $2\pi_u$ (3π) MO (see Figure 42). In the region from 180 to 100°, however, the angular behavior of the orbital energies is quite similar to that in symmetric triatomics, with the 2π (π_g) components becoming less stable and the 3π ($2\pi_u$) species becoming more stable, respectively, with bending out of the linear nuclear arrangement.

The aforementioned orbital energy trends are *evident* in comparing the calculated SCF potential curves for various states of NNO shown in Figure 43. First of all, the molecule is linear in its ground state (curve 1) just as all other covalently bonded symmetric triatomics with 16 valence electrons. Transferring two electrons from the 2b to the 10a MO yields a state (denoted 2) in which the molecule is strongly bent, just as for the analogous change in occupation for symmetric diatomics, in this case involving the $1a_2$ (2b) and $6a_1$ (10a) MO's, respectively (the analogous *potential curve* for N_3^- in Figure 9a is also labeled 2). A two-electron transition from the 9a ($4b_2$) to the 3b ($2b_1$) relative to the NNO ground state leaves the system linear but less strongly so, also just as in the analogous change in symmetric N_3^- (curve 3 of Figure 9a). In addition, the *actual* angular potential curves for asymmetric and symmetric triatomics should be even more similar than the respective *calculated SCF* species since a CI treatment will for all practical purposes remove any distinctions between these two types of systems which might be thought to result from the unusual correlation of the 9a and 10a MO's for angles smaller than 100°; this conclusion follows from the fact that in multideterminantal wave functions electron transfer between orbitals of different symmetry is not forbidden by the noncrossing rule, unlike the situation for single-determinantal (SCF) species. The agreement between potential curves of symmetric and nonsymmetric systems has also been found to be quite good in a comparison[70] of ethane C_2H_6 and ammonia-borane BNH_6 (see section III.B.6) and seems to be of quite general significance.

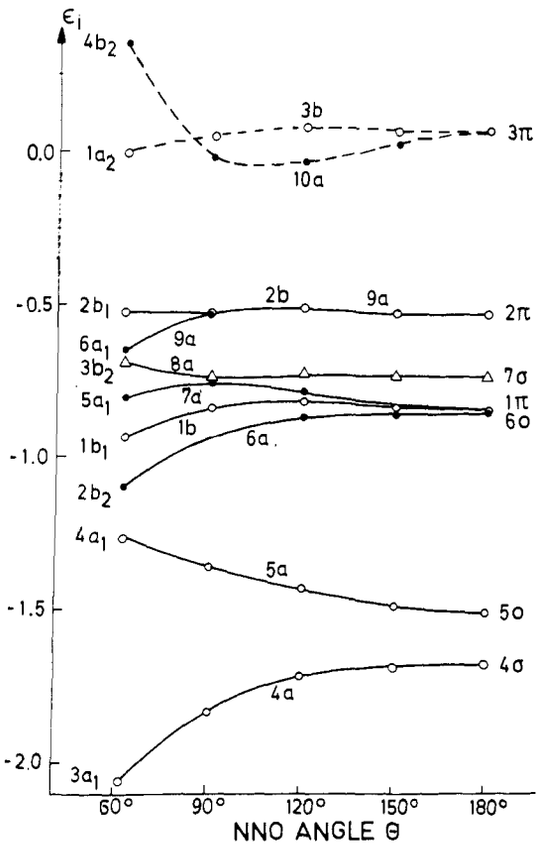

Figure 42. Calculated canonical orbital energies as a function of internuclear angle for the ground state of NNO.[74]

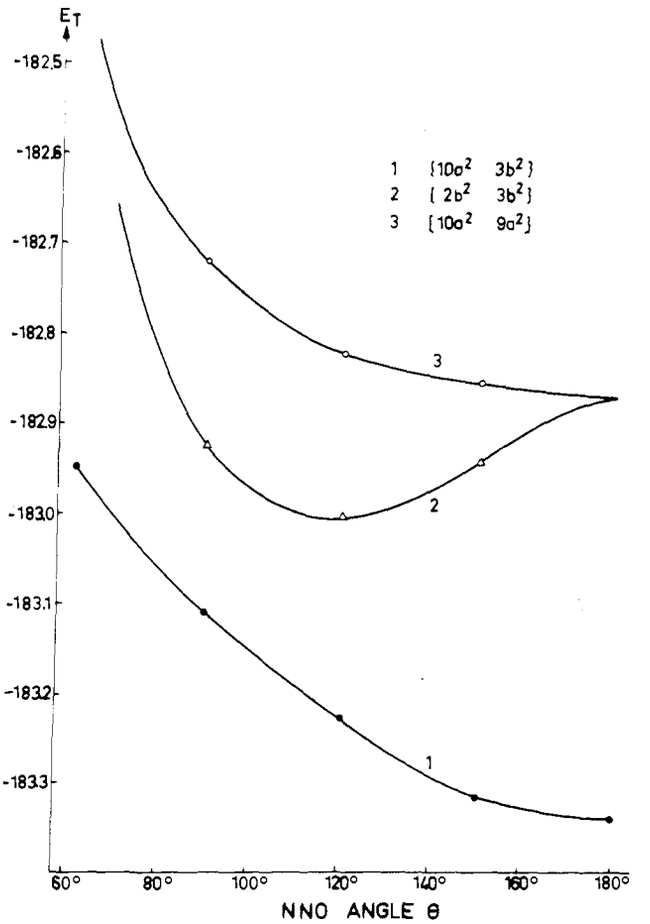

Figure 43. Calculated angular potential curves for the $^1A_1$ states of NNO. The notation $\{10a^2\ 3b^2\}$ indicates that of the four MO's 9a, 10a, 2b, and 3b the orbitals 10a and 3b are not occupied.[74]

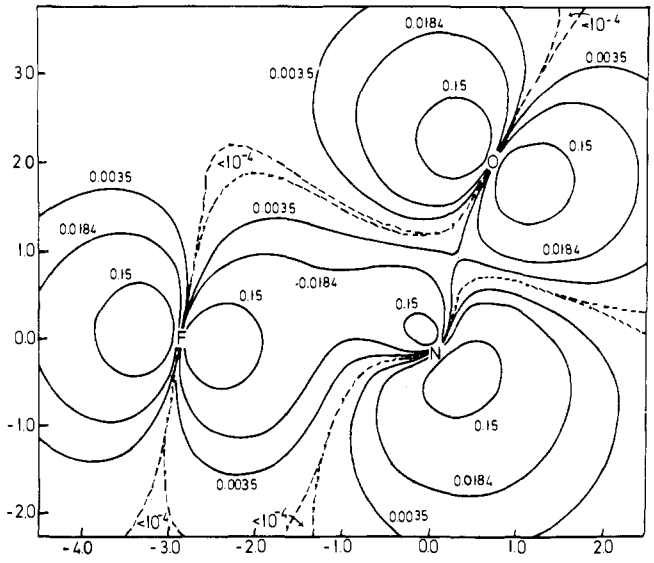

Figure 44. Calculated charge density contours for the 10a (highest occupied) MO in FNO in its equilibrium geometry.

Furthermore the same trends which are found to be operative for *bond lengths* in symmetric triatomics are also observed in the case of asymmetric species; for example, both addition and removal of electrons from systems with 16 valence electrons lead to an increase in the corresponding internuclear distances (see Table I). Obviously, compared to symmetric triatomics there is much less likelihood in these cases that the two bond lengths are equal,[182] and in order to predict which of these is the larger as well as the approximate magnitude of the observed difference between them it is again found that the horizontal correction of eq 12 can be of considerable utility. The NN and NO bond lengths in NNO of 1.128 and 1.184 Å are roughly equal to R_{CO} in isovalent CO_2 (1.16 Å), for example, but because of the smaller polarity of the bond between the two nitrogens in this system the NN distance is decreased (see section II.B.3) whereas the NO species shows the opposite change relative to the corresponding value for the symmetric molecule. In FNO the FN bond is much more polar than the OO counterpart in isoelectronic ozone, and hence the F^-N^+ bond length is much larger (2.872 bohrs) than the equilibrium distance in O_3 (2.413 bohrs); on the other hand, the NO bond in FNO is only 2.135 bohrs. It is worth noting that in both comparisons the two bond lengths in the nonsymmetric system straddle that of the corresponding isovalent symmetric species, with the magnitude of the bond length differences depending quite heavily on the respective bond polarities.

The finding that this effect is much smaller for NNO than for FNO is clearly related to the fact that the AO's in NNO are strongly interacting whereas those in FNO are not. Thus FNO can be described rather accurately[185,186] as $F^- + NO^+$, and, in fact, of all the MO's in this system only the 10a is accurately described as a mixture of both fluorine and NO character (Figure 44); the latter orbital is quite similar to a typical $6a_1$ MO of a symmetric triatomic, with its tendency toward a bent nuclear framework (compare Figure 39a,b). Despite the weak mixing of its AO's, however, FNO is found to possess an internuclear angle (110°) which is rather close to that of O_3 (117°). In turn the fact that the FNO angle is somewhat smaller is quite consistent with what is expected from eq 12 on the basis of the relatively negative end atoms of this system (see section II.B.3). A summary of the geometrical trends in nonsymmetric as well as symmetric triatomic molecules (all heavy atoms) is also given in Tables VIII and IX.

b. Replacement of Fluorine by Hydrogen

In the present context it is worthwhile to briefly compare and analyze the shapes of molecules which differ only in the substitution of fluorene atoms for hydrogens (often with formal loss of symmetry). Historically systems such as H_2O and F_2O have been treated in different classes in the MW model because of rather obvious distinctions in both the number and constitution of their respective occupied valence MO's, but it is well known that systems which are so related generally do possess quite similar shapes (although certainly not bond lengths), and this resemblance seems to be more than just coincidence, as can be judged from a recent review of this general subject by Gillard.[187]

A comparison of the systems FNO[185] and HNO[134] shows that the similarity between F and H atoms is quite understandable from the standpoint of *ab initio* SCF calculations, especially in cases for which the fluorine AO's are only capable of rather weak mixing with the AO's of the other atoms contained in the compound. The electronic structures of both FNO and HNO can be described in terms of a perturbed NO (or NO^+) system (recall the perturbed sphere model discussion in section III.A) accompanied by either a spherical H^+ or F^- ion;[188] to be sure the bonds to fluorine and hydrogen in such cases are still best described as covalent, but the important point is that the degree of electron sharing is very nearly the same in both types of systems. As a result in both cases the preferred location of the H or F nucleus is determined to a large extent *by the manner in which the charge density of the rest of the molecule becomes* (slightly) *perturbed by the presence of the latter.*

Not surprisingly there are still some differences in equilibrium angles of corresponding systems of the two types,[189] but for the most part these distinctions can easily be understood in terms of the fact that F atoms tend to possess net negative charges while H atoms are more likely to be somewhat positive. As a result according to the general analysis of horizontal corrections to the MW model in terms of eq 12 it follows that V_{ee} should *increase faster with bending* for F compounds than those with substituted H atoms and hence that the fluorine-containing substances generally possess slightly smaller equilibrium angles[47] (for example, F_2O 100°, H_2O 105°). Nevertheless as usual these discrepancies are generally *far less important* than the *basic similarity* observed between the shapes of corresponding pairs of such systems. This point will be pursued further in connection with a discussion of tetratomic molecules in section III.D.

c. Order of Heavy Atoms in Triatomic Molecules

The fact that the MO's of an asymmetric system such as NNO are not greatly different from those of symmetric AB_2 molecules (see Figure 41a,b) raises the rather obvious question of what factors actually determine *the order of nuclei* in this and other classes of polyatomic systems. The key to the understanding of this point has been shown[74] to lie in the fact that although MO composition may be roughly equivalent for NNO and NON, for example, the *relative* stabilities of their orbitals are definitely affected by such a change in the order of nuclei. To see why this is so it is necessary to recall that the $1\pi_g$ MO (and also the 2π) is composed entirely of end-atom AO's, whereas the $2\pi_u$ shows very nearly the opposite composition (the $1\pi_u$ also has considerable end-atom

AO character). It follows then that in NNO the MO's with considerable end-atom character are relatively more stable, because of the higher nuclear charge of O, than in NON (in which case both end atoms are nitrogens); at the same time the opposite situation holds for MO's of central-atom character such as the $2\pi_u$. *Therefore the* $1\pi_g$–$2\pi_u$ *energy separation is found*[74] *to be substantially less in NON than the analogous* 2π–3π *splitting in NNO.* The same type of argument has been used by Walsh[2] to explain the fact that transition energies to various states in NNO are uniformly *lower* than the corresponding values in CO_2 (with two O end atoms, of course).

This observation concerning the relative orbital stability is critical in determining the preferred order of nuclei because obviously the tendency in such systems is to occupy the lower lying $1\pi_u$ and $1\pi_g$ orbitals with their predominantly end-atom character before the less stable $2\pi_u$ species of opposite composition. For triatomics with 16 valence electrons the $1\pi_g$ (or 2π) is fully occupied, for example, while the $2\pi_u$ is vacant. For a combination of two nitrogen atoms and one oxygen, by far the most stable π_g (and $1\pi_u$) orbital is obtained if the more highly charged oxygen nucleus is located at one of the termini, and indeed the aforementioned SCF calculations[74] indicate that *the NNO arrangement is preferred over the more symmetric NON conformation by at least 100 kcal/mol;* the stability of the $2\pi_u$ is immaterial in this case since it is not occupied. Consequently it is not at all surprising that the order of nuclei in triatomics quite generally is such as to locate the most electronegative elements at the termini (FOF, FOO, FNO, FCO, NNO, NCN, OCO, OBO, ONO, $ONO^{\pm}$, FCN, and many other examples, as in Table I).

Furthermore, the above argument indicates that the trend toward placing the most electropositive atom at the central position *should reach its zenith for systems with 16 valence electrons*, such as NNO, CO_2, NO_2^+, and BeF_2. For systems with fewer electrons and hence lower $1\pi_g$ occupation the stability difference between symmetric and asymmetric arrangements should be significantly smaller, as is in fact indicated by the finding[190] that CCN and CNC (with 13 valence electrons) are *both* sufficiently stable to be studied experimentally. By the same token, it seems clear that systems with substantially more than 16 valence electrons, such as FOO and F_2O, which occupy the central atom $2\pi_u$ MO (more stable with the heavier atom in the center) with three or four electrons, respectively, show a much smaller stability difference between symmetric and nonsymmetric structures than does either NNO or CO_2.

A more detailed discussion of this general subject is given elsewhere;[74] yet another experimental result which throws additional light on this interesting subject is the finding that the thio analog of nitrosyl fluoride (FNO) *prefers the structure NSF.* This result emphasizes that the most important single factor in the above argument is the relationship between *the stability of MO's and their AO composition.* In FNO there is no question that O AO's are generally more stable than those of nitrogen; hence the order FNO is preferred with the most electropositive element in the central position. In NSF, however, the situation is not as clear since N and S possess roughly equal electronegativity (*cf.* Pauling's diagonal rule for the periodic table[7]). The fact that NSF is the preferred structure in the latter case is quite consistent with the calculated finding[191] that the *orbital energy of a nitrogen 2p is slightly lower than that of a sulfur 3p,* thereby making the π_g-type orbital more stable with N in the terminal position. At the same time, however, it seems clear that the alternative structure FNS must also represent a relatively stable conformation for this combination of nuclei. In summary, the fundamental principle operative in all these cases is seen to be the *desirability of locating atoms with the lowest orbital energies in the positions of greatest electronic density,* which for virtually all triatomics simply turns out to be the termini of such systems.

3. H_nABC Molecules (Open Chain and Ring Compounds)

The great similarity observed between the correlation diagrams and ultimately the geometries of hydrogenic and corresponding fluoro-substituted compounds points out a desirable goal in the study of the MW model, namely the enlargement of the classes of systems for which a given Walsh diagram is applicable. This subject has been considered in great detail in an earlier publication by the authors[87] and the results of that study will be summarized in the remaining part of this section. The specific experimental observation which has prompted this work is the generally close relationship found to exist between the *skeletal* geometries of certain hydrogen-containing systems on the one hand and the *structures of corresponding isovalent molecules not containing hydrogen* (or containing different numbers of hydrogen atoms) on the other; examples of this phenomenon may be found in Table I of ref 87, such as the propane-F_2O, propene-O_3, and allene–CO_2 comparisons, respectively.

Although structural relationships of this type are well known and quite numerous, however, certain exceptional cases easily come to mind; cyclopropane and cyclopropene, which quite obviously possess greatly different nuclear geometries from those of the corresponding isoelectronic AB_2 systems O_3 and N_3^-, respectively, represent but a few examples of hydrogen-containing systems which do not at all follow the usual geometrical trends of the parent family of nonhydrogenic molecules. Because of the high percentage of cases in which the aforementioned isovalent rule *is* adhered to, it is certainly worthwhile to obtain a clear understanding of why these similarities in the equilibrium geometries of such systems occur when they do and even more importantly to explain how the so-called *exceptional* cases fit into this general pattern.

A logical point to begin this investigation is in connection with a comparison of the electronic structures of O_3 and $HCOO^-$, respectively (section II.C.2), systems whose individual MO's have been shown to bear a close one-to-one relationship to one another[86] (see Figure 15a,b for the charge densities of the $6a_1$ orbitals for these two systems, for example). As usual it is found that the similarity in MO composition is carried over into the shapes of corresponding orbital energy curves,[86] as can be seen from a comparison of the pertinent data in Figure 45a,b; the resemblance between the two correlation diagrams is especially clear in the case of the important upper valence MO's, namely the $3b_2$, $4b_2$, $1a_2$, $6a_1$, and $2b_1$ (the last of which is not occupied for either molecule), respectively. As a result it is indeed found that the shapes of corresponding angular potential curves for these two molecules (in both ground and excited states) are also quite similar to one another, as can be seen from a comparison of the calculated results[192] for $HCOO^-$ shown in Figure 46 with the analogous data for O_3 given earlier in Figure 4a (the labeling of electronic states is the same in both figures). As discussed in section II.B.2 all such potential curve relationships can be explained on a nearly quantitative basis in terms of the differential form of Koopmans' theorem (eq 9) once it

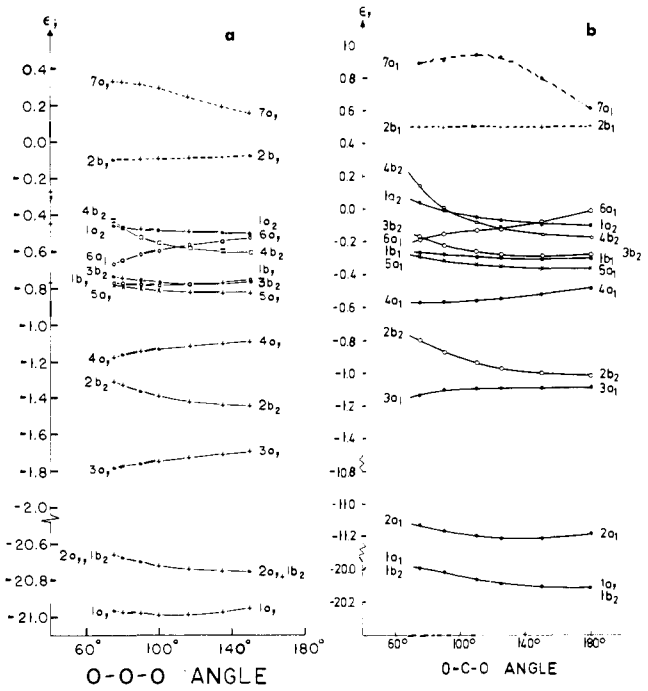

Figure 45. Calculated angular correlation diagram for the ground state of O_3 (a) and the ground state of $HCOO^-$ (b).

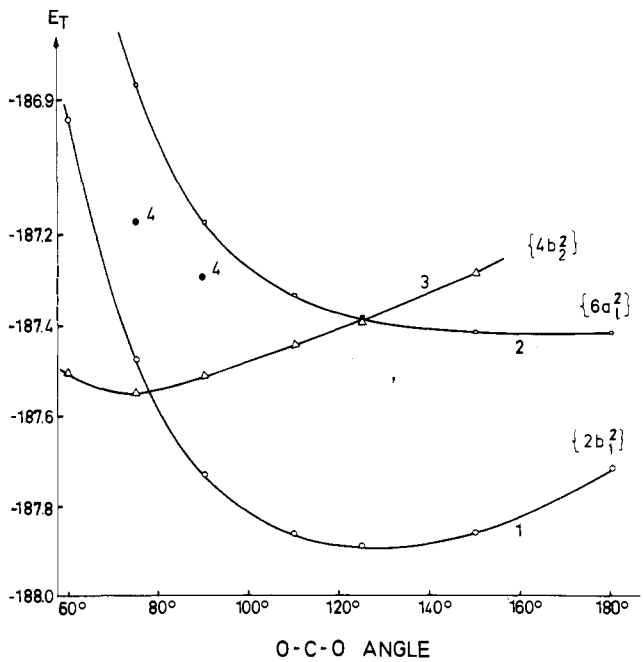

Figure 46. Total SCF energy E_T for various closed-shell states of $HCOO^-$; the electronic configurations are the same as for the corresponding states of ozone in Figure 4.

has been demonstrated that the angular correlation diagrams of the systems being compared resemble each other to a high degree. Clearly the fact that the similarity in the shapes of corresponding potential curves of the two systems holds for *excited states as well as ground states* argues strongly for the existence of a well-defined theoretical principle of *general applicability* in determining such structural relationships between isovalent systems.

Despite such observations, however, it is important to note that the *spacing* in the potential curves of the two systems under consideration is not at all the same, with the excited states of $HCOO^-$ lying at much higher relative energies than those of ozone. Recalling the relationship between orbital stability and the positioning of the nuclei of a given system, as discussed in the preceding subsection, it is clear that such distinctions can easily be explained on the basis of the fact that the $2b_1$ orbital, with its predominantly *central* atom character, is much more stable in O_3 than it is in the formate ion[86] (with a much smaller nuclear charge at the center of this system). Experimental observations of the electronic spectra of these systems (and also of NO_2^-, an example intermediate between these two cases)[86] confirm that these calculated relationships do, in fact, accurately represent the actual physical situation in these cases, thereby emphasizing that while the interchange of nuclei does not generally affect the *shapes* of individual orbital and total energy curves, it can greatly alter the separations between them (see section II.C.2).

Protonation of the formate ion does very little to alter these general structural trends, as can be inferred, for example, from the total charge density contours of formic acid, HCOOH, for both the nonsymmetric (equilibrium) and symmetric placement of the acidic proton[193] (Figure 47a,b); again the proton appears to cause only a relatively minor perturbation in the *overall* charge density of this system. Yet both $HCOO^-$ and HCOOH are isoelectronic not only with O_3 (with roughly the same internuclear angle), but also with cyclopropane, ethylene oxide, and ethylenimine, all of which are well known to possess quite different nuclear structures which are cyclic in nature.

The explanation for such large geometrical differences might well be thought to lie in the basic *dissimilarity* between the MO's of such cyclic systems and those of corresponding nonhydrogenic molecules, an approach which has been stressed in the work of Walsh[194] and Coulson and Moffitt,[195] but actual SCF calculations indicate that the usual one-to-one relationship between corresponding MO's of such systems *holds just as well in the cyclopropane–ozone comparison as for any other pair of isovalent molecules with a triatomic skeleton.* The $1a_2$ MO of cyclopropane (in C_{2v} symmetry), for example, consists of the usual antibonding combination of terminal $p\pi$ AO's, albeit greatly influenced by the presence of the out-of-plane hydrogen atoms of this system (see Figure 48 and compare with the general AO composition of the $1a_2$ in simple AB_2 systems as shown in Figure 37). More importantly, the calculations[89] show that the *shapes of corresponding orbital energy curves for a system such as cyclopropane are also found to be quite similar to those of ozone and/or the formate ion* (compare the C_3H_6 ground state correlation diagram of Figure 49 with analogous results for O_3 and $HCOO^-$ in Figure 45a,b, respectively).

This similarity in the shapes of corresponding orbital energy curves for ozone and cyclopropane *does not,* however, *rule out the possibility* that the structural differences between these two systems can be explained in the usual manner *by means of the differential form of Koopmans' theorem,* for the simple reason that *the MO's which are occupied in the ground state of cyclopropane are not completely the same as those occupied in the most stable electronic state of O_3.* In fact, it is easily seen from a comparison of Figure 49 with Figure 45a,b, respectively, that the *ground-state electronic configuration* of cyclopropane doubly occupies the $2b_1$ MO (with its bent tendency) instead of the $4b_2$ species (strong tendency toward linear geometry) preferred by each of the noncyclic systems. Therefore, what is *the ground-state configuration in cyclopropane is that of an excited state in O_3 or $HCOO^-$ and vice versa.* Furthermore, this difference in ground-state electronic configuration can, in fact,

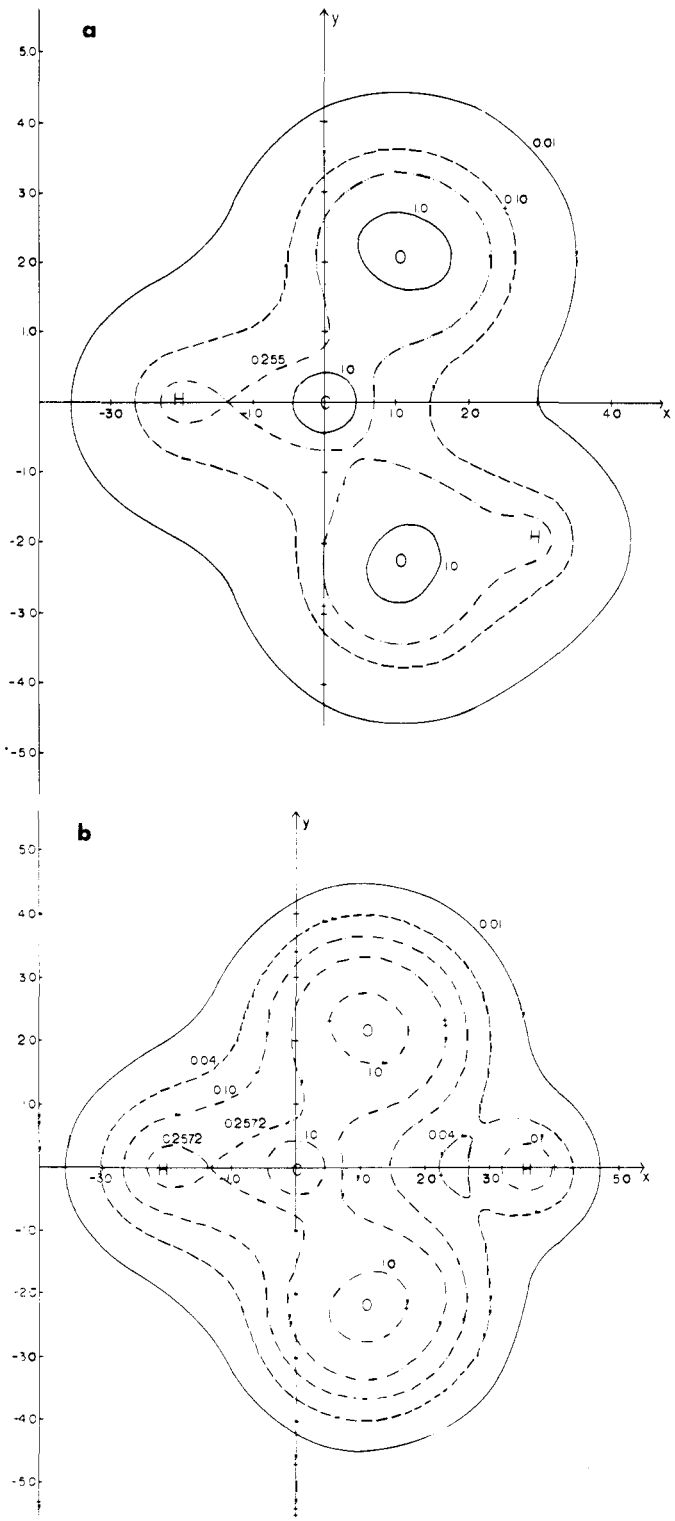

Figure 47. Total molecular charge density for HCOOH calculated for the optimal arrangement of nuclei (a) and for a more symmetric conformation (b).

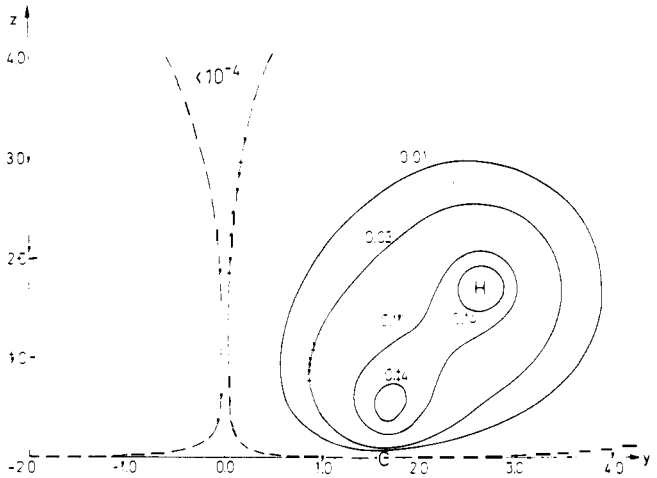

Figure 48. Calculated charge density contours for the $1e'^{1}$ MO of cyclopropane in a plane perpendicular to the plane of carbons and containing the bisector of ∠CCC.

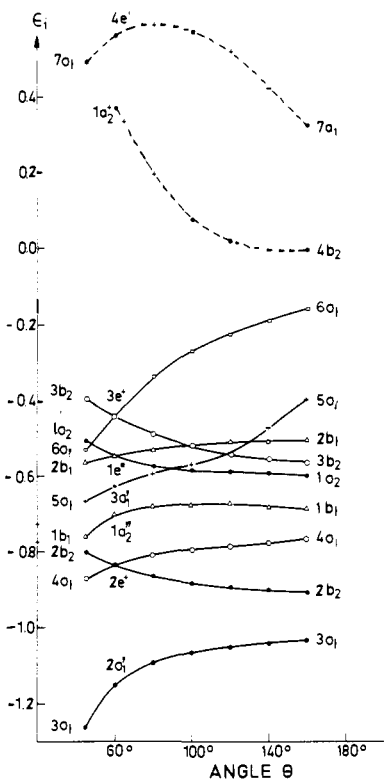

Figure 49. Calculated canonical orbital energies as a function of internuclear angle for the ground state of cyclopropane C_3H_6.

be predicted on the basis of a group theoretical analysis of the VB structures of cyclopropane (with its three CC and six CH bonds) and the formate ion, respectively, as illustrated in Table Xa,b. This general technique of predicting MO ground-state configurations is derived from standard hybrid orbital analyses described in conventional textbooks on group theory[196] and was first used by the authors in connection with a study of the equilibrium geometry of cyclobutadiene and various other systems containing four nonhydrogenic atoms.[151,197]

Once it is realized that the ground-state electronic configuration of cyclopropane corresponds to a doubly excited state of a simple triatomic, it is clear that the geometry of the former system is completely understandable in terms of a *conventional application of the MW model.* There is still a one-to-one correspondence between the potential curves of this system and those of the other isovalent species; it is only that the *stability order of the various electronic configurations is not the same in the two cases* (compare Figure 50 for cyclopropane with Figures 4a and 46 for O_3 and $HCOO^-$, respectively). Whenever a given cyclopropane state is compared with an O_3 species of identical electronic configuration, the resemblance between the associated potential curves is every bit as close as in earlier cases involving only *nonhydrogenic members of the same molecular family.* Furthermore it should be clear that this difference

TABLE X. Symmetry of Occupied Orbitals Derived from Group Theoretical Analysis of VB Structures of (a) Cyclopropane and (b) the Formate Ion (C_{2v} Notation)

VB description	Corresponding occupied MO's
(a) Cyclopropane	
3 × 1s	a_1, a_1, b_2
3 × CC bonds	a_1, a_1, b_2
4 × CH bonds ("terminal")	a_1, b_2, b_1, a_2
2 × CH bonds ("central")	a_1, b_1
(All CH bonds are perpendicular)	
Total occupied	$6\times a_1, 3\times b_2, 2\times b_1, 1\times a_2$
(b) Formate Ion	
3 × 1s	a_1, a_1, b_2
2 × CO bonds	a_1, b_2
π bond	b_1
CH bond	a_1
5 × O lone pairs	a_1, a_1, b_2, b_2, a_2
Total occupied	$6\times a_1, 4\times b_2, 1\times b_1, 1\times a_2$

TABLE XI. Symmetry of Occupied Orbitals Derived from Group Theoretical Analysis of the VB Structures of (a) Cyclopropene, (b) the Cyclopropyl Cation, and (c) the Allyl Cation (C_{2v} Notation)[a]

VB description	Corresponding occupied MO's
(a) Cyclopropene	
3 × 1s	a_1, a_1, b_2
3 × CC	a_1, a_1, b_2
2 × CH ("central", perpendicular)	a_1, b_1
2 × CH ("terminal", planar)	a_1, b_2
π	b_1
Total occupied	$6\times a_1, 3\times b_2, 2\times b_1$
(b) Cyclopropyl Cation	
3 × 1s	a_1, a_1, b_2
3 × CC	a_1, a_1, b_2
1 × CH (central, planar)	a_1
4 × CH (terminal, perpendicular)	a_1, b_2, b_1, a_2
Total occupied	$6\times a_1, 3\times b_2, 1\times b_1, 1\times a_2$
(c) Allyl Cation	
3 × 1s	a_1, a_1, b_2
2 × CC	a_1, b_2
1 × CH (central, planar)	a_1
4 × CH (terminal, planar)	a_1, a_1, b_2, b_2
π	b_1
Total occupied	$6\times a_1, 4\times b_2, 1\times b_1$

[a] These results are to be compared with the "normal" ground-state configuration of isovalent triatomics (such as CO_2, N_3^-, and NO_2^+, for example) in which $5\times a_1$, $4\times b_2$, $1\times b_1$, and $1\times a_2$ MO's are doubly occupied.

in the stability order of the states of cyclopropane and O_3 results from very much the same circumstances as have been seen to produce the distinctions in the electronic spectra of the latter system and $HCOO^-$, respectively; the change in the relative spacing of the energy levels in the formate ion compared to that found in O_3 is merely less pronounced than in the cyclopropane–ozone comparison, for which the order of electronic states is actually altered from one system to another.

The most important conclusion resulting from this observation is simply that the geometries of such unusual systems as cyclopropane, ethylene oxide, and others *are no more exceptions in terms of the MW model* than are structures exhibited by the *excited states of more conventional systems*, such as the members of the AB_2 family of molecules. The same types of MO's are involved in

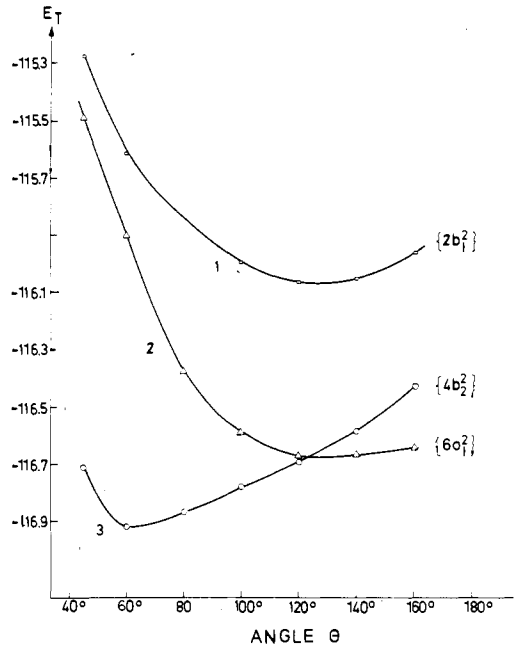

Figure 50. Total SCF energy E_T for various closed-shell states of cyclopropane; they should be compared with the analogous states of $HCOO^-$ in Figure 46 and those of ozone given in Figure 4a.

all cases, the same shapes of orbital energy curves; it is only that the order of these orbitals is *altered as a result of selective mixing with hydrogen AO's*. The same type of analysis[88] can be made for the existence of such nonlinear 16-valence-electron species as cyclopropene (51°), the cyclopropyl cation (85°), and the allyl cation (120°), whose VB structures are translated into ground-state MO electronic configurations in Tables XIa–c, respectively. The great similarity between the shapes of the angular potential curves of these systems and those obtained for the corresponding (excited) electronic configurations of N_3^- (Figure 9a) is again quite apparent from the calculated results (Figure 51).

Thus in order to predict the ground-state geometries of any molecule with a triatomic skeleton, it is first necessary to simply ascertain the correct electronic configuration for this species and then assume that the associated equilibrium nuclear arrangement will be quite similar to that of the same (perhaps excited) configuration of some simple nonhydrogenic triatomic system. Formally such a procedure can be carried out *entirely within the framework of the differential form of Koopmans' theorem* (eq 9), since no significant horizontal correction (eq 12) to the MW model is really required (because all these systems are of essentially equal covalency). Furthermore, the group theoretical VB analysis mentioned before is generally quite sufficient for determining the correct ground-state electronic configuration in a given case, requiring only knowledge of the approximate orientation (in-plane or out-of-plane) of the hydrogen atoms. In fact, it is just this orientation of hydrogen atoms which ultimately determines the change in MO stability relative to the standard order and therefore is clearly the primary determining factor for the distinctive skeletal equilibrium geometries of such H_nAB_2 systems whenever they occur.

In summary then the MW model clearly succeeds in the description of ground and excited state geometries of such "exceptional" molecules as cyclopropane,[89] the various C_3H_4 isomers,[88] and allyl and cyclopropyl cations, radicals, and anions,[198] whereas the VB scheme has considerably more difficulties in describing the same types of phenomena. In particular, it follows from the MW

model that cyclopropane in its lower valence states (obtained by electron promotion into the $4b_2$ MO with its strongly linear tendency) should possess a noncyclic structure similar to that of trimethylene (another C_3H_6 isomer with yet a different electronic configuration). Similarly the ring opening of cyclopropane in addition reactions is easily explained as the logical consequence of occupying the $4b_2$ MO in the incipient stages of such processes. More details on these and other related subjects may be found in the more specific treatment of this subject alluded to above[87] and also in the original series of papers[88,89,198] dealing with these points as they pertain to the study of various cyclic hydrocarbons with a triatomic skeleton. It should be clear from what has been included in the present section, however, that if sufficient attention is given to the question of which electronic configuration is preferred by a given system, the information contained in the original correlation diagrams of Mulliken and Walsh can be applied to a much larger class of systems than was once believed possible.

D. Molecules Containing Four Nonhydrogenic Atoms

1. AB_3 and $H_nA(BCD)$ Systems (Three-Coordinated Central Atom)

The geometry of AB_3 systems, one of the original molecular classes treated by Walsh,[2] has yet to be investigated *via ab initio* SCF calculations, but experience with AH_2 and AB_2 species (see section II.C.2) suggests strongly that the important features of the MW model as applied to the AB_3 family may be deduced to a large extent from analogous results for AH_3 molecules such as BH_3 and NH_3. A close connection can be made by considering the fluoro-substituted analogs of the latter species and assuming that the upper valence MO's in such AB_3 molecules are quite similar to those corresponding AH_3 systems; in other words, those orbitals which are *localized* at the highly electronegative fluorine atoms (with $3 \times 6 = 18$ more valence electrons than in corresponding hydrogen-containing systems) are assumed to have substantially no geometry-determining influence. In this way AH_3 molecules with six valence electrons (planar systems) are expected to have the same geometries as AF_3 species with 24 (6 + 18); also addition of two more electrons should have a similar effect in both cases, so that 26 valence-electron AF_3 molecules are expected to possess bent geometries, quite similar to those of AH_3 systems with 18 less valence electrons (such as NH_3 and PH_3). Furthermore once these geometrical trends have been isolated for AF_3 systems, it seems clear from the MW model that the same types of structural patterns should be equally apparent for more general members of the AB_3 molecular family. Geometrical differences between *isovalent* fluorides and oxides, for example, should result only because of relatively small differences in their respective charge distributions and hence are not expected to be adequately accounted for in terms of the MW model until some form of horizontal correction, such as that of eq 12, is applied to it.

Experimental studies of the geometry of AB_3 molecules (as well as of AB_2C and any other systems with three-coordinate central atoms) certainly bear out the essential accuracy of the foregoing analysis, as has been pointed out in Walsh's original papers on this general subject, with 24-valence-electron systems such as BF_3, CO_3^{2-}, NO_3^-, NO_2F, and almost surely CF_3^+ exhibiting planar geometries while their counterparts with 26 valence electrons, such as NF_3, PO_3^{3-}, PF_3, and $SOCl_2$, are found to possess bent structures. Furthermore, AB_3 correlation diagrams obtained *via* EHT calculations by Gimarc and Chou[57] indicate that the MW orbital energy trends discussed above are, in fact, actually observed in more quantitative investigations. The semiempirical calculations also indicate that the trend toward planar geometries becomes less strong when electrons are removed from the e-type MO (with its planar geometrical tendency; see Figure 21) as, for example, in going from strongly planar CO_3^{2-} with 24 valence electrons to CO_3 with only 22 (recall the analogous discussion of AH_3 species with four valence electrons in section III.A.2); in fact, a somewhat more distorted conformation in which the OCO angles are not all equal seems to be favored. Also just as for AH_3 systems addition of more electrons than are needed to fill both the e and a_1 (lone-pair) MO's is found to produce a tendency toward planar structures for this family of molecules, as, for example, in ClF_3 or XeO_3 with 28 valence electrons. It is interesting that the latter tendency is generally explained in terms of d-orbital hybridization effects in VB models while in the MW theory it is anticipated even on the basis of molecular orbitals composed exclusively of s and p AO's. The fact that molecules of this type for either the AH_3 or AB_3 families are only observed if the central atom belongs to the second or higher rows of the periodic table would thus seem to indicate that d AO's may be essential for the overall *stability* of such systems, but that they do not greatly affect the essential details of the *shapes* of such molecules.[199]

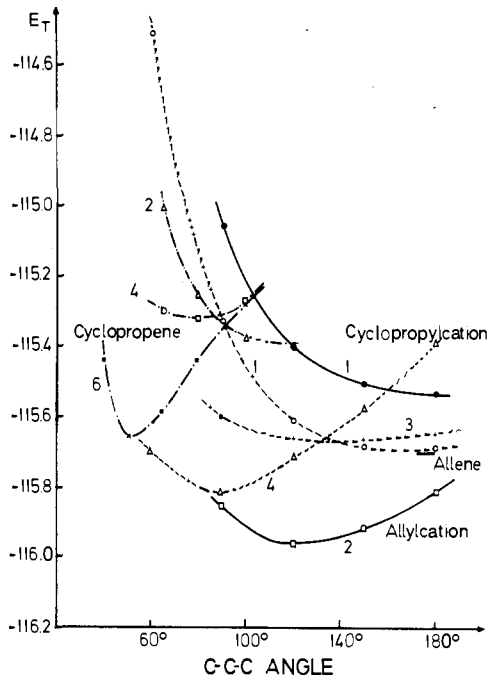

Figure 51. Total SCF energy E_T for several states of the allyl cation (solid lines), the cyclopropyl cation (dashed lines), cyclopropene (dotted-dashed lines), and allene. The labeling of the curves is the same as in Figure 9, indicating the electronic configuration of the respective states.

Systems of the AB_3 family with 25 electrons are clearly analogous to AH_3 species with only 7 valence electrons, which as discussed in section III.A.2 are generally weakly planar systems (although BeH_3^{2-} is calculated to be slightly nonplanar *via* Koopmans' theorem). Nevertheless, as pointed out above in section III.C.2, fluorides are generally expected to favor planar geometries less strongly than corresponding hydrogen-containing systems (at least as long as the central lone-pair MO is occupied), and thus it should not be surprising that CF_3 actually prefers a slightly bent geometry ($\angle FCF = 112°$), even though CH_3 is believed to be a (weakly) planar system.

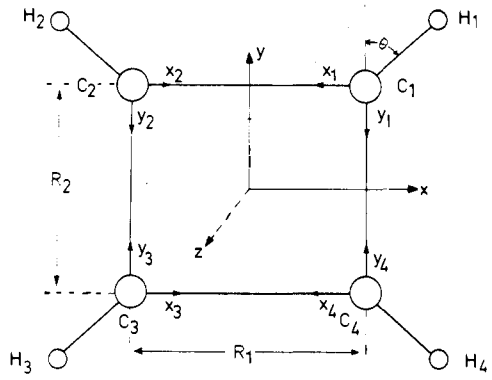

Figure 52. Coordinate system for a general C_4H_4 system.

The horizontal correction of eq 12 is really no larger in this comparison from the *standpoint of energy differences* than in other hydrogen–fluorine substitutions; it is only that when this effect is translated into a change in equilibrium angle relative to that of the weakly planar molecule CH_3 it appears to be unusually large.

In fact, the evidence is that the horizontal correction between corresponding hydrides and fluorides is less than between members of the hydride group itself for different central atoms (for example, PH_3 and NH_3 have angles that differ by nearly 15°); it also seems to be quite small among isovalent fluorides, since, for example, NF_3 and PF_3 have virtually equal internuclear angles (although both are smaller at 103–104° than that of NH_3). This effect probably results because the orbital energy term in eq 12 is relatively more important for fluorides than for the corresponding hydrides and hence is better able to cancel out the opposite tendency in the V_{ee} term.[200] This difference in the geometrical trends observed among isovalent fluorides and hydrides, respectively, certainly appears to indicate that such relatively minor distinctions in the equilibrium structures of these systems cannot be explained in a consistent manner *solely on the basis of electron repulsion effects*, in disagreement with what is generally assumed in connection with application of the VSEPR model to problems of this type.

The effect of adding hydrogen atoms to AB_3 or AB_2C skeletons (with a three-coordinate central atom) also follows the same pattern as for their triatomic counterparts discussed in section III.C.3. Once again it appears that the *skeletal geometry* in both nonhydrogenic parent systems and in their hydrogen-containing analogs is determined primarily on the basis of the number of valence electrons contained by them. In H_nAB_3 systems, however, there are apparently no cases in which the additional hydrogen atoms produce a change in the ground-state electronic configuration and hence, contrary to the situation discussed above for H_nAB_2 species, there are no known cases in which the equilibrium structures of such molecules are significantly different from those of their isovalent nonhydrogenic counterparts. One of the clearest examples of the aforementioned relationships occurs for the isobutene–isobutane comparison; the alkene is planar as one expects for a system of this type with 24 valence electrons, whereas the alkane, with two more electrons, is not. The *tert*-butyl radical [$C(CH_3)_3\cdot$], with 25 valence electrons, represents the usual intermediate case and is expected to be weakly planar (probably somewhat more strongly so than CH_3 itself in light of the electron-donating properties of the constituent methyl groups). Many other hydrogen-containing systems in this family with 24 valence electrons are also known to have a planar skeleton of heavy atoms, such as HNO_3, HCO_3^-, $C(NH_2)_3^+$, H_3CNO_2, and the acetate ion CH_3COO^-, while analogous nonplanar systems with two more valence electrons also abound. Furthermore, the experience with H_nAB_2 systems (section III.C.3) indicates quite strongly that very definite similarities exist between the angular correlation diagrams of H_nAB_3 molecules and those of the parent AB_3 family and hence that as usual the aforementioned geometrical trends can be explained quite easily in terms of the differential form of Koopmans' theorem.

2. H_nABCD Systems

A large number of molecules with four heavy atoms do not contain a three-coordinated central atom and thus are not described satisfactorily by means of AB_3 correlation diagrams. The experience with other molecular families suggests strongly, however, that the MW model can be applied in the usual manner in this case as long as at least one calculated SCF correlation diagram is available; furthermore, judging from the results discussed above for cyclopropane, $HCOO^-$, and various simple AB_2 molecules (section III.C.3), it should not be critical whether such a diagram is obtained for some parent nonhydrogenic tetratomic species or for a more complex derivative which does contain additional hydrogen atoms.

An *ab initio* investigation of a system of the latter type, namely cyclobutadiene C_4H_4, has in fact been reported some time ago.[151] Since one of the main points of interest in this study was whether cyclobutadiene possesses a square or rectangular equilibrium structure, the specific geometrical parameter considered is somewhat complicated involving simultaneous stretching of one pair of CC bonds while the other two are contracted according to a prescribed relationship. Details of the specific nuclear arrangements considered can be found in the original paper; a schematic coordinate system for this molecule is given in Figure 52 for easy reference in the following discussion. Although the nuclear conformations treated in these calculations[151] are all of the cyclic variety, it will become apparent that the results of this study are also pertinent to the understanding of how open-chain structures arise in systems of this type.

Typical schematic diagrams for the important upper valence MO's (both σ and π species) of cyclobutadiene are given in Figure 53. Interpretation of these results is again aided by means of a group theoretical analysis of the VB structure of the molecule in question, as summarized in Table XIIa; the four inner-shell MO's and also the three most stable valence species ($2a_g$, $2b_{2u}$, $2b_{3u}$; essentially CC bonding orbitals, as can be seen from the respective charge density contours in Figures 9a and 10a,b, respectively, of ref 151) are not shown in Figure 53 since they are always occupied in any stable molecule of this family and hence have essentially a constant geometrical effect throughout this series. Of the σ MO's actually plotted in the diagram, all but the $4b_{3u}$ species, which is antibonding along the (long) R_1 bond (Figure 52), are occupied in cyclobutadiene at equilibrium (Table XIIa). The π (p_z) MO's are, of course, the familiar Hückel-type species discussed in π-electron theories; for rectangular geometries (long R_1 and short R_2) the $1b_{2g}$ (bonding along R_2) is more stable than the $1b_{3g}$ (bonding along R_1) while in the square conformation these species are completely equivalent (e_g). The *ab initio* SCF and CI calculations have indicated that the ground state of this system is a rectangular singlet, a finding which is quite understandable in light of the fact that distortions out of the square structure result in increased stability for one of the e_g components (b_{2g}), while the opposite behavior is noted

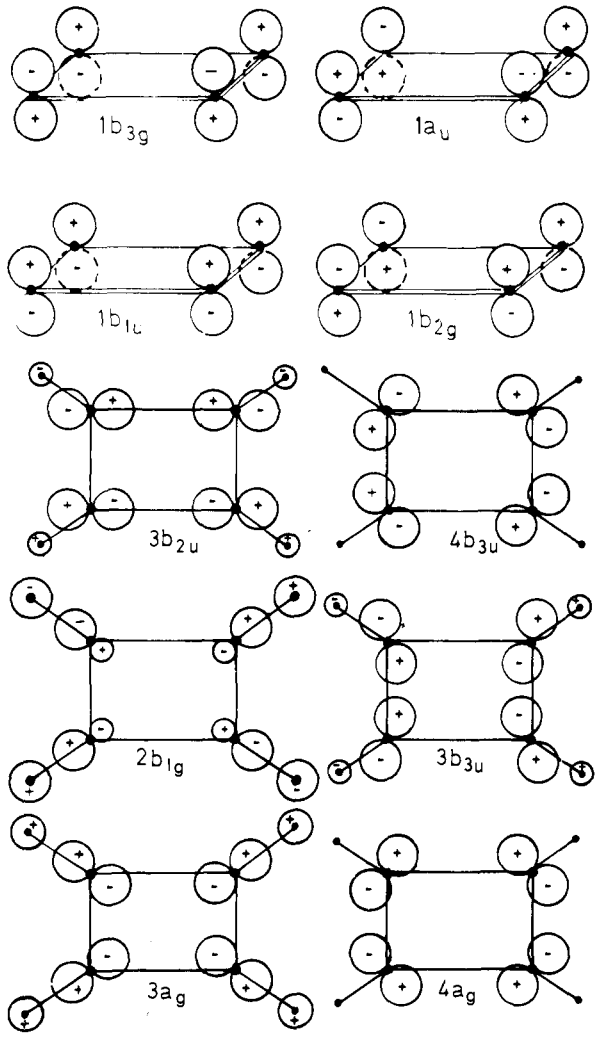

Figure 53. Schematic diagram of the upper valence orbitals in an A_4H_4 system.

for the other[201] (b_{3g}). These orbital energy trends and others are readily observed in the calculated C_4H_6 correlation diagram given in Figure 54 (note that as R_1 is increasing in this diagram, R_2 is simultaneously decreasing[151]). For the upper valence MO's described in Figure 53 the shapes of corresponding orbital energy curves are seen to correlate quite well with the respective bonding and antibonding character of these species along R_1 and R_2, respectively;[202] further details may be found in ref 151. These orbital energy trends are summarized in Table XIII and as usual will serve as the basis for applying the MW model to the study of other systems in the same molecular family.

The equilibrium geometry of cyclobutadiene (20 valence electrons) is extremely rare among other isovalent systems containing the same number of heavy atoms, and it is therefore a challenge for any geometrical model emphasizing a close relationship between geometry and number of electrons to explain why such a cyclic structure is favored in this particular case. The experience with cyclopropane and cyclopropene and other systems with a triatomic skeleton (section III.C.3) indicates that such exceptional situations can be explained consistently in terms of the MW model *once it is realized that they are caused by a difference in ground-state electronic configuration.* The general procedure to be followed thus involves first determining the electronic configuration for the ground state of each molecule of interest and then using the orbital energy trends summarized in Table XIII

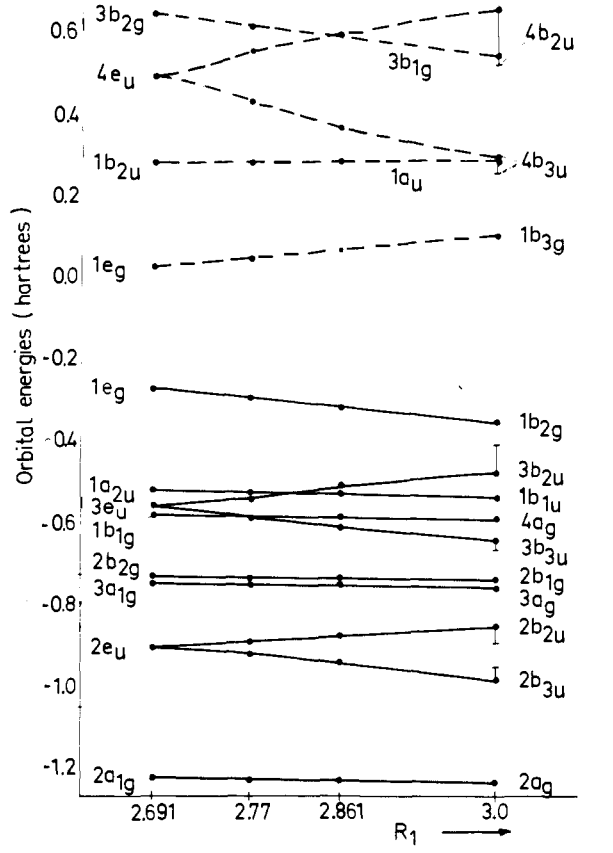

Figure 54. Calculated canonical orbital energies for the ground state of cyclobutadiene C_4H_4 as a function of the R_1 distance (see Figure 52).

TABLE XII. Symmetry of Occupied Orbitals Derived from Group Theoretical Analysis of the VB Structures of (a) (Rectangular) Cyclobutadiene, C_4H_4, and (b) Two Acetylene Fragments Separated to Infinity (D_{2h} Notation)

VB description	Corresponding occupied MO's
(a) Cyclobutadiene	
4 × 1s	a_g, b_{1g}, b_{2u}, b_{3u}
4 × CC	a_g, a_g, b_{2u}, b_{3u}
4 × CH (planar)	a_g, b_{1g}, b_{2u}, b_{3u}
2 × π	b_{1u}, b_{2g}
Total occupied	$4\times a_g$, $2\times b_{1g}$, $3\times b_{2u}$, $3\times b_{3u}$, $1\times b_{1u}$, $1\times b_{2g}$
(b) Two C_2H_2 Molecules	
4 × 1s	a_g, b_{1g}, b_{2u}, b_{3u}
2 × CC	a_g, b_{3u}
4 × CH	a_g, b_{1g}, b_{2u}, b_{3u}
2 × π (in-plane)	a_g, b_{3u}
2 × π (perpendicular)	b_{1u}, b_{2g}
Total occupied	$4\times a_g$, $2\times b_{1g}$, $2\times b_{2u}$, $4\times b_{3u}$, $1\times b_{1u}$, $1\times b_{2g}$

to deduce any differences in the equilibrium geometries of these systems on the basis of their distinctive orbital occupations.

A group theoretical analysis of an important C_4H_4 "isomer," namely, two acetylene molecules separated at infinity (Table XIIb), shows that the ground-state electronic configuration (simply a combination of the two ground-state acetylenes in this case) is, in fact, different from that favored by cyclobutadiene; specifically the products of decomposition are seen to occupy the $4b_{3u}$ (π_{u1}-π_{u2}) MO in place of the $3b_{2u}$ species formed from positive overlap (π_{g1} + π_{g2}) of the two π_g (π^*) orbitals of C_2H_2.

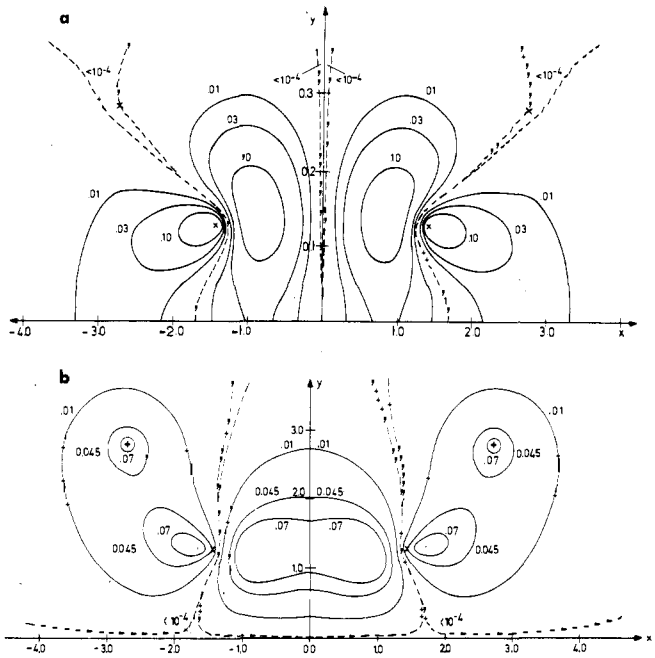

Figure 55. Calculated charge density contours for the $4b_{3u}$ MO (a) and the $3b_{2u}$ MO (b) of cyclobutadiene, C_4H_4. (Only the upper half of the molecule is shown in each case.)

The calculated orbital charge density contours for these two MO's in cyclobutadiene itself shown in Figures 55a and 55b, respectively, indicate clearly why the change in occupation occurs. The $4b_{3u}$ is bonding along the short CC distance (R_2 in Figure 52) but antibonding along the other (R_1) and is thus favored for the separated acetylene molecules, whereas the $3b_{2u}$ possesses virtually the opposite characteristics, *favoring small* R_1 *values* and hence a bound cyclobutadiene molecule (see Table XIII). This finding means that orbital symmetry is not conserved in the decomposition of cyclobutadiene into two acetylene fragments; thus even though the SCF and CI calculations[151] indicate that the combined system is not stable with respect to two acetylene molecules separated at infinity, it still appears quite likely that the former system may still have a bound state because of the relatively high activation energy necessary for the decomposition process.

The ground-state electronic configuration of the stable C_4H_4 isomer vinylacetylene (butatriene), with two hydrogens at one of the end carbons (linear skeleton) and none at one of the central species, is indeed also different from that of cyclobutadiene (see Table XIV for a summary of the electronic configurations of a series of C_4H_n and A_2B_2 systems[203]), with the $4b_{3u}$ (see Figure 55a) doubly occupied in place of the $2b_{1g}$ species favored by the cyclic system. The charge density contours of the latter MO (Figure 56) show it to possess considerable CH bonding character, thereby compensating for the fact that it is an exclusively CC *antibonding* species (as indicated in Figure 53). If the hydrogen atoms are not distributed equally among the carbons in such C_4H_4 systems, the effect is almost surely to emphasize the CC antibonding character of this orbital, thereby making its occupation less favorable in a system such as vinylacetylene. In view of the strongly R_1 antibonding character of the $4b_{3u}$ MO (Table XIII), it is not at all surprising that occupation of this species instead of the $2b_{1g}$ is marked by a decided tendency away from a cyclic arrangement of the carbon atoms, as is observed in going from cyclobutadiene to the linear equilibrium geometry of the vinylacetylene system.

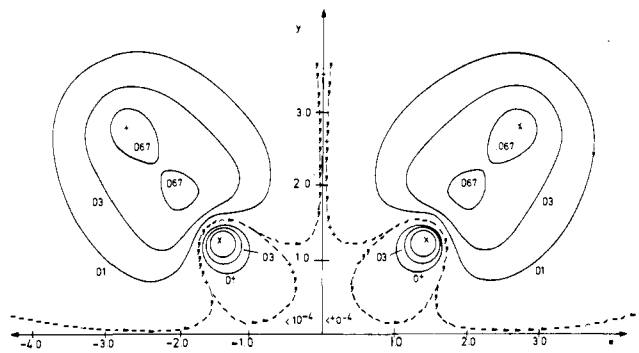

Figure 56. Calculated charge density contours for the $2b_{1g}$ MO of cyclobutadiene,[151] C_4H_4. (Only the upper half of the molecule is shown.)

TABLE XIII. Orbital Energy Trends in Systems with Tetratomic Skeletons[a]

MO	R_1 character[b] (long bond)	R_2 character[b] (short bond)	CH bonding
σ-Type $3a_g$	Bonding (σ)	Bonding (π)	Strong
$4a_g$	Bonding (σ)	Bonding (π)	Very weak
$3b_{3u}$	Antibonding (σ)	Bonding (σ)	Strong
$2b_{1g}$	Weakly antibonding	Weakly antibonding	Very strong
$3b_{2u}$	Bonding (σ)	Antibonding (π)	Weak
$4b_{3u}$	Antibonding (σ)	Bonding (π)	Very weak
π-Type $1b_{1u}$	π bonding	π bonding	None[c]
$1b_{2g}$	π antibonding	π bonding	None[c]
$1b_{3g}$	π bonding	π antibonding	None[c]
$1a_u$	π antibonding	π antibonding	None[c]

[a] Schematic diagrams of corresponding MO's in C_4H_4 may be found in Figure 53. [b] For notation see Figure 52. [c] At least for planar systems. If hydrogen atoms are placed out of the molecular plane, CH bonding becomes an important factor in the composition of these π-type species.

The latter observation as well as the foregoing discussion of the decomposition of cyclobutadiene into two acetylenes suggests quite strongly that it is impossible to have a small-angle C_4 skeletal structure as long as the (R_1 antibonding) $4b_{3u}$ MO is occupied. This situation is completely analogous to that found in the study of H_nAB_2 systems (section III.C.3), for which the $4b_2$ species (Figure 38b) plays a very similar role, being left vacant for all stable cyclic structures of this type. At the same time it underscores the great importance of bonding with H AO's in the attainment of stable cyclic structures since it is clear from the aforementioned charge density contours that without the effect of heavy CH bonding the $2b_{1g}$ species itself would be strongly R_1 and R_2 antibonding, thereby becoming less stable than the $4b_{3u}$ and quite likely just as detrimental to the formation of ring compounds. In retrospect the $2b_{1g}$ is seen to be closely akin to the $2b_1$ of triatomic systems, which must be occupied instead of the $4b_2$ in order to obtain cyclic structures, and which at the same time can be stabilized considerably by (out-of-plane) CH bonding.

The importance of bonding with H AO's in this connection is also emphasized by the fact that there is apparently no stable ring isomer with a C_4H_2 formula. The removal of two hydrogens relative to cyclobutadiene makes occupation of the $2b_{1g}$-type MO much less favorable for systems of this type (see Table XIV). In fact, at equilibrium the most stable C_4H_2 isomer diacetylene, HCCCCH, occupies the $4b_{3u}$ ($2\pi_u$) instead of either the $3b_{2u}$ or $2b_{1g}$ species, by reason of the fact that the strongly bonding character of the former MO along both R_2 (in this case triple) bonds outweighs the opposite effect

TABLE XIV. Electronic Configurations of Various Systems with Tetratomic Skeletons[a]

System	Occupation number[b] $4b_{3u}$	$2b_{1g}$	$3b_{2u}$	$1b_{3g}$	$1a_u$
C_4H_2 (18) Diacetylene, also C_2N_2	2	0	0	0	0
C_4H_4 (20) Cyclobutadiene	0	2	2	0	0
$2C_2H_2$ Two separated acetylene fragments	2	2	0	0	0
C_4H_4 Vinylacetylene	2	0	2	0	0
C_4H_6 (22) Butadiene, also N_2O_2	2	2	2	0	0
Cyclobutene	0	2	2	2	0
Bicyclobutane	0	2	2	0	2
Dimethylacetylene, also C_2F_2	2	0	2	2	0
C_4H_8 (24) Cyclobutane, also O_4	0	2	2	2	2
1-, 2-Butene, also N_2F_2	2	2	2	2	0
C_4H_{10} (26) *n*-Butane, also F_2O_2	2	2	2	2	2

[a] The number of valence electrons for each system is given in parentheses. D_{2h} notation is used throughout; schematic diagrams for each of the valence MO's in this table may be found in Figure 53. [b] In addition to the MO's listed here the following MO's are all doubly occupied in each case: $1a_g$, $1b_{3u}$, $1b_{2u}$, $1b_{1g}$, $2a_g$, $2b_{3u}$, $2b_{2u}$, $3a_g$, $3b_{3u}$, $4a_g$, $1b_{1u}$, $1b_{2g}$.

along the lone R_1 species (see Figures 52 and 55a), particularly for such a linear arrangement of the four carbon atoms. One can anticipate, however, that double occupation of the $2b_{1g}$ MO in place of the $4b_{3u}$ species would lead to an excited state which does, in fact, prefer a cyclic geometry somewhat similar to that of cyclobutadiene, albeit probably somewhat more rectangular (since the $3b_{2u}$ is not occupied in C_4H_2).

In hydrocarbons with 22 valence electrons the same close relationship between electronic configuration and skeletal geometry is equally apparent. The cyclic C_4H_6 isomer cyclobutene is again observed to occupy the $2b_{1g}$ and not the $4b_{3u}$ (Table XIV); relative to cyclobutadiene the differentiating orbital in cyclobutene is the $1b_{3g}$ species, which is heavily CH bonding in this system as a result of the perpendicular orientation of its methylene groups (Figure 53). The latter MO is R_1 bonding (Table XIII) but more strongly so between the nonmethylene carbons (in the neighborhood of the methylene carbons the charge is more localized in the CH bonds), and hence it is not surprising that the equilibrium structure of cyclobutene is distinctly trapezoidal in nature (in the notation of the coordinate system in Figure 57, R_b is significantly smaller than R). In most other cases the close relationship between the MO's of cyclobutene and cyclobutadiene is even more apparent, as can be seen from a comparison of their $3b_{2u}$-type orbital charge densities shown in Figures 58 and 55b, respectively.

If the additional electrons of a C_4H_6 species are placed in a $1a_u$-type orbital of cyclobutadiene instead of the $1b_{3g}$ species favored by cyclobutene, it is still possible to maintain a stable ring structure, again as long as the $4b_{3u}$ MO remains unoccupied. Just as before with the cyclobutene ground state, however, the change in occupation relative to cyclobutadiene does have an important structural effect, this time tending to promote bending *across the ring* (since $1a_u$ is antibonding along each of the normal ring bonds in such systems; see Figure 53 and Table XIII). The most favored structure for the resulting electronic configuration (see Table XIV) is exemplified quite nicely by the unusual nuclear arrangement of another C_4H_6 isomer bicyclobutane, which is known to possess a π-type bond across a ring of four CCσ species.[204,205] In this case the four-membered ring is strongly puckered and the CH bonds at the π-bonding carbons are tilted upward by at least 50°; both of these

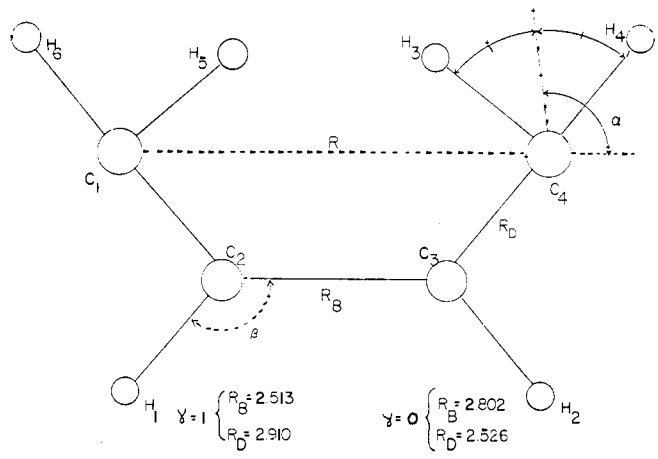

Figure 57. Coordinate system for a general C_4H_6 system.

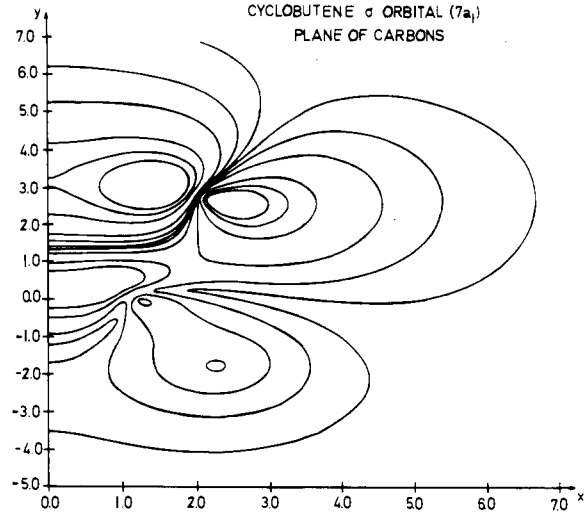

Figure 58. Calculated charge density contours[73] of the $7a_1$ (σ) MO of cyclobutene in the plane containing the four carbon atoms. (Only the right side of the molecule is shown.) Note the similarity between this contour diagram and that of the corresponding ($3b_{2u}$) MO in cyclobutadiene given in Figure 55b.

effects are easily understandable in light of the added stability they produce for the normally strongly antibonding $1a_u$ MO.

In both cyclobutene and butadiene an important factor in promoting occupation of π-type MO's instead of the R_1-antibonding $4b_{3u}$ species is the perpendicular orientation of their constituent methylene groups. Rotating the CH_2 species into the C_4 plane clearly has the opposite effect, and as a result such a planar C_4H_6 nuclear arrangement as that favored by either cis or trans butadiene strongly prefers occupation of the $4b_{3u}$ instead of either the $1b_{3g}$ or $1a_u$ species (Table XIV); consequently, the possibility of a stable cyclic structure for either of the latter C_4H_6 isomers is effectively removed. The butadiene example illustrates quite clearly that while occupation of the $2b_{1g}$- and $3b_{2u}$-type MO's is quite important for maintaining a cyclic structure, it is not sufficient to guarantee a ring system as long as the $4b_{3u}$ is not vacant. Nevertheless, it is still found that whether such MO's are occupied in C_4H_6 isomers or C_4H_4 species, the orbital energy trends observed for them remain essentially unchanged, as can be seen by comparing calculated cyclobutene and *cis*-butadiene R_1-stretch (or $\angle$CCC) correlation diagrams (Figure 59a,b) with that shown earlier for cyclobutadiene (Figure 54); in the C_4H_6 diagrams the $7a_1$ or σ MO is to be compared with the former $3b_{2u}$ and the $6b_2$ with the $4b_{3u}$, while the correspondence between the various π-

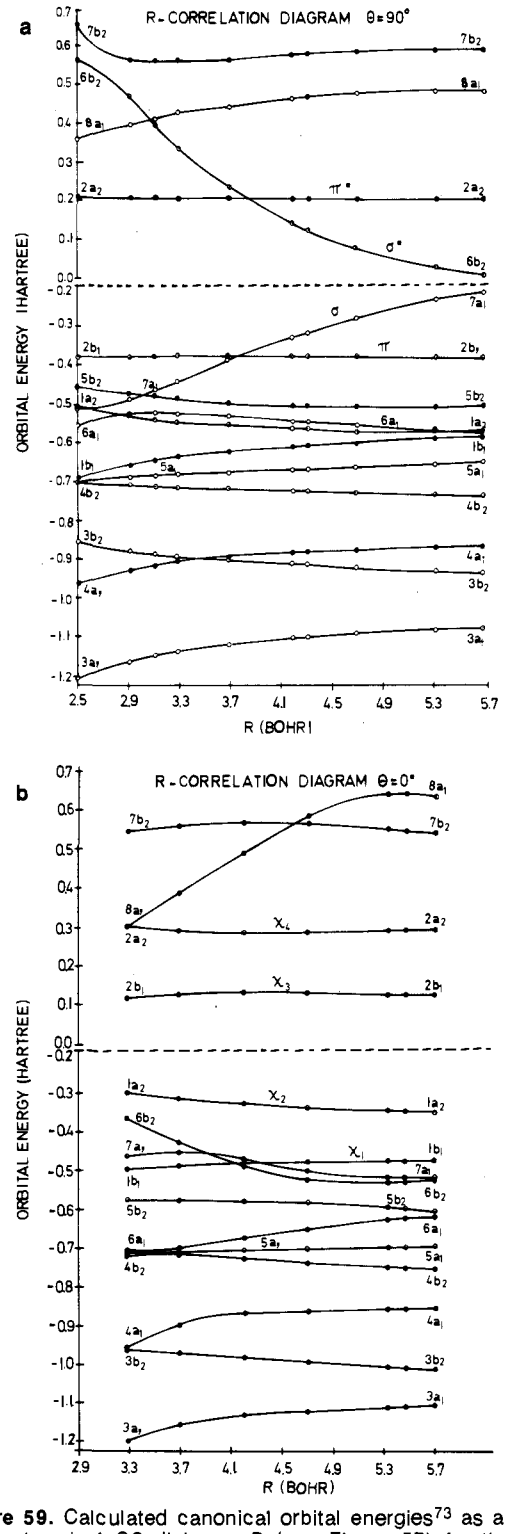

Figure 59. Calculated canonical orbital energies[73] as a function of the terminal CC distance R (see Figure 57) for the ground states of (a) cyclobutene (θ = 90°) and (b) *cis*-butadiene (θ = 0°), respectively.

type orbitals should be more obvious. Finally it can be shown by means of a group theoretical analysis that dimethylacetylene has yet another ground-state electronic configuration in which the C_1–C_3 antibonding π -type $1b_{3g}$ species (Table XIV) is occupied;[203] since this orbital replaces the (weakly) C_1–C_3 bonding $2b_{1g}$ orbital in butadiene (Figure 54 or Figure 59a,b), it is to be expected that this system has an even larger CCC bond angle than the dienyl structure, as is, of course, observed.[206]

The C_4H_8 isomers have still two more valence electrons, making 24 in all, and it should be clear from what has been written that the only way such a system could possess a small-angle (cyclic) equilibrium structure is if the $4b_{3u}$ MO is left unpopulated. In order to accomplish this objective in cyclobutane, it is necessary to occupy both the π-type $1a_u$ and $1b_{3g}$ orbitals (Figure 53). As mentioned above, these MO's are most stable if all the hydrogen atoms are positioned above and below the C_4 plane so the greatest possible mixing of hydrogen AO's with the corresponding p_z AO's of the carbons can be effected, and this nuclear arrangement is known to be favored in the case of the only known cyclic system of this formula. The antibonding character of the $1a_u$ nevertheless has its effect, causing the molecule to assume a somewhat skewed nuclear structure, in close analogy to the situation which ensues upon occupation of the $1b_{2g}$ MO in A_2H_2 systems, as, for example, in hydrogen peroxide H_2O_2 (section III.B.3). If the $4b_{3u}$ is occupied, on the other hand, as in 2-butene, the resulting structure definitely possesses an open-chain form. The skeletal geometry of the carbons in this C_4H_8 isomer is closely akin to that of butadiene, as should be expected from the fact that this alkene results from hydrogenation of dimethylacetylene (and hence from differential occupation of the C_1–C_3 bonding $2b_{1g}$ species, thereby experiencing the usual tendency away from linear geometries).

If two more electrons are added to either of the C_4H_8 isomers, the $4b_{3u}$ must become occupied, and hence all possibility of attaining a stable cyclic C_4H_{10} structure is removed; hydrogenation thus leads to the open-chain system *n*-butane (Table XIV) in either case. In the language of MO theory the saturated hydrocarbon results when all of the constituent valence orbitals become occupied (except, of course, the strongly antibonding σ^* species, whose population inevitably leads to decomposition of the combined system into smaller fragments).

Finally, although the discussion in this section has centered upon hydrocarbons in the H_nABCD class, the principles employed are clearly of much more general validity. Thus substitution of N for CH, NH and O for CH_2 and NH_2, OH and F for CH_3 should preserve to a large extent the skeletal nuclear geometry observed for the original hydrocarbons. In drawing such analogies, however, it should not be overlooked that certain MO's and hence certain electronic states are considerably less stable in the absence of significant mixing with H AO's. Thus reduction in the number of attached hydrogen atoms may often be of critical importance in determining the ground-state electronic configuration in such systems and as a result may lead to a substantially different equilibrium nuclear arrangement than that exhibited by the parent hydrocarbon; examples of this kind will be taken up in the next subsection. Nevertheless, experimental structural studies offer ample evidence to support the conclusion that the calculated correlation diagrams discussed above for cyclobutadiene and cyclobutene provide quite specific details about the equilibrium nuclear geometries of all the molecules in the H_nABCD family.

3. *Tetratomics without Hydrogens*

As indicated at the beginning of the previous section it should be possible to pursue the study of the geometry of nonhydrogenic tetratomic systems along the same lines as for hydrogen-containing analogs such as cyclobutadiene or dimethylacetylene. It is not at all surprising, for example, that 18-valence electron C_2N_2 (NCCN) is a linear system since it possesses the same ground-state electronic configuration as linear diacetylene HCCCCH (see Table XIV). In like manner since C_2F_2 has the same electronic configuration as dimethylacetylene it is expect-

ed that both these systems should have the same (linear) equilibrium geometries, a point which was discussed in connection with the aforementioned SCF calculations for cyclobutadiene.[151] The same conclusion can be reached by taking advantage of the usual rule for fluorine-substituted compounds since of course C_2H_2 is also a linear molecule, with the upper π_u MO fully occupied and the corresponding π_g vacant (section III.B.3).

The question remains, however, as to whether other types of geometrical structures are possible for A_2B_2 systems with from 18 (such as C_2N_2) to 22 (C_2F_2) valence electrons, particularly those of the cyclic form, such as are observed for cyclobutadiene and cyclobutene with 20 and 22 valence electrons, respectively. Among the molecules with 20 valence electrons C_2O_2 undoubtedly favors an electronic configuration with π_g only doubly occupied ($^3\Sigma_g^-$ ground state) and hence a linear nuclear arrangement, but a substance such as N_4, which is more closely related to cyclobutadiene, might well be expected to assume a ground-state configuration characteristic of a cyclic equilibrium geometry. In actuality N_4 probably does not possess a very stable cyclic structure, however, since in the absence of H AO mixing the key $2b_{1g}$ MO (see Table XIV) becomes fairly strongly antibonding along both R_1 and R_2 (see Figures 53 and 56). The second-row analog P_4 is known and is believed to possess a tetrahedral geometry,[207] but it is unlikely that N_4 is a stable system at all in view of the high stability of N_2 itself. At the same time the possibility of a tetrahedral C_4H_4 isomer might seem quite likely on the basis of the P_4 geometry, but the results of *ab initio* SCF and CI calculations[208] indicate that such a tetrahedrane isomer is less stable than cyclobutadiene by approximately 70 kcal/mol. Although this result is clearly subject to some degree of uncertainty, the sheer magnitude of the energy difference found militates heavily against the existence of tetrahedrane, especially in light of the rather tenuous existence of cyclobutadiene itself.

The situation with A_2B_2 systems of 22 valence electrons is somewhat clearer, however, because of the existence of N_2O_2 isomers as well as that of the linear C_2F_2 species. The experimental evidence is that N_2O_2 exists in both trans and cis bent conformations, quite similar to those believed to be optimal for butadiene. That these two systems should also favor the same electronic configuration is only to be expected since an N atom can replace a CH in butadiene while O is isoelectronic with CH_2. Thus N_2O_2 occupies the in-plane $2b_{1g}$-type orbital in preference to the out-of-plane $1b_{3g}$-type species favored by both dimethylacetylene and difluoroacetylene (Table XIV). It may be that a cyclobutene-like *excited state* of N_2O_2 is also relatively stable but such a species must occupy the $1b_{3g}$-type MO in preference to the $4b_{3u}$–$6b_2$ species (Figure 55a) which has been seen to be so unfavorable for cyclic geometries, and without the influence of bonding with H AO's such an exchange would seem to involve a fairly large loss in stability.

There is yet another possibility for a stable N_2O_2 structure, namely one which is analogous to the C_4H_6 isomer bicyclobutane; its structure would be in valence bond notation

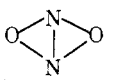

with a dihedral angle of approximately 120° between the two ONN planes. In order to achieve such a structure N_2O_2 would have to assume an electronic configuration in which both $4b_{3u}$ and $1b_{3g}$ MO's are vacant but in which the $1a_u$-type orbital is filled (see Table XIV). Again, without the aid of H AO mixing, it is unlikely that such a structure could be very stable since the $1a_u$ undoubtedly possesses a higher orbital energy in N_2O_2 than does $4b_{3u}$; nevertheless, an excited state with this electronic configuration should almost certainly possess an equilibrium geometry which is quite similar to that of bicyclobutane.

The system N_2F_2 with 24 electrons is analogous to N_2H_2 in the family of A_2H_2 molecules or to 2-butene in the group of hydrocarbons. Either way it must be expected that a bent geometry is favored, with cis and trans isomers of roughly equal stability. In order to get a cyclic A_2B_2 structure analogous to cyclobutane, the most likely possibility seems to be O_4, obtained by substituting an O atom for each CH_2 species in the hydrocarbon. A skewed ring would be expected in analogy to the C_4H_8 species, but thus far O_4 has apparently only been observed in condensed liquid form[209,210] and the experimental indication is that all the O–O bonds are not equal; hence it would appear that once again the existence of a stable cyclic isomer for such nonhydrogenic systems is unlikely.

Systems with 26 valence electrons in this family such as F_2O_2 and Cl_2S_2 should be similar to both H_2O_2, on the one hand, and isovalent *n*-butane, on the other; *i.e.*, they should have bent structures which are also somewhat skewed. This expectation is again borne out in experimental investigations.[211]

In summary then, with the aid of H_2A_2 and $H_nA_2B_2$ analogs it is a very simple matter to explain the equilibrium geometries of known A_2B_2 systems, and also to predict what types of nuclear arrangements should be expected for the corresponding excited states. In general, it seems as if all cyclic structures of this family are unstable because the essential hydrogen AO mixing which makes the analogous $H_nA_2B_2$ nuclear arrangements possible is obviously not present in these cases. Nevertheless, the relationship between equilibrium geometry and electronic configuration appears to be equally valid for all these systems, and the explanation for this phenomenon can be found in the great similarities exhibited by their respective orbital energy correlation diagrams, as borne out by actual calculations employing the *ab initio* SCF method.

IV. Summary and Conclusion

At the beginning of this paper a series of six criteria was given for the purpose of judging the extent to which a given theoretical method is successful in obtaining a quantitative realization of the Mulliken–Walsh structural model. A review of these points shows quite unambiguously that the procedure of constructing angular correlation diagrams from the *canonical orbital energies of ab initio SCF calculations* satisfies at least the first five of these criteria very well. For example, the corresponding MO's are well known to possess the necessary symmetry characteristics, and this fact in turn allows for a straightforward interpretability of the orbital energy curves themselves. In addition it is clear because of Koopmans' theorem that such orbital energy quantities are easily identifiable with molecular ionization potentials, and it has also been shown that differences between them can be correlated quite effectively with spectral transition energies.[212] Even more importantly the correlation diagrams constructed from these calculated quantities for different members of the same molecular family are invariably found to bear a quite close resemblance to one another. As a result the only real question about employing the SCF canonical orbital energies in the MW model has concerned the manner in which to use them to obtain the

geometrical predictions which are the ultimate goal of the original theory.

The most obvious approach, namely to use the sum of canonical orbital energies to approximate the SCF total energy, must be discarded. To be sure, for a large number of cases it has been found that the orbital energy sum $\Sigma\epsilon_i$ (or $\Sigma^{val}\epsilon_i$) behaves very nearly the same as the total energy E_T, but a detailed investigation of the relationships between these two quantities for many systems and also for different types of geometrical variables, particularly equilibrium bond lengths, has shown that the orbital energy sum by itself is *not a sufficiently reliable indicator of equilibrium molecular geometry.*

On the other hand, it is found that even in cases for which the *sum of orbital energies* is not capable of giving an *absolute* determination of the favored nuclear arrangement, it is still possible to use the information available from the *individual orbital energy curves themselves* to predict *differences* in geometry between systems in the same molecular family but *with different numbers of valence electrons*. Relationships such as these follow directly in a quantitative manner simply by making use of Koopmans' theorem. In particular it has been shown that *successive application of the differential form of Koopmans' theorem* (eq 9) using the results of *ab initio* SCF calculations for one system yields potential curves for a wide variety of related species (in both ground and excited states) which, in fact, approximate the true energy surfaces in such cases quite satisfactorily. The success of this approach is clearly based on the fact that it does not seek an *absolute* determination of the molecular geometry of any of these systems but rather merely an assessment of what *differences in geometry* are to be expected *between such species.* And indeed closer scrutiny of the manner in which the MW model itself is actually applied shows that such *relative* structural information is all that is ever really forthcoming from the empirical theory with which identification is being sought. Once this basic point is grasped, it is possible to use the SCF canonical orbital energy curves with the same degree of effectiveness as has generally been claimed for the corresponding empirical quantities given by Mulliken and Walsh.

To see how the MW model is used to describe geometrical effects, it is useful to consider a schematic diagram such as that given in Figure 12, in which all the systems in a given molecular family are arranged in rows according to the number of valence electrons each contains. In order to deal with excited as well as ground states of molecules it is necessary to expand the diagram somewhat to include a separate row *for each valence electronic configuration,* rather than just for each number of valence electrons, commonly observed for such systems. The MW model (and also the Koopmans' theorem analysis discussed above) simply gives a prescription for predicting geometrical changes *between but not within* different rows of the resulting diagram (that is, by adding or subtracting appropriate orbital energy curves to the corresponding total energy surface of some parent system); in effect *the model merely assumes that all systems with the same valence electronic configuration possess completely equivalent equilibrium nuclear arrangements.*

The latter assumption is clearly based on the idea that specific distinctions in the AO composition of the various MO's for different systems have no effect on molecular geometry; the underlying premise of Koopmans' theorem, namely that the two systems being compared use exactly the same MO's in representing their electronic charge distributions, is obviously consistent with this general point of view. To improve upon this situation and thus account for known *distinctions in the molecular geometries of isovalent systems*, it is obviously necessary to allow for the fact that the individual MO's do actually change from one species to another, particularly in comparisons involving systems with greatly different ionic character. In terms of Figure 12 it is useful to speak of the resulting *subsidiary* principle of molecular geometry as a horizontal correction to the MW model, and analysis of the SCF total energy expression shows that it involves changes in both the individual orbital energy terms and the total electronic repulsion V_{ee} from one isovalent system to another (eq 12).

Taking account of such distinctions makes it possible to explain rather small differences in geometry between such species as O_3 and FNO or NH_3 and PH_3 and also much larger discrepancies, such as those which exist between very ionic systems such as Li_2O and BaF_2 and their isovalent (covalent) counterparts water and CO_2, respectively. Basic trends in the behavior of this horizontal correction term are generally quite apparent from observation of a relatively small number of systems in each molecular family, and this information has been summarized in various tables given in this paper. From such results it must simply be concluded that while molecular geometry is determined first and foremost (in the MO framework) by the valence electronic configuration, that is, by an effect which does not depend on the identity of the constituent nuclei in a given case, there still is an important secondary principle to be considered which is much more specific, namely the manner in which the AO composition of the individual MO's varies from one system to another.

In fact, there is theoretical evidence which indicates that the MO composition may vary significantly from *one multiplet to another within a given electronic configuration of the same system.* Such considerations seemingly add a new dimension to this study because the resulting distinctions in electronic charge distribution again imply that discrepancies in the shapes of corresponding potential curves are again to be expected, particularly in cases for which the amount of exchange energy differs greatly between individual multiplets. Again the MW model in its original form is not capable of accounting for such details in the study of the molecular geometry of these systems, since it does not allow for any variation in the AO composition for the individual orbitals, either for different combinations of constituent nuclei or for changes in the multiplet character of a particular electronic state.

In addition to showing how the MW model can be related to results of *ab initio* SCF MO calculations as well as how it can be improved to account for rather subtle structural distinctions among systems with identical valence electronic configurations, the present study has also emphasized that the application of this theoretical model can be extended to much larger classes of systems than was originally thought. For example, correlation diagrams of systems which differ only in the replacement of hydrogen by fluorine atoms are found to bear great similarity to one another, thereby allowing an explanation for the close relationship observed between geometrical trends in AH_2 and AH_3 systems, on one hand, and AB_2 and AB_3 species, on the other. In addition it has been shown that hydrogen atoms can be added to a heavy-atom skeleton without affecting the basic methodology of the MW model.[87]

In most cases the correspondence between equilibrium geometries of isovalent AB_m and H_nAB_m systems, respectively, is quite apparent, but there are well-known

exceptions to this pattern such as in the ozone–cyclopropane and the C_2F_2–cyclobutene comparisons. In fact, however, even cases of the latter type are capable of being explained consistently in terms of the MW model, once it is realized that the ground-state electronic configurations of the hydrogenic species are not necessarily the same as those of the corresponding systems not containing hydrogen. If the geometries corresponding to the same electronic configuration are compared in each case, as is proper in applying the MW model, the apparent exceptions vanish simply because sometimes such a procedure requires correlating the ground state of one system with the excited state of another and *vice versa*. No significant horizontal correction is really required in these examples since the *ab initio* SCF calculations indicate that the shapes of corresponding orbital energy curves are quite similar for (covalent) AB_m and typical H_nAB_m species.

Explicit SCF calculations also demonstrate that the essential features of the various correlation diagrams are not significantly altered by a reduction of symmetry of the system under consideration, despite the acknowledged utility of symmetry characteristics in analyzing the nature of the various orbital energy trends associated with the parent family. In such cases, however, a horizontal correction such as that of eq 12 is often necessary to explain relatively small discrepancies between the structures of asymmetric species and those of isovalent systems of higher molecular symmetry.

Finally it has been shown that the Koopmans' theorem analysis described above can actually be used for any type of geometrical variable, not simply for the various internuclear angles usually considered in connection with applications of the MW model. *In principle it is only necessary to obtain total and orbital energies as a function of the desired geometrical coordinate for a single member representing a given molecular family and then apply eq 9 to predict the nature of the corresponding potential curves for all other systems in this class which possess a different valence electronic configuration.* Again such relationships are often obscured by the existence of rather large horizontal corrections which arise because of distinctions in the electronic charge distributions of various systems being compared, but once such effects are accounted for by means of eq 12 the generality of the MW trends for any geometrical variable is easily demonstrated. The key distinction between the comparative approach of the Koopmans' theorem analysis discussed in this work, on the one hand, and the earlier procedures involving various orbital energy sums, on the other, is clearly that in the latter case data obtained for one system are only used internally to approximate the total energy curve of the same molecule, whereas in the former case the calculated results for one family member are taken over directly to study corresponding properties of whole groups of related systems. Indeed in many cases the orbital energy sum methods actually lead to *information loss*, in marked contrast to the situation which results from the Koopman's theorem analysis, in which just as for the original MW model one is continually impressed with the amount of new structural information which can be deduced from such a deceptively simple object as an orbital energy correlation diagram.

Finally it should be pointed out that virtually all of the aforementioned geometrical conclusions arise in a straightforward manner *without consideration of CI effects*, and exclusively within the framework of basis sets consisting of only s and p AO's.[213] Examination of existing calculations at the Hartree–Fock level emphasizes, however, that such CI and basis set effects can be significant for structural studies in certain cases, and that it is therefore important to be aware of what changes in geometry can result because of such improvements in the level of the theoretical treatment. Structural changes effected by inclusion of CI are essentially interpretable in terms of the concepts of the original MW model, simply by taking into account the geometrical trends of the MO's whose occupation is altered relative to an SCF treatment. The situation with respect to d-orbital effects is less clear, but it seems safe to conclude that their influence on molecular geometry is relatively small as long as such species are not formally occupied. Inclusion of d orbitals in the basis is more likely to affect the shapes of fairly shallow potential curves, but in such cases the same result can also be obtained through the use of other types of polarization functions. In general, slight discrepancies in calculated equilibrium geometries which result from deficiencies in the basis set employed can be accounted for effectively in terms of the same horizontal correction formula (eq 12) as that used above to describe differences in the observed nuclear arrangements of isovalent systems possessing somewhat different electronic charge distributions.

In summary it has been found that the MW model can, with certain modifications, be used to explain virtually every trend observed in the equilibrium geometries of polyatomic molecules in their ground and excited states. Furthermore, the fact that such analyses can be carried out on the basis of canonical orbital energy diagrams calculated using the *ab initio* SCF method establishes a clear connection between the well-defined mathematical formalism of the SCF or Hartree–Fock theory and the aforementioned empirically deduced model of electronic structure. These findings demonstrate that *ab initio* calculations (both SCF and CI) can be used quite effectively to elicit extremely general relationships among a large body of empirical data and thus that their role in electronic structure studies need not be restricted to the realm of numerical comparison with specific experimental results.[214]

Acknowledgment. The authors wish to express their deep appreciation for the continued financial support of the Deutsche Forschungsgemeinschaft in this work.

V. References and Notes

(1) R. S. Mulliken, *Rev. Mod. Phys.*, **14**, 204 (1942).
(2) A. D. Walsh, *J. Chem. Soc.*, 2260 (1953), and following articles.
(3) J. Cassie, *Nature (London)*, **131**, 438 (1933).
(4) W. G. Penney and G. B. Sutherland, *Proc. Roy. Soc. Ser. A*, **156**, 654 (1936).
(5) N. V. Sidgwick and H. M. Powell, *Proc. Roy. Soc. Ser. A*, **176**, 153 (1940).
(6) G. Kimball, *J. Chem. Phys.*, **8**, 188 (1940).
(7) L. Pauling, "The Nature of the Chemical Bond," Cornell University Press, Ithaca, N. Y., 1960.
(8) The relationship between SCF canonical orbital energies and Walsh's rules was first discussed by means of actual *ab initio* calculations in a series of four papers: S. D. Peyerimhoff, R. J. Buenker, and L. C. Allen, *J. Chem. Phys.*, **45**, 734 (1966) [AH_2, AH_3]; R. J. Buenker, S. D. Peyerimhoff, L. C. Allen, and J. L. Whitten, *ibid.*, **45**, 2835 (1966) [B_2H_6 and C_2H_6]; R. J. Buenker and S. D. Peyerimhoff, *ibid.*, **45**, 3682 (1966) [F_2O, Li_2O, FOH, LiOH]; S. D. Peyerimhoff and R. J. Buenker, *ibid.*, **47**, 1953 (1967) [O_3, N_3^-].
(9) Subsequent calculations on this subject carried out by the authors and coworkers are: S. D. Peyerimhoff, R. J. Buenker, and J. L. Whitten, *J. Chem. Phys.*, **46**, 1707 (1967) [CO_2, BeF_2]; R. J. Buenker, S. D. Peyerimhoff, and J. L. Whitten, *ibid.*, **46**, 2029 (1967) [C_2H_{2n}]; S. D. Peyerimhoff, *ibid.*, **47**, 349 (1967) [$HCOO^-$]; S. D. Peyerimhoff and R. J. Buenker, *Theor. Chim. Acta*, **9**, 103 (1967) [FNO]; R. J. Buenker and S. D. Peyerimhoff, *J. Chem. Phys.*, **48**, 354 (1968) [C_4H_4, cyclobutadiene]; R. J. Buenker, *ibid.*, **48**, 1368 (1968) [C_2H_4, allene]; S. D. Peyerimhoff and R. J. Buenker, *ibid.*, **49**, 312 (1968) [BNH_6, $C_2H_6^{2+}$]; **49**, 2473 (1968) [N_2O]; **50**, 1846 (1969) [HCOOH]; R. J. Buenker and S. D. Peyerimhoff, *J. Phys. Chem.*, **73**, 1299 (1969) [cyclopropane]; S. D.

Peyerimhoff and R. J. Buenker, *Theor. Chim. Acta*, **14**, 305 (1969) [C_3H_4 isomers]; R. J. Buenker and S. D. Peyerimhoff, *J. Amer. Chem. Soc.*, **91**, 4342 (1969) [C_4H_4, tetrahedrane]; S. D. Peyerimhoff and R. J. Buenker, *J. Chem. Phys.*, **51**, 2528 (1969) [$C_3H_5^{\pm}$]; R. J. Buenker and S. D. Peyerimhoff, *ibid.*, **53**, 1368 (1970) [H_2CO]; R. J. Buenker, S. D. Peyerimhoff, and K. Hsu, *J. Amer. Chem. Soc.*, **93**, 5005 (1971) [cyclobutene, butadiene]; W. E. Kammer, *Chem. Phys. Lett.*, **6**, 529 (1970); Ph.D. Thesis, Giessen, 1970 [C_2H_2]; B. Wirsam, Ph.D. Thesis, Giessen, 1971; *Theor. Chim. Acta*, **25**, 169 (1972) [Si_2H_2]; unpublished work by S. Shih [H_2O, H_2S, NH_3, Ph_3], W. E. Kammer and H. L. Hsu [N_2H_2], R. J. Buenker and S. D. Peyerimhoff [$NO_2^{\pm}$], A. Wu [HNO], K. Vasudevan [HN_2^+], P. Bruna [HCO^+, H_2CS].

(10) Related calculations carried out by other authors: B. D. Joshi, *J. Chem. Phys.*, **43**, S40 (1965) [NH_3]; E. F. Hayes, *ibid.*, 70, 3740 (1966) [CaF_2]; B. D. Joshi, *ibid.*, **46**, 875 (1967); **47**, 2793 (1967) [AH_3]; D. C. Pan and L. C. Allen, *ibid.*, **46**, 1797 (1967) [HCN]; W. H. Fink, *ibid.*, **49**, 5054 (1968) [NO_2]; J. J. Kaufmann, L. M. Sachs, and M. Geller, *ibid.*, **49**, 4369 (1968) [BeH_2]; L. Burnelle, A. M. May, and R. A. Gaugi, *ibid.*, **49**, 561 (1968) [NO_2]; G. V. Pfeiffer and L. C. Allen *ibid.*, **51**, 190 (1969) [$NO_2^{\pm}$]; L. M. Sachs, M. Geller, and J. J. Kaufman, *ibid.*, **51**, 2771 (1969) [CH_2]; L. M. Sachs, M. Geller, and J. J. Kaufman, *ibid.*, **52**, 974 (1970) [BH_2^-]; A. Rauk, E. Clementi, and L. C. Allen, *ibid.*, **52**, 4133 (1970) [NH_3]; D. C. Pan, W. H. Fink, and L. C. Allen, *ibid.*, **52**, 6291 (1970) [N_2H_2]; R. E. Kari and I. G. Csizmadia, *ibid.*, **56**, 4337 (1972) [NH_3, CH_3^-]; D. H. Liskow, C. F. Bender, and H. F. Schaefer, III, *ibid.*, **56**, 5075 (1972) [C_3].

(11) C. E. Wulfman, *J. Chem. Phys.*, **31**, 381 (1959).

(12) C. E. Wulfman, *J. Chem. Phys.*, **33**, 1567 (1960).

(13) W. A. Bingel in "Molecular Orbitals in Chemistry, Physics and Biology," P. O. Löwdin and B. Pullmann, Ed., Academic Press, New York, N. Y., 1964, p 191.

(14) A. F. Saturno, *Theor. Chim. Acta*, **7**, 273 (1967).

(15) H.-H. Schmidtke and H. Preuss, *Z. Naturforsch. A*, **16**, 790 (1961).

(16) H.-H. Schmidtke, *Z. Naturforsch. A*, 17, 121 (1962).

(17) H.-H. Schmidtke, *Z. Naturforsch. A*, **18**, 496 (1963).

(18) C. A. Coulson and A. H. Neilson, *Discuss. Faraday Soc.*, **35**, 71 (1963).

(19) C. A. Coulson and A. H. Neilson, *Discuss. Faraday Soc.*, **35**, 217 (1963).

(20) D. Peters, *Trans. Faraday Soc.*, **62**, 1353 (1966).

(21) S. D. Peyerimhoff, R. J. Buenker, and L. C. Allen, *J. Chem. Phys.*, **45**, 734 (1966).

(22) R. J. Buenker, S. D. Peyerimhoff, L. C. Allen, and J. L. Whitten, *J. Chem. Phys.*, **45**, 2835 (1966).

(23) R. J. Buenker and S. D. Peyerimhoff, *J. Chem. Phys.*, **45**, 3682 (1966).

(24) S. D. Peyerimhoff and R. J. Buenker, *J. Chem. Phys.*, **47**, 1953 (1967).

(25) J. C. Leclerc and J. C. Lorquet, *Theor. Chim. Acta*, **6**, 91 (1966).

(26) L. C. Allen and J. D. Russell, *J. Chem. Phys.*, **46**, 1029 (1967).

(27) B. Nelander, *J. Chem. Phys.*, **51**, 469 (1969).

(28) Y. Takahata and R. G. Parr, *Chem. Phys. Lett.*, **4**, 109 (1969).

(29) R. J. Gillespie, "Molecular Geometry," Van Nostrand-Reinhold, London, 1972. See also the articles by C. E. Mellish and J. W. Linnett, *Trans. Faraday Soc.*, **50**, 657 (1954), and P. G. Dickens and J. W. Linnett, *Quart. Rev., Chem. Soc.*, 11, 291 (1957).

(30) C. A. Coulson and B. M. Deb, *Int. J. Quantum Chem.*, **5**, 411 (1971).

(31) This historical summary has not included a review of the structure theory based on the second-order Jahn–Teller effect. For a discussion of this interesting work see, for example: R. G. Pearson, *J. Amer. Chem. Soc.*, **91**, 4947 (1969); *J. Chem. Phys.*, **52**, 2167 (1970); *Chem. Phys. Lett.*, **10**, 31 (1971); R. F. W. Bader, *Mol. Phys.*, **3**, 137 (1960); *Can. J. Chem.*, **40**, 1164 (1962); L. S. Bartell, *J. Chem. Educ.*, **45**, 754 (1968); D. H. W. den Boer and H. C. Longuet-Higgins, *Mol. Phys.*, **5**, 387 (1962); H. C. Longuet-Higgins, *Proc. Roy. Soc. Ser. A*, **235**, 537 (1956).

(32) J. C. Slater, "Quantum Theory of Molecules and Solids," Vol. I, McGraw-Hill, New York, N. Y., 1963.

(33) R. S. Mulliken, *Phys. Rev.*, **32**, 186, 388, 761 (1928); **40**, 55 (1930); **41**, 49, 751 (1932). Also see the review by C. A. Coulson, in ref 13, p 1.

(34) F. Hund, *Z. Phys.*, **51**, 759 (1928); **73**, 1, 565 (1931, 1932).

(35) T. Koopmans, *Physica*, 1, 104 (1933).

(36) C. C. J. Roothaan, *Rev. Mod. Phys.*, **23**, 69 (1951).

(37) Nevertheless, the energy gap between unoccupied and occupied MO's appears to be greatly overestimated on the basis of canonical orbital energies because of the definition of the latter quantities (see eq 1).

(38) R. G. Parr, *J. Chem. Phys.*, **19**, 799 (1951).

(39) F. O. Ellison and H. Shull, *J. Chem. Phys.*, **23**, 2348 (1955).

(40) E. R. Davidson, *J. Chem. Phys.*, **57**, 1999 (1972); S. T. Elbert, S. R. Langhoff, and E. R. Davidson, *ibid.*, **57**, 2005 (1972).

(41) F. P. Boer, M. D. Newton, and W. N. Lipscomb, *Proc. Nat. Acad. Sci. U.S.*, **52**, 890 (1964).

(42) Throughout this discussion we assume simple potential curves with single minima. The same arguments are still valid for species with multiple minima, however, as long as they are related to one another by symmetry.

(43) D. C. Pan and L. C. Allen, *J. Chem. Phys.*, **46**, 1797 (1967).

(44) S. D. Peyerimhoff, R. J. Buenker, and J. L. Whitten, *J. Chem. Phys.*, **46**, 1707 (1967).

(45) The original papers by Mulliken[1] and Walsh,[2] for example, do not allow a clear-cut decision as to the nature of the geometrical changes which occur when equal numbers of electrons are removed from both the $6a_1$ and $4b_2$ MO's of AB_2 systems (one strongly favoring bent geometries, the other equally strongly favoring linear structures).

(46) In this case, of course, equivalence would simply require the addition of the inner-shell orbitals of the Li atom to the original system (water). In general, an equivalent charge distribution is assumed to be one in which the *net* charges for both systems are equal at all points in space.

(47) To avoid confusion in applying eq 12, emphasis will always be placed on the additive potential terms in this expression, hence on $\Delta\Sigma\epsilon_i$ and $(-\Delta V_{ee})$. Then it simply must be remembered that if any such additive term *increases* with bending (or bond contraction), the tendency is toward *larger* angles (distances); if such a term *decreases* with bending, on the other hand, the trend is obviously in the opposite direction, toward *smaller* angles (or distances).

(48) Unpublished *ab initio* SCF calculations by the authors for water in various nuclear conformations.

(49) In both Li_2O and water the orbital energy sums are observed to favor bent geometries, but the additional terms in eq 12 produce the opposite tendency. It is thus the fact that $\Sigma\epsilon_i$ for Li_2O favors *bent* geometry *less* than in H_2O that ultimately causes the former system to prefer a linear structure.

(50) Strictly speaking, this statement will be correct only if one uses the curvature $\partial^2E/\partial\Theta^2$ for this criterion; the usual definition of bending force constants, namely the quotient of the curvature and the square of the bond length, may not always exhibit the same general trends as the curvature itself.

(51) Hence $(-\Delta V_{ee})$ as well as $\Delta\Sigma\epsilon_i$ decreases with bending, thereby combining to produce the tendency away from linearity in the sulfide.[47]

(52) The decreased interaction between the AO's in such systems is expected to change the *magnitude* of the slope of $\Sigma\epsilon_i$ but not its sign.

(53) Unpublished *ab initio* SCF results for the angular potential surfaces of CO_2 and BeF_2.

(54) E. F. Hayes, *J. Phys. Chem.*, 70, 3740 (1966).

(55) Concentrating the electronic charge at the F atoms in BeF_2 undoubtedly leads to an overall *increase* in V_{ee} itself but at the same time it leads to a *decrease* in the *rate* of change in this quantity with R, which of course is the only factor of significance in the determination of equilibrium geometry.

(56) L. Burnelle, P. Beaudouin, and L. J. Schaad, *J. Phys. Chem.*, 71, 2240 (1967).

(57) B. M. Gimarc and T. S. Chou, *J. Chem. Phys.*, **49**, 4043 (1968).

(58) B. M. Gimarc, *J. Amer. Chem. Soc.*, **92**, 266 (1970).

(59) B. M. Gimarc, *J. Amer. Chem. Soc.*, **93**, 593 (1971).

(60) B. M. Gimarc, *J. Amer. Chem. Soc.*, **93**, 815 (1971).

(61) L. C. Allen in "Sigma Molecular Orbital Theory," O. Sinanoglu and K. B. Wiberg, Ed., Yale University Press, New Haven, Conn., 1970, p 227.

(62) L. C. Allen, *Theor. Chim. Acta*, **24**, 117 (1972).

(63) R. Hoffmann and W. N. Lipscomb, *J. Chem. Phys.*, **36**, 2179, 3489 (1962).

(64) A similar orbital energy quantity can of course be defined so that the sum over only the valence quantities varies exactly as E_T, simply by distributing the change in core orbital energies equally among the valence species.

(65) In Li_2O, for example, the additive term has a magnitude of only 0.015 hartree or 0.4 eV at fully 90° away from the (180°) equilibrium angle.

(66) Basis sets for *ab initio* calculations can alternatively be chosen so as to produce maximum consistency between calculated and experimental geometrical and/or dissociation energy data.

(67) U. Kaldor and I. Shavitt, *J. Chem. Phys.*, **48**, 191 (1968).

(68) R. J. Buenker, *J. Chem. Phys.*, **48**, 1368 (1968).

(69) M. J. S. Dewar and E. Haselbach, *J. Amer. Chem. Soc.*, **92**, 590 (1970).

(70) S. D. Peyerimhoff and R. J. Buenker, *J. Chem. Phys.*, **49**, 312 (1968).

(71) R. B. Woodward and R. Hoffmann, *J. Amer. Chem. Soc.*, **87**, 395 (1965).

(72) H. C. Longuet-Higgins and E. W. Abrahamson, *J. Amer. Chem. Soc.*, **87**, 2045 (1965).

(73) R. J. Buenker, S. D. Peyerimhoff, and K. Hsu, *J. Amer. Chem. Soc.*, **93**, 5005 (1971).

(74) S. D. Peyerimhoff and R. J. Buenker, *J. Chem. Phys.*, **49**, 2473 (1968).

(75) G. Verhagen and W. G. Richards, *J. Chem. Phys.*, **45**, 1828 (1966).

(76) W. G. Richards, G. Verhagen, and C. M. Moser, *J. Chem. Phys.*, **45**, 3226 (1966).

(77) G. Verhagen, W. G. Richards, and C. M. Moser, *J. Chem. Phys.*, **46**, 160 (1967).

(78) E. Clementi, *J. Chem. Phys.*, **46**, 3842 (1967).

(79) Experience with *ab initio* calculations for ethylene, formaldehyde, and many other systems also shows that corresponding orbital energy curves obtained for *open-shell* SCF states exhibit the same types of general characteristics universally found for their *closed-shell* counterparts. Such observations should dispel the doubts recently raised by M. P. Melrose and P. J. Briggs, *Theor. Chim. Acta*, **25**, 181 (1972).

(80) In this application the virtual orbital energy curves are also quite satisfactory for use in the MW model because an essentially minimal basis set of contracted gaussians has been used in the calculations and hence the virtual MO's are effectively constrained to

be reasonable approximations to the true upper-valence species to which they correspond. Indeed, for such restricted basis sets, it is invariably found that the shapes of corresponding occupied (in one system) and virtual (in another) orbital energy curves are very similar.[21,23,24] Such observations clearly run contrary to what is claimed in ref 30, p 426.

(81) For a single excitation from the *i*th to the *j*th orbital energy level (relative to a closed-shell ground state) the total energies of the resultant excited triplet (^3E_T) and singlet (^1E_T) are related to the ground state energy (E_T) by the relationships $^{3,1}E_T = E_T + \epsilon_j - \epsilon_i - (J_{ij} - K_{ij}) \pm K_{ij}$, where J_{ij} and K_{ij} are Coulomb and exchange integrals, respectively, and the upper sign refers to the singlet state (see ref 36). As a result the geometrical dependence of such electron repulsion integrals is also a *potentially* important factor in determining the shapes of the excited state potential curves.

(82) It is, of course, not generally true that the total energies of ground and excited or (multiply) ionized states differ by only orbital energy quantities. Nevertheless, the results of section II.B.2 indicate quite strongly that it is only such terms which *commonly* are sensitive to geometrical changes.

(83) F. A. Cotton, "Chemical Applications of Group Theory," Wiley, New York, N. Y., 1963.

(84) R. S. Mulliken, *Phys. Rev.*, **41**, 751 (1932); **43**, 294 (1933); *Chem. Rev.*, **41**, 207 (1947).

(85) R. J. Buenker, S. D. Peyerimhoff, and J. L. Whitten, *J. Chem. Phys.*, **46**, 2029 (1967).

(86) S. D. Peyerimhoff, *J. Chem. Phys.*, **47**, 349 (1967).

(87) R. J. Buenker and S. D. Peyerimhoff, *Theor. Chim. Acta*, **24**, 132 (1972).

(88) S. D. Peyerimhoff and R. J. Buenker, *Theor. Chim. Acta*, 14, 305 (1969).

(89) R. J. Buenker and S. D. Peyerimhoff, *J. Phys. Chem.*, **73**, 1299 (1969).

(90) A Müller and H. J. Schuman, solution of a problem set within a course at the University of Mainz.

(91) S. D. Peyerimhoff, *J. Chem. Phys.*, **43**, 908 (1965).

(92) J. R. Platt, *J. Chem. Phys.*, **18**, 932 (1950).

(93) The bond distance for BH_2^- is calculated to be 2.35 bohrs (1.243 Å) in ref 94, but it still seems quite likely that the earlier calculation of ref 44 obtains a quite accurate estimation of the differences in bond lengths for different systems such as BH_2^- and NH_2^+, for example (since equivalent basis sets are used in each case).

(94) L. M. Sachs, M. Geller, and J. J. Kaufman, *J. Chem. Phys.*, **52**, 974 (1970).

(95) T. F. Moran and L. Friedmann, *J. Chem. Phys.*, **39**, 2491 (1963); **40**, 860 (1964). Note that R_{NeH} is calculated therein to be 1.53 bohrs for NeH^+, considerably less than the presently accepted value of 1.83 bohrs.[91]

(96) R. S. Mulliken, *J. Amer. Chem. Soc.*, 77, 887 (1955).

(97) Unfortunately the $1b_1$ orbital energy curve is not plotted in the BH_2^- correction diagram of ref 94 while, in the case of the semiempirical calculations of Gimarc,[60] it is apparently calculated to be constant with changes in ∠HAH. In the latter case, however, the author states that this result holds quite generally for all AH_2 correlation diagrams, contrary to what is observed in *ab initio* calculations, as discussed above.

(98) See Appendix II of ref 21.

(99) This trend toward increasingly larger equilibrium angles apparently continues through the case of H_2O^{2+}, with ∠HOH for this system calculated to be approximately 150° by means of Koopmans' theorem (eq 9) based on the aforementioned calculations for H_2O.[48,90]

(100) In this case it is not really necessary to use eq 12 but rather to simply compare directly the calculated NH_2^+ and BH_2^- results. For such comparisons it is, of course, necessary to also consider V_{nn} explicitly since $R_{NH} \neq R_{BH}$, but it is readily seen from actual calculations that this term represents only a minor effect because of the relatively small nuclear charge of the protons. The same statement is valid for any comparison of HAH angular (but not stretching) potential curves.

(101) "Tables of Interatomic Distances and Configurations in Molecules," *Chem. Soc. Spec. Publ.*, **No.** 11 (1958); *ibid.*, **No.** 18 (1965).

(102) S. Shih, unpublished data for H_2S; calculations are at the same level as those for H_2O (ref 48 and 90).

(103) J. M. Lehn, *Mol. Phys.*, **23**, 91 (1972); also XXIIIrd International Congress of Pure and Applied Chemistry, Vol. 1.

(104) J. F. Harrison and L. C. Allen, *J. Amer. Chem. Soc.*, **91**, 807 (1969); J. F. Harrison, *ibid.*, **93**, 4112 (1971).

(105) C. F. Bender and H. F. Schaefer, III, *J. Amer. Chem. Soc.*, **92**, 4984 (1970); S. V. O'Neil, H. F. Schaefer, III, and C. F. Bender, *J. Chem. Phys.*, **55**, 162 (1971).

(106) G. Herzberg and J. W. Johns, *J. Chem. Phys.*, **54**, 2276 (1971).

(107) E. Wassermann, W. A. Yager, and V. Kuck, *J. Amer. Chem. Soc.*, **92**, 7491 (1970).

(108) The calculations discussed above for BH_2^- and NH_2^+ have dealt exclusively with the closed-shell $^1A_1$ state, which possesses a significantly smaller equilibrium internuclear angle.

(109) It should be pointed out, however, that the angle obtained solely on the basis of Hartree-Fock calculations is approximately 5° smaller than the more probable one resulting from a quite large CI treatment.[104,105]

(110) B. D. Joshi, *J. Chem. Phys.*, **43**, S40 (1965); **46**, 875 (1967); **47**, 2793 (1967).

(111) A. Rauk, E. Clementi, and L. C. Allen, *J. Chem. Phys.*, **52**, 4133 (1970).

(112) Unpublished calculations for BeH_3^+ by the authors.

(113) On the other hand, it appears that isoelectronic systems such as BH_3^{2+} and CH_3^{+3} do prefer planar geometries, but even these systems become nonplanar upon further ionization from the $1e-1e'$ MO.

(114) H. B. Thompson and L. S. Bartell, *Inorg. Chem.*, 7, 488 (1968).

(115) C. Edminston and K. Ruedenberg, *Rev. Mod. Phys.*, **35**, 457 (1963).

(116) C. Edminston and K. Ruedenberg, *J. Chem. Phys.*, **43**, 597 (1965), and in "Quantum Theory of Atoms, Molecules and the Solid State," P. O. Löwdin, Ed., Academic Press, New York, N. Y., 1966, p 263.

(117) This point has recently been reviewed by W. England, L. S. Salmon, and K. Ruedenberg in "Fortschritte der chemischen Forschung," Vol. 23, Springer-Verlag, 1971, p 31, taking advantage of the localized orbital technique. It has also been discussed in ref 62.

(118) S. Shih, unpublished data for NH_3 and PH_3.

(119) R. J. Gillespie and R. S. Nyholm, *Quart. Rev. Chem. Soc.*, 11, 339 (1957).

(120) More detailed investigation of these points will be published separately.

(121) G. Herzberg, *Proc. Roy. Soc. Ser. A*, **262**, 291 (1961).

(122) J. Arents and L. C. Allen, *J. Chem. Phys.*, **53**, 73 (1970).

(123) In C_2, for example, the $1\pi_u$ MO is fully occupied in the $^1\Sigma_g^+$ ground state with the $3\sigma_g$ unoccupied, whereas in N_2 the opposite ordering appears to be favored on the basis of the canonical orbital energy results.

(124) P. E. Cade, K. D. Sales, and A. C. Wahl, *J. Chem. Phys.*, **44**, 1973 (1966).

(125) Second-row diatomics are generally much less stable than their first-row analogs. The relationship between bond lengths and binding energies in all such systems is of course well known.[126]

(126) G. Herzberg, "Spectra of Diatomic Molecules," Van Nostrand, Princeton, N. J., 1950.

(127) More generally it is necessary to examine which of the MO's of the original nonhydrogenic species are most affected by the addition of hydrogen atoms in order to predict the effect upon the $\Sigma\epsilon_i$ term in eq 12. If, for example, the hydrogen AO's interact almost exclusively with MO's of *antibonding* type, a tendency toward relatively *smaller bond distances* results because of the consequent shift in the balance between bonding and antibonding character in such systems. In C_2H_2, for which mixing with hydrogen AO's occurs primarily in a normally bonding ($3\sigma_g$) MO, the trend is clearly toward a larger bond length than that of N_2 (see sections III.B.2-4).

(128) The ionic system LiOH is an obvious exception to this regularity, simply because the electron transfer from lithium to oxygen is so nearly complete as to rule out the possibility of a sufficiently strong LiH bond.

(129) For both types of systems, R_{AB} depends strongly on this electronegativity difference, as discussed in the preceding subsection, and hence a system such as BF has a larger heavy-atom separation (1.262 Å) than that of isoelectronic HCN.

(130) The HNO potential curve in Figure 11 is of course a better approximation to that of FOH^{2+}, obtained as it is by means of eq 9 and the SCF results of FOH itself.

(131) G. Herzberg and K. K. Innes, *Can. J. Phys.*, **35**, 842 (1957).

(132) F. W. Dalby, *Can. J. Phys.*, **36**, 1336 (1958).

(133) G. Herzberg, "Electronic Spectra of Polyatomic Molecules," Van Nostrand, Princeton, N. J., 1966.

(134) Unpublished data for HNO by A. Wu and for HCO by P. Bruna, this laboratory.

(135) D. C. Pan, W. H. Fink, and L. C. Allen, *J. Chem. Phys.*, **52**, 6291 (1970).

(136) In the A_2H_2 angular correlation diagrams, the linear conformation is denoted by $\theta = 0°$, following the notation of Kammer[138] and Wirsam,[140] rather than by the 180° value generally adopted for the analogous nuclear arrangement for other molecular families.

(137) W. E. Kammer, Ph.D. Thesis, Giessen, 1970.

(138) W. E. Kammer, *Chem. Phys. Lett.*, **6**, 529 (1970).

(139) B. Wirsam, Ph.D. Thesis, Giessen, 1970.

(140) B. Wirsam, *Theor. Chim. Acta*, **25**, 169 (1972); *Chem. Phys. Lett.*, **10**, 180 (1971).

(141) This distinction is caused by the increased effect of hydrogen AO bonding in the $p\sigma$ MO of A_2H_2 systems relative to that in the corresponding orbital in HAB molecules (with only one H AO). Hence $p\sigma$ is much more stable than 1π in A_2H_2 systems, while in the HAB class the corresponding MO's are very nearly isoenergetic (see Figure 24).

(142) The Coulomb integral between the $3a_1$ and $4a_1$ MO's, respectively, *increases* from 0.402 to 0.421 upon a 60° cis bend, while the analogous quantity decreases from 0.402 to 0.397 for the same range of angle for the trans bending motion.

(143) A. Trombetti, *Can. J. Phys.*, **46**, 1005 (1968).

(144) B. Cadioli, P. Patella, U. Pincelli, and D. J. David, *Atti Soc. Natur. Mat. Modena*, **97C**(VI), 47 (1969).

(145) W. E. Kammer and H. L. Hsu, SCF and CI calculations for N_2H_2, to be published.

(146) J. Alster and L. A. Burnelle, *J. Amer. Chem. Soc.*, **89**, 1261 (1967).

(147) The SOJT model predicts the cis conformer to be more stable in contrast to the conclusion resulting from application of the MW model (ref 31).

(148) C. K. Ingold and G. W. King, *J. Chem. Soc.*, 2702 (1953).

(149) K. K. Innes, *J. Chem. Phys.*, **22**, 863 (1954).

(150) I. G. Ross, *Trans. Faraday Soc.*, **48**, 973 (1952).

(151) R. J. Buenker and S. D. Peyerimhoff, *J. Chem. Phys.*, **48**, 354 (1968).
(152) Again such geometrical distinctions can be predicted with good accuracy by means of a Koopmans' theorem analysis of the type discussed in section II.B.2.
(153) For the latter families of molecules it is obviously necessary to consider the behavior of the orbital energies for *bent geometries*, in which case the MO's in question are no longer degenerate. In this way it is easy to see that the in-plane π_g component is much less antibonding than the corresponding out-of-plane species (see Figures 23 and 25, respectively); this follows mainly as a result of the fact that the H AO's mix strongly with the in-plane orbital for bent nuclear arrangements (such as are observed for HNO, N_2H_2, FOH, and H_2O_2) but not with the other component, thereby producing the substantial difference in their respective antibonding characteristics (in-plane component less antibonding and more stable in each case). The weakly antibonding character of the in-plane π_g component in HAB, A_2H_2, and H_2AB molecules is also an important factor in explaining the finding that while ten-valence-electron species such as HCN, C_2H_2, and, undoubtedly, H_2BN possess significantly larger R_{AB} values than isoelectronic N_2, those with 12 valence electrons (HNO, N_2H_2, and H_2CO, respectively) have bond lengths which are nearly equal to that of their isoelectronic homonuclear diatomic O_2 (see section III.B.2).
(154) R. J. Buenker and S. D. Peyerimhoff, *J. Chem. Phys.*, **53**, 1368 (1970).
(155) V. A. Job, V. Sethuraman, and K. K. Innes, *J. Mol. Spectrosc.*, **30**, 365 (1969).
(156) V. T. Jones and J. B. Coon, *J. Mol. Spectrosc.*, **31**, 137 (1969).
(157) A. B. Callear, J. Connor, and D. R. Dickson, *Nature (London)*, **221**, 1238 (1969); J. Fabian and A. Mehlhorn, *Z. Chem.*, **9**, 271 (1969).
(158) P. Bruna, unpublished calculations.
(159) The boro-nitrogen analog of ethylene is known but is believed to possess a significantly larger AB bond length than ethylene.
(160) Diamond-shaped isomers of Be_2H_4 and B_2H_4 are possible; they will be treated in connection with hydrogen-bridged species such as diborane (section III.B.6).
(161) S. D. Peyerimhoff, R. J. Buenker, and H. L. Hsu, *Chem. Phys. Lett.*, **11**, 65 (1971).
(162) T. H. Dunning, W. J. Hunt, and W. A. Goddard, *Chem. Phys. Lett.*, **4**, 147 (1969).
(163) H. Basch and V. McKoy, *J. Chem. Phys.*, **53**, 1628 (1970).
(164) R. J. Buenker, S. D. Peyerimhoff, and W. E. Kammer, *J. Chem. Phys.*, **55**, 814 (1971).
(165) R. S. Mulliken, *Chem. Phys. Lett.*, **14**, 141 (1972).
(166) C. C. J. Roothaan, *Rev. Mod. Phys.*, **32**, 179 (1960).
(167) In-plane and out-of-plane excitations are characterized by the relative orientation of initial and final MO's in the transitions.
(168) Details of the exact geometrical path employed in these calculations may be found in ref 22.
(169) The order of $p\sigma$ and AH orbital energies in ethane is opposite to that of diborane because of the differences in the strength of boron and carbon $p\sigma$ bonds in these systems.[22,70]
(170) W. H. Fink and L. C. Allen, *J. Chem. Phys.*, **46**, 2261 (1967).
(171) J. P. Lowe, *J. Amer. Chem. Soc.*, **92**, 3799 (1970).
(172) R. M. Pitzer and W. N. Lipscomb, *J. Chem. Phys.*, **39**, 1995 (1963).
(173) R. M. Stevens, *J. Chem. Phys.*, **52**, 1397 (1970).
(174) I. R. Epstein and W. N. Lipscomb, *J. Amer. Chem. Soc.*, **92**, 6094 (1970).
(175) Unpublished calculations by the authors for NO_2^+ and NO_2^-.
(176) L. Burnelle, A. M. May, and R. A. Gaugi, *J. Chem. Phys.*, **49**, 561 (1968).
(177) G. V. Pfeiffer and L. C. Allen, *J. Chem. Phys.*, **51**, 190 (1969).
(178) L. M. Sachs, M. Geller, and J. J. Kaufman, *J. Chem. Phys.*, **51**, 2771 (1969).
(179) D. H. Liskow, C. F. Bender, and H. F. Schaefer, III, *J. Chem. Phys.*, **56**, 5075 (1972).
(180) W. H. Smith and G. E. Leroi, *J. Chem. Phys.*, **45**, 1784 (1966).
(181) R. G. Body, D. S. McClure, and E. Clementi, *J. Chem. Phys.*, **49**, 4916 (1968).
(182) In the following it has generally been assumed that the two bond lengths in AB_2 and A_3 systems are equal. There are cases for which such an assumption does not seem to be valid, as has been pointed out recently by T. W. Archibald and J. R. Sabin, *J. Chem. Phys.*, **55**, 1821 (1971).
(183) Rydberg states possess equilibrium geometries which are quite similar to those of the corresponding positive ion and hence are also easily dealt with in the MW model.
(184) W. H. Fink, *J. Chem. Phys.*, **54**, 2911 (1971); **49**, 5054 (1968).
(185) S. D. Peyerimhoff and R. J. Buenker, *Theor. Chim. Acta.* **9**, 103 (1967).
(186) The magnitude of the NO bond distance is actually intermediate between its values in the diatomics NO and NO^+, respectively.
(187) R. D. Gillard, *Rev. Port. Quim.*, 11, 70 (1969).
(188) See Figure 3 of ref 185 for the total charge density of FNO.
(189) Equilibrium bond distances are much larger in the fluorine-substituted compounds, however, emphasizing the fact that the polarity of AH and AF bonds is essentially opposite; this fact leads to a quite large horizontal correction for bond stretching in the two types of systems but to only a relatively small distinction for bending motions.
(190) A. J. Merer and D. N. Travis, *Can. J. Phys.*, **43**, 1795 (1965); **44**, 353 (1966).
(191) E. Clementi, *IBM J. Res. Develop.*, **9**, 2 (1965).
(192) The main differences occur in the region of $\theta = 180°$ since the O_3 potential curves necessarily have to be symmetric with respect to this angle while the corresponding ones for $HCOO^-$ do not.
(193) S. D. Peyerimhoff and R. J. Buenker, *J. Chem. Phys.*, **50**, 1846 (1969).
(194) A. D. Walsh, *Trans. Faraday Soc.*, **45**, 179 (1949).
(195) C. A. Coulson and W. E. Moffitt, *Phil. Mag.*, **40**, 1 (1949).
(196) Reference 83, part II.6.
(197) At about the same time Thompson and Bartell[114] used the same type of analysis to point out certain basic similarities between the VB or VSEPR[29] models of electronic structure and those of MO type such as that proposed by Mulliken and Walsh.[117]
(198) S. D. Peyerimhoff and R. J. Buenker, *J. Chem. Phys.*, **51**, 2528 (1969).
(199) Trihydrogen fluoride FH_3, for example, is undoubtedly most stable in a planar conformation (for a given HF distance), even though 3d AO's are not critical for the representation of its electronic structure.
(200) Recall that $\Sigma^{val}\epsilon_i$ in PH_3 favors nonplanar geometry less than in NH_3 (see section III.A.2 and Table IV).
(201) Cyclobutadiene represents another example of a system which, at least in *ab initio* treatments, is not adequately represented without CI. The calculated finding[151] (after CI) of a singlet ground state is at least superficially in conflict with Hund's rules, but the fact that equilibrium is attained for a nonsquare geometry is, of course, consistent with the Jahn-Teller effect.
(202) Note that the two components of the e_g MO for the square geometry do not have equal orbital energies. This result is a consequence of the fact that one component is occupied while the other is not.[36] The explanation for this phenomenon has been given earlier.[24] The other degenerate MO's do possess equal orbital energies for their respective components, however.
(203) The symmetry orbital notation in Table XIV always refers to the D_{2h} point group, even though the specific molecule may not possess this symmetry. Such a procedure is employed only to emphasize the *essential similarity between corresponding MO's* in such systems, regardless of the symmetry of the complete molecule. The same notational procedure has been employed for the triatomic systems in section III.C.2, in which ABC systems are discussed in terms of C_{2v} symmetry orbitals.
(204) K. W. Cox, M. D. Harmony, G. Nelson, and K. B. Wiberg, *J. Chem. Phys.*, **50**, 1976 (1969); **53**, 858 (1970).
(205) K. Hsu, unpublished results.
(206) In comparing linear and bent (not cyclic) isomers it is the interaction between C_1 and C_3 that is the most important. From Figure 53 it is clear that the $2b_{1g}$ is bonding between these two centers (just as the $2b_1$ in AB_2 systems) while the $1b_{3g}$ has the opposite character (just as the $1a_2$ in AB_2 molecules). Hence occupying the $1b_{3g}$ in place of the $2b_{1g}$ causes the C_1C_3 distance to increase.
(207) R. L. Kuczkowski and E. B. Wilson, *J. Chem. Phys.*, **39**, 1030 (1963).
(208) R. J. Buenker and S. D. Peyerimhoff, *J. Amer. Chem. Soc.*, **91**, 4342 (1969).
(209) V. I. Dianov-Klokov, *Opt. Spectrosc.*, **6**, 290 (1959).
(210) S. J. Arnold, E. A. Ogryzlo, and H. Witzke, *J. Chem. Phys.*, **40**, 1769 (1964).
(211) R. J. Jackson, *J. Chem. Soc.*, 4585 (1962).
(212) Again this use for orbital energies presupposes that account is taken for the general overestimation of the energy gap between occupied and unoccupied MO's in the SCF method.[36,81]
(213) That is unless d AO's are formally occupied in the electronic configuration of the system under consideration.
(214) Note Added in Proof. After completion of this review article new work appeared on the subject of the shapes and energetics of polyatomic molecules by G. Schnuelle and R. G. Parr [*J. Amer. Chem. Soc.*, **94**, 8974 (1972)] which is relevant to the present discussion. In their work the authors have used a simple electrostatic model in a localized MO framework to obtain a consistent description of details of the geometry and spectra of polyatomic systems. In particular, a new prescription for the localization of canonical SCF MO's has been suggested and an alternative means of constructing diagrams from *ab initio* techniques has been considered. This work has special bearing on the question of how to relate MO and VB models of electronic structure, as discussed in section III.A.2 of the present article.